PRODUCTION OF LOW-ENERGY CEMENTS USING VARIOUS INDUSTRIAL WASTES

A THESIS SUBMITTED TO
THE GRADUATE SCHOOL OF NATURAL AND APPLIED SCIENCES
OF
MIDDLE EAST TECHNICAL UNIVERSITY

BY

OĞULCAN CANBEK

IN PARTIAL FULFILLMENT OF THE REQUIREMENTS
FOR
THE DEGREE OF MASTER OF SCIENCE
IN
CIVIL ENGINEERING

SEPTEMBER 2018

Approval of the thesis:

PRODUCTION OF LOW-ENERGY CEMENTS USING VARIOUS INDUSTRIAL WASTES

submitted by **OĞULCAN CANBEK** in partial fulfillment of the requirements for the degree of **Master of Science in Civil Engineering Department**, **Middle East Technical University** by,

Prof. Dr. Halil Kalıpçılar
Dean, Graduate School of **Natural and Applied Sciences** _____

Prof. Dr. İsmail Özgür Yaman
Head of Department, **Civil Engineering** _____

Assoc. Prof. Dr. Sinan Turhan Erdoğan
Supervisor, **Civil Engineering Dept., METU** _____

Examining Committee Members:

Prof. Dr. İsmail Özgür Yaman
Civil Engineering Dept., METU _____

Assoc. Prof. Dr. Sinan Turhan Erdoğan
Civil Engineering Dept., METU _____

Assoc. Prof. Dr. Berna Unutmaz
Civil Engineering Dept., Hacettepe University _____

Asst. Prof. Dr. Çağla Meral Akgül
Civil Engineering Dept., METU _____

Asst. Prof. Dr. Seda Yeşilmen
Civil Engineering Dept., Çankaya University _____

Date: 07.09.2018

I hereby declare that all information in this document has been obtained and presented in accordance with academic rules and ethical conduct. I also declare that, as required by these rules and conduct, I have fully cited and referenced all material and results that are not original to this work.

Name, Last Name: Oğulcan Canbek

Signature:

ABSTRACT

PRODUCTION OF LOW-ENERGY CEMENTS USING VARIOUS INDUSTRIAL WASTES

Canbek, Oğulcan

M.S., Department of Civil Engineering

Supervisor: Assoc. Prof. Dr. Sinan Turhan Erdoğan

September 2018, 129 pages

Calcium sulfoaluminate ($C\bar{S}A$) cements are of interest since their production promises lower environmental impact than portland cement (PC) due to the lower kiln temperatures required to form the main phase of $C\bar{S}A$ clinker than that of PC. Unlike PC, alite does not form in $C\bar{S}A$ cements instead ye'elimite forms.

In this study, laboratory production of $C\bar{S}A$ cement has been realized. Limestone, bauxite and gypsum were used as natural raw materials. Red mud, fly ash and desulfogypsum, high-volume industrial wastes generated in Turkey, were also used as raw materials. Minimizing the use of natural raw materials, especially bauxite, was targeted during the production of $C\bar{S}A$ clinker. Several parameters that affect the properties of $C\bar{S}A$ cements were investigated such as clinker fineness, kiln temperature, kiln residence time, source and amount of added calcium sulfates and raw mixture proportioning. Properties of various $C\bar{S}A$ cements produced were explored through compressive strength tests, X-ray diffraction (XRD), isothermal conduction calorimetry, thermogravimetric analysis (TGA) and scanning electron microscopy (SEM). Optimum burning parameters for clinker production were determined as 1250 °C for 90 minutes. Most of the strength gain of mortars prepared with the $C\bar{S}A$ cements produced, was achieved up to 3 days because of rapid ettringite formation. Desulfogypsum was found to be more beneficial than natural gypsum when it was

added to clinker pastes, in terms of strength gain. > 40 MPa 28-day compressive strengths were achieved when red mud and fly ash were incorporated into the clinker raw mixture. Carbonation of cement pastes was also observed.

Keywords: Alternative cement, calcium sulfoaluminate, clinker production, waste material accomodation, strength development

ÖZ

ÇEŞİTLİ ENDÜSTRİYEL ATIKLAR KULLANILARAK DÜŞÜK ENERJİLİ ÇİMENTOLAR ELDE EDİLMESİ

Canbek, Oğulcan

Yüksek Lisans, İnşaat Mühendisliği Bölümü

Tez Yöneticisi: Doç. Dr. Sinan Turhan Erdoğan

Eylül 2018, 129 sayfa

Kalsiyum sülfoalüminat (KSA) çimentosu ve Portland çimentosu (PÇ) klinker ana fazlarını oluşturmak için gereken fırın sıcaklığının KSA çimentosu için daha düşük olması üretim esnasında çevresel etkiyi azaltabileceğinden, KSA çimentoları ilgi odağı haline gelmiştir. KSA çimentosunda PÇ' dekinin aksine alit fazı oluşmaz, yerine ye'elimit oluşur.

Bu çalışmada, KSA çimentolarının laboratuvarda üretimi gerçekleştirilmiştir. Doğal hammaddeler olarak kalker, boksit ve alçıtaşı kullanılmıştır. Ayrıca, ülkemizde yoğun olarak ortaya çıkan endüstriyel atıklardan olan uçucu kül, kırmızı çamur ve desülfojips de (yapay alçı) hammadde olarak kullanılmıştır. Doğal hammaddelerin, özellikle de boksitin, KSA çimentosu üretimi esnasında kullanımının minimize edilmesi hedeflenmiştir. Klinker inceliği, yakma sıcaklığı, yakma süresi, klinkere katılan kalsiyum sülfatın kaynağı ve miktarı ve hammadde karışım oranları gibi KSA çimentosunun özelliklerini etkileyebilecek birçok parametre araştırılmıştır. Üretilen farklı KSA çimentolarının özellikleri; dayanım testi, X-ışını kırınım (XRD), izotermal iletim kalorimetresi, termogravimetrik analiz ve taramalı elektron mikroskopisi (SEM) kullanılarak incelenmiştir. Klinker üretimi için gereken optimum yakma değerleri 1250 derece ve 90 dakika olarak belirlenmiştir. Üretilen KSA çimentoları kullanılarak hazırlanan harç numunelerinin dayanım gelişiminin büyük bölümü hızlı etrenjit

oluşumu sebebiyle ilk 3 günde elde edilmiştir. Desülfojips alçıtaşına göre dayanım gelişimi açısından daha yararlı bulunmuştur. Klinker hammadde karışımında kırmızı çamur ve uçucu kül kullanıldığında 40 MPa' dan yüksek 28. gün basınç dayanımlarına ulaşılmıştır. Ayrıca, çimento hamurlarında karbonatlaşma gözlenmiştir.

Anahtar Kelimeler: Alternatif çimento, kalsiyum sülfoalüminat, klinker üretimi, atık malzeme ikamesi, dayanım gelişimi

Dedicated to my family

ACKNOWLEDGEMENTS

I wish to express my heartfelt gratitude to my supervisor, Dr. Sinan Turhan Erdoğan who has been more than a supervisor to me during my studies. I was so lucky to meet him when I first came to METU. This dissertation could not have been realized if he had not provided me with a research assistanship in his research project. I will always be grateful to him for his guidance throughout my M.S. and knowledge he has shared with me.

Special thanks to Dr. Mustafa Tokyay from whom I learned much about construction materials. His recommendations for this research kept me motivated. I am also appreciated for the valuable contributions of the jury members.

I am thankful for the friendship of my colleagues Baki Aykut Bilginer, Kadir Can Erkmen, Sahra Shakouri, Meltem Tangüler Bayramtan and Muhammet Atasever. I am also indebted to Dr. Burhan Aleessa Alam and Kemal Ardoğa for their help and support.

Many thanks to Gülşah Bilici and Cuma Yıldırım for their friendship and assistance in the laboratory.

I thank Votorantim Hasanoğlan Cement Plant, Seydişehir Eti Aluminum Plant and Afşin Elbistan Thermal Power Plant for providing the raw materials used in this research.

Finally, I want to thank The Scientific and Technological Research Council of Turkey (TÜBİTAK) for funding this research project (Project Number: 116M233).

TABLE OF CONTENTS

LIST OF TABLES

LIST OF FIGURES

LIST OF ABBREVIATIONS

AFm	Al_2O_3-Fe_2O_3 (mono)
AFt	Al_2O_3-Fe_2O_3 (tri)
AMCSD	American Mineralogist Crystal Structure Database
ASTM	American Society for Testing and Materials
C-S-H	Calcium-silicate-hydrate
$C\bar{S}A$	Calcium sulfoaluminate
$C\bar{S}AC$	Calcium sulfoaluminate cement
DTA	Differential thermal analysis
EDX	Energy-dispersive X-ray spectroscopy
L.O.I	Loss on ignition
OPC	Ordinary Portland cement
SEM	Scanning electron microscopy
TGA	Thermogravimetric analysis
w/b	Water-to-binder ratio by mass
w/c	Water-to-cement ratio by mass
wt.%	Weight percentage
XRD	X-Ray diffraction
XRF	X-Ray fluorescence

CHAPTER 1

INTRODUCTION

1.1 Background

The Kyoto Protocol, signed in 1997, specified targets for each signatory country to decrease its greenhouse gas emissions to prevent global warming. It was also affirmed that CO_2 emissions play a significant part in the alteration of the Earth' s climate (Sharp et al., 1999). The cement industry is under increasing pressure, since it is one of the major global emitters of CO_2, to search for ways to reduce CO_2 emissions in both the production and utilization of hydraulic cements for large scale implementations (Gartner, 2017). In 2015, approximately 4.6 billion tons of cement were produced worldwide which is equal to about 626 kg per capita, higher than the sum of human food consumption (FAO, 2013; CEMBUREAU, 2015). Portland cement (PC) is the most widely used binder and its raw materials are limestone and clay. Also, minor amounts of gypsum rock are used to control the hydration mechanism. PC clinker is produced by appropriate proportioning of raw materials and burning the raw mixture at 1450-1500 °C. The oxide composition of PC clinker mainly consists of lime (CaO), silica (SiO_2) and alumina (Al_2O_3). Considering the CO_2 emissions of the PC manufacturing process, 60 % of comes from the calcination of limestone only ($CaCO_3 \rightarrow CaO + CO_2$), not from the fuel used in the kiln, and that's why the cement industry plays a major role in CO_2 emissions (Scrivener et al., 2016a). Moreover, 4.2 GJ of energy is consumed and about 0.87 t of CO_2 emerges per ton of cement produced (Juenger et al., 2011; Tokyay, 2016). Thus, 6 to 7 % of global man-made CO_2 emissions come from cement production (Shi et al., 2011). Along with the demands to reduce CO_2 emissions, the cement industry also deals with waste materials from other industries. These wastes do not have much usage and are mostly landfilled where they can cause environmental problems. Portland cement can be combined with

industrial waste materials such as fly ash, a residue of coal combustion, ground granulated blast furnace slag, a co-product of iron production, or silica fume from the production of silicon metal or ferrosilicon alloys. However, these materials can be combined with PC in limited quantities and there is an interest in incorporating as much waste as possible into cementitious systems. In addition, environments with high acidity and high sulfate concentrations are able to cause durability problems for PC and also some rapid-repair implementations are in need of higher early strength than that of PC. Hence, there is a need to find an alternative to PC (Juenger et al., 2011).

Regarding the situations above, both academia and industry are seeking new binders to replace PC clinker and calcium sulfoaluminate ($C\bar{S}A$) cement is one of interest. Its ability to be produced at about 200 °C lower kiln temperatures, relatively low lime requirement, higher early strength gain than that of PC and the possible production of its clinker using wastes make calcium sulfoaluminate a promising alternative to PC. Also, since the typical $C\bar{S}A$ clinker contains large amounts of sulfur due to its major phase ye'elimite, it is possible to incorporate waste materials that contain large amounts of sulfur into $C\bar{S}A$ cement, unlike into PC.

However, the greater need for alumina to form the main $C\bar{S}A$ clinker compound ye'elimite, makes the use of bauxite necessary as a raw material. Bauxite is not an abundant material like limestone or gypsum and it is in demand by the aluminum industry. Therefore, its use increases the cost of $C\bar{S}A$ cement. Partial or complete replacement of bauxite with an industrial waste can make $C\bar{S}A$ cement even more attractive in terms of both being a customer for wastes and being cheaper.

1.2 Research Objectives and Scope

This study had several objectives:

a) To investigate the possible laboratory production of $C\bar{S}A$ cement by using both natural (traditional) raw materials and industrial wastes
b) To investigate the influence of clinker fineness on the properties of $C\bar{S}A$ cement
c) To investigate the influence of calcination parameters such as firing temperature and kiln residence time on the properties of $C\bar{S}A$ cement

d) To investigate the influence of added gypsum amount on the properties of C$\bar{S}$A cement
e) To investigate the influence of clinker raw mixture proportioning including both wastes and natural raw materials on the properties of C$\bar{S}$A cement
f) To investigate the influence of calcium sulfate from different sources on the properties of C$\bar{S}$A cement

Within the scope of this study, several tests were conducted to investigate the hydration mechanism, strength development, thermal stability, heat evolution and microstructure of C$\bar{S}$A cements produced. Grindability of various C$\bar{S}$A clinkers was also evaluated.

This dissertation includes five chapter and begins with the introduction. Chapter 2 introduces the literature review about C$\bar{S}$A cements. This chapter firstly looks at the history and importance of C$\bar{S}$A cements and continues with the technical knowledge such as the formation and hydration mechanism of C$\bar{S}$A clinkers. Utilization of wastes in C$\bar{S}$A systems which was one of the objectives in this study, is also surveyed in Chapter 2. Chapter 3 covers the experimental procedure. This chapter begins introducing raw materials used and explains methods applied to follow the research objectives. Tests and standards used during the study, are also introduced in Chapter 3. Results of experiments are given and evaluated in Chapter 4. Discussions are focused on each experimental result, separately. Conclusions about the research and recommendations for future work are presented in Chapter 5.

1.3 Nomenclature

Cement chemistry notations used in the text, are given below:

$A = Al_2O_3$

$C = CaO$

$\hat{C} = CO_2$

$F = Fe_2O_3$

$H = H_2O$

$K = K_2O$

M = MgO

N = Na_2O

S = SiO_2

$\bar{S}$ = SO_3

T = TiO_2

CHAPTER 2

LITERATURE REVIEW

2.1 History and Importance of the Calcium Sulfoaluminate Cement

The OPEC (Organization of Petroleum Exporting Countries) oil embargo occurred in the 1970s which was a prohibition of exporting oil to the United States. This incident led to increased R&D activities for all industries including the cement industry, to decrease their dependence on oil (Gartner, 2004). Therefore, being the most popular type of cement for many years, Portland cement (PC) attracts great attention about manufacturing an alternative binder that could eliminate PC, in terms of energy savings, conservation of natural materials and lowered gas emissions.

Ordinary PC clinker (OPC) consists of minerals such as alite (C_3S), belite (C_2S), tricalcium aluminate (C_3A) and ferrite (C_4AF). Alite itself constitutes a major part of the clinker composition, usually about 60-65 %, and is mostly responsible for the energy consumption of OPC since it is produced at temperatures relatively higher (1450-1500 °C) than other phases. Also, because of its chemical composition, Ca_3SiO_5, abbreviated as C_3S, has the greatest dependence on lime among the cement phases. Therefore, due to the decarbonation of lime within the kiln, most of the CO_2 liberated during the production of PC clinker comes from the formation of alite. Belite itself, the second major phase within OPC clinker, can be formed at 1000-1200 °C and also the overall chemical enthalpy for its formation is lower than that of alite, as shown in Table 2.1.

Table 2.1 Energy requirement and liberated CO_2 during formation of clinker phases (Sharp et al., 1999)

Cement Compound	**Enthalpy of formation: kJ/kg clinker**	**Carbon dioxide released:**
C_3S	1848.1	0.578
β-C_2S	1336.8	0.511
CA	1030.2	0.278
$C_4A_3\bar{S}$	800	0.216

Hence, academia and industry have been focusing on binders that can eliminate alite as much as possible. However, there is a fundamental concern about entirely removing or decreasing the amount of alite since the hydration of belite is relatively slower. Even though, belite contributes to the ultimate strength of cement, its contribution to early strength is not great. In order to fulfill the demand for early strength development, two basic approaches are taken. One is the improvement of the reactivity of the belite phase and the other, incorporation of an additional phase into the clinker that can give early strength. The latter idea led to the production of sulfoaluminate-belite cements which includes calcium sulfoaluminate cements abbreviated as $C\bar{S}A$ (Sharp et al., 1999).

Ragozina (1957) described the calcium sulfoaluminate (ye'elimite) phase first. However; Fukuda (1961) was the researcher who correctly identified its composition as $4CaO.3Al_2O_3.SO_3$. In the 1960s Alexander Klein from the University of California, Berkeley performed advanced experiments with sulfoaluminate cements and, as such, ye'elimite is also referred to as "Klein's Compound". Development of $C\bar{S}A$ goes back to the early 1970s and was realized by the China Building Materials Academy for the purpose of producing self-stressed concrete pipes (Shi et al., 2011). It is called "third cement series" (TCS), preceded by the first and second series which are Portland cement and calcium aluminate cements, respectively (Wang and Su, 1997; Zhang et al., 1999). Also, Mehta (1980) described energy-saving cements that can be produced by modifying the PC composition through the incorporation of $C_4A_3\bar{S}$ and $C\bar{S}$ replacing C_3S and C_3A with the intention of higher early strength development together with later strength as well.

In 1997, the production of $C\bar{S}A$ cement in China was reported as 1 million tons and it is assumed that this rate has increased until now. By modifying its phase proportions,

C$\bar{S}$A cements has the ability to serve many purposes such as non-expansive, expansive, shrinkage compensating and rapid setting due to the readily formation of ettringite from the hydration of ye'elimite. Also, it can be combined with PC to produce Type K cement (Hargis et al., 2014).

C$\bar{S}$A cement have been used for a wide variety of field applications, especially in China. For instance, due to the aforementioned properties, production of road bridges, precast concrete beams, self-stressing concrete pipes with some coal-mining and concrete repair applications have been realized with C$\bar{S}$A cement as a binder. Also, they are suitable for low temperature and marine constructions since they have low heat of hydration and good sulfate resistance (Sharp et al., 1999; Juenger et al., 2011). Yet, their broad utilization to produce concrete is still limited, even in China (Gartner, 2004). On the other hand, alternative raw materials are necessary to widely expand its application since the cost of natural raw materials are increasing and especially the bauxite, used as the source of aluminum, is limited in supply.

2.2 Formation and Composition

C$\bar{S}$A clinker can be synthesized by combining limestone, bauxite and gypsum as sources of lime (CaO), alumina (Al_2O_3) and sulfur trioxide (SO_3), respectively. Also, ferroaluminate clinker abbreviated as FAC, which is a derivative of C$\bar{S}$A clinker can be produced, depending upon the iron oxide content in clinker. Typical oxide compositions of C$\bar{S}$A and FAC clinkers are given in Table 2.2.

Table 2.2 Typical **o**xide compositions of C$\bar{S}$A and FAC clinkers (Zhang et al., 1999)

Clinker	**SiO_2 (%)**	**Al_2O_3 (%)**	**Fe_2O_3 (%)**	**CaO (%)**	**SO_3 (%)**
C$\bar{S}$A	3-13	25-40	1-3	36-45	8-15
FAC	6-15	20-30	6-13	41-50	7-12

The main compounds of C$\bar{S}$A clinker are; ye'elimite, belite, ferrite and anhydrite. Also, depending on the raw mixture, it can include minor amounts of free lime (C), periclase (M), mayenite ($C_{12}A_7$), gehlenite (C_2AS), merwinite (C_3MS_2) and monocalcium aluminate (CA) (Odler, 2000). Phase composition of a typical C$\bar{S}$A clinker is shown in Table 2.3.

Table 2.3 Typical phase composition of C$\bar{S}$A clinker (Odler, 2000)

Phase	Amount (%)
Belite (C_2S)	10-60
Ye'elimite ($C_4A_3\bar{S}$)	10-55
Ferrite (C_4AF)	0-40
Anhydrite ($C\bar{S}$)	0-25
Monocalcium aluminate (CA)	0-10
Mayenite ($C_{12}A_7$)	0-10
Free Lime (C)	0-25

Instead of the alite phase in OPC clinker, ye'elimite is the key component in C$\bar{S}$A clinker and is mostly responsible for its early strength development owing to its hydration with calcium sulfate resulting in ettringite formation. Also, ye'elimite is preferable since its lime content is the lowest among the cement phases given in Table 2.4.

Table 2.4 Lime contents of cement phases (Mehta, 1980)

Phase	Lime content (%)
C_3S	73.7
C_2S	65.1
C_3A	62.2
C_4AF	46.2
$C_4A_3\bar{S}$	36.7

Polymorphism of ye'elimite has been investigated by several researchers (Zhang et al., 1992; Andac and Glasser, 1994; Singh et al., 1997; Hargis et al., 2014;). Zhang et al. (1992) defined the crystalline structure of ye'elimite as a tetragonal system consisting of a three-dimensional framework of AlO_4 tetrahedra in the corners with Ca^{2+} and SO_4^{2-} ions located in the cavities. It is also known that ye'elimite can possess cubic or orthorhombic structure due to the impurities in its structure at ambient temperature (Andac and Glasser, 1994; Hargis et al., 2014). Singh et al. (1997) stated the possibility of partial substitution between Al^{3+} and Fe^{3+} ions since the ionic size of Fe^{3+} (0.675 Å) is merely 20% larger than that of Al^{3+} (0.535 Å). In this case, the main compound can be defined as $C_4A_{(3-x)}F_x\bar{S}$. There exist several claims about the range of the proportion of Fe_2O_3 that may replace Al_2O_3. Between 9-20 % of replacement has been reported (Zdorov and Bernshtein, 1987; Osokin et al., 1992; Krivoborodov and Samchenko, 1992; Xi, 1992). Such a phenomenon may be observed by X-ray

diffraction (XRD) analysis. Considering the larger ionic size of Fe^{3+} than that of Al^{3+}, substitution among these ions results in a growth of cell volume therefore, diffraction of ye' elimite occurs at larger d-spacings (Bullerjahn et al., 2014). The incorporation of different foreign ions such as K^+, Na^+, Mg^{2+} or Ba^{2+} into $C_4A_3\bar{S}$ could be considered as well.

Typical kiln temperatures to form $C\bar{S}A$ clinker range between 1250-1350 °C considering the formation of ye'elimite (Sharp et al.,1999; Martin-Sedeňo et al., 2010). To avoid the decomposition of ye'elimite, a burning temperature of 1350 °C should not be exceeded (Puertas et al., 1995). Ye'elimite can form in various ways such as solid-state reactions between CaO, Al_2O_3 and $CaSO_4$, between $C_{12}A_7$ and $C\bar{S}$, or from a solid-gas reaction between C_3A and SO_2 (Odler, 2000). These formulations are given below:

$$3CaCO_3 + 3Al_2O_3 + CaSO_4.2H_2O \rightarrow 4CaO.3Al_2O_3.SO_3 + 3CO_2 + 2H_2O \quad (1)$$

$$3(12CaO.7Al_2O_3) + 7CaSO_4 \rightarrow 7(4CaO.3Al_2O_3.SO_3) + 15CaO \quad (2)$$

$$3(3CaO.Al_2O_3) + SO_2 + 0.5O_2 \rightarrow 4CaO.3Al_2O_3.SO_3 + 5CaO \quad (3)$$

Belite usually exist as its β form in $C\bar{S}A$ clinkers. It is formed at temperatures between 1000-1200 °C. It is known to be primarily responsible for ultimate strength (Sharp, 1999). There also exist four other polymorphic forms of belite (α, α'_H, α'_L and γ) but the β form is known as the most reactive. β-C_2S is not thermodynamically stable at any temperature whereas only the γ form is thermodynamically stable at room temperature and recognized as hydraulically inactive (Gosh et al., 1979; Odler, 2000; Ramachandran et al., 2002). Mehta and Monteiro (2006) wrote:

> *The irregular coordination of the oxygen ions around calcium leaves large voids, which account for the high reactivity of C_3S. On the other hand, γ–C_2S has a regularly coordinate structure and is, therefore, nonreactive.*

The β to γ conversion has always been an issue for the cement industry. It mostly occurs with slow cooling or grinding (Thomas and Stephenson, 1978; Grooves, 1983; Odler, 2000). It is thought that the conversion of the β to γ can be avoided if some appropriate dopants like boron are used or the clinker produced can be cooled rapidly (Kriskova et al., 2013). Li et al. (2007) found that the incorporation of dopants into the $C\bar{S}A$ system stabilized the α'-belite form resulting in faster hydration and higher

early compressive strength than undoped clinker containing the β-C_2S form. However, despite the advantages of using dopants, primarily boron, such as to increase belite reactivity and to delay setting by reducing the reactivity of the ye'elimite phase, high cost is a serious matter for boron doping (Gartner, 2017).

When the raw mixture contains sufficient amounts of Fe_2O_3, the ferrite phase also forms in C$\bar{S}$A clinker and contributes both to early and later strength (Odler, 2000). Minor amounts of magnesium, sodium and potassium may be incorporated in the ferrite solid solution. Due to the presence of alkalies, the crystal structure is orthorhombic with large structural holes explaining the high reactivity (Mehta and Monteiro, 2006). However, its composition in C$\bar{S}$A clinker may not be similar to that in portland cement and may range from C_4AF to C_6AF_2 (Strigac et al., 2000).

Furthermore, within the C$\bar{S}$A clinker, free SO_3, free lime and various calcium aluminate phases such as CA and $C_{12}A_7$ can be formed depending on the raw meal. Free SO_3 may lead to free $CaSO_4$ if it is not consumed during ye'elimite formation. On the other hand, the amount of $CaSO_4$ in such clinkers is important since the aluminate-bearing phases react with anhydrite to form ettringite. Free lime in C$\bar{S}$A clinker is known to be more reactive than in PC due to the lower firing temperature of C$\bar{S}$A clinker and its amount should be limited since its hydration with water causes the formation of $Ca(OH)_2$ that could lead to expansion and unsoundness (Odler, 2000; Mehta and Monteiro, 2006). Still, minor amounts (< 2 %) of free lime can contribute to early strength development (Sudoh et al., 1980; Sahu and Majling, 1994).

Regarding the oxide compositions of the raw materials used, a set of modified Bogue equations can predict the phase composition of the C$\bar{S}$A clinker produced (Majling et al., 1993):

$$C_4AF\ \% = 3.043(Fe_2O_3\ \%) \quad (4)$$

$$C_4A_3\bar{S}\ \% = 1.995(Al_2O_3\ \%) - 1.273(Fe_2O_3\ \%) \quad (5)$$

$$C_2S\ \% = 2.867(SiO_2\ \%) \quad (6)$$

$$C\bar{S}\ \% = 1.700(SO_3\ \%) - 0.445(Al_2O_3\ \%) + 0.284(Fe_2O_3\ \%) \quad (7)$$

$$C\ \% = 1.000(CaO\ \%) - 1.867(SiO_2\ \%) - 1.054(Fe_2O_3\ \%) - 0.550(Al_2O_3\ \%) - 0.700(SO_3\ \%) \quad (8)$$

$$M\ \% = 1.000(MgO\ \%) \quad (9)$$

However, these equations may be illusive for predicting the phase composition since they do not consider the calcination parameters during the production and the possibility of ion substitution within the clinker.

2.3 Hydration Mechanism

The main hydration product of C$\bar{S}$A clinker is ettringite ($C_6A\bar{S}_3H_{32}$, AFt) and it is mainly responsible for early strength development as it appears within the first 20 minutes of mixing (Glasser and Zhang, 2001). According to Kasselouri et al. (1995), hydration of ye'elimite produces significant amounts of ettringite with needle-like morphology in the early hours. During hydration, these crystals fill empty spaces. They convert to prismatic shape at later stages however, they are not very visible unlike in OPC owing to their denser accumulation (Glasser and Zhang, 2001).

Ettringite forms simultaneously with aluminum hydroxide from the reaction of either ye'elimite or other aluminate-bearing phases with calcium sulfate, through the following reactions (Mindess et al., 2003; Martin-Sedeňo et al., 2010; Pinazo et al., 2013):

$$C_4A_3\bar{S} + 2C\bar{S} + 38H \rightarrow C_6A\bar{S}_3H_{32} + 2AH_3 \quad (10)$$

$$C_4A_3\bar{S} + 6CH + 8C\bar{S} + 90H \rightarrow 3C_6A\bar{S}_3H_{32} \quad (11)$$

$$2C_4A_3\bar{S} + 2C\bar{S} + 52H \rightarrow C_6A\bar{S}_3H_{32} + C_4A\bar{S}H_{12} + 4AH_3 \quad (12)$$

$$C_4A_3\bar{S} + 18H \rightarrow C_4A\bar{S}H_{12} + 2AH_3 \quad (13)$$

$$C_{12}A_7 + 12C\bar{S}H_2 + 113H \rightarrow 4C_6A\bar{S}_3H_{32} + 3AH_3 \quad (14)$$

$$3CA + 3C\bar{S}H_2 + 32H \rightarrow C_6A\bar{S}_3H_{32} + 2AH_3 \quad (15)$$

$$C_4AF + 3C\bar{S}H_2 + 30H \rightarrow C_6A\bar{S}_3H_{32} + FH_3 + CH \quad (16)$$

$$C_4AF + 3C\bar{S}H_2 + 21H \rightarrow C_6(A,F)\bar{S}_3H_{32} + 2(A,F)H_3 \quad (17)$$

If the system contains portlandite (Eqn. (11)), the ettringite formed shows expansive behavior whereas if portlandite is absent, it does not cause such a phenomenon (Telesca et al., 2014). Expansion occurs due to ettringite formed after hardening and decreases the compressive strength of the C$\bar{S}$A cement (Odler, 2000).

Ettringite forms alone if the molar ratio of anhydrite to ye'elimite is at least 2. If this ratio becomes less than 2 or calcium sulfate becomes fully depleted, monosulfate (AFm), which is poorly crystalline, forms (Odler, 2000; Winnefeld and Barlag, 2010; Telesca et al., 2014), as illustrated in Equation (12). This phase is deemed trivial for strength development (Bernardo et al., 2007). Also, when the ye'elimite and other aluminate bearing phases are depleted, ettringite can still occur at later stages from the reaction of present AH_3, calcium sulfate and portlandite formed from the later hydration of belite, as shown in Equation (18). But, if the calcium sulfate amount is not sufficient for ettringite formation while consuming AH_3 and CH, then conversion occurs (Eqn. (19)) from ettringite to monosulfate that ends with cracking (Odler, 2000).

$$AH_3 + 3C\bar{S}H_2 + 3CH + 20H \rightarrow C_6A\bar{S}_3H_{32} \quad (18)$$

$$C_6A\bar{S}_3H_{32} + 2AH_3 + 6CH \rightarrow 3C_4A\bar{S}H_{12} + 8H \quad (19)$$

Aluminum hydroxide (AH_3) starts to form simultaneously with ettringite during the hydration of ye'elimite. It is known as poorly crystalline or amorphous therefore hard to identify with XRD. On the contrary, thermogravimetric analysis (TGA) is able to indicate its presence observed as mass loss between 250-280 °C (Winnefeld and Barlag, 2010). Its role in the $C\bar{S}A$ system is still under investigation. Song et al. (2015) concluded that AH_3 colloids accumulate and surround the ettringite particles leading to a more compact structure. Chang et al. (2017) found a correlation between the amorphous AH_3 content and the compressive strength of synthetic $C\bar{S}A$ clinker. By increasing the AH_3 content in samples, higher compressive strength was reached due to the denser pore structure.

Unlike the ye'elimite whose hydrations readily result in ettringite formation, belite does not hydrate much at early stages and it starts to react at later stages as it hydrates 40 % at most up to 28 days (Sudoh et al., 1980; Kasselouri et al., 1995; Malami et al., 1996). Such reactions have been suggested for the hydration of belite:

$$C_2S + AH_3 + 5H \rightarrow C_2ASH_8 \quad (20)$$

$$2C_2S + 4H \rightarrow C_3S_2H_3 + CH \quad (21)$$

Stratlingite (C_2ASH_8) formed in Equation (20), is merely stable when CH is absent in the system based on the hydration studies of Damidot and Glasser (1995) and Pinazo et al. (2013). C-S-H yielded from the hydration of the C_2S with only water as given in the Equation (21), contributes to the ultimate strength of C$\bar{S}$A cement (Odler, 2000).

Water/binder ratio required for the complete hydration of C$\bar{S}$A cement is higher than that of PC. From the composition stoichiometry using Equation (10), it is obvious that for the complete hydration of pure ye'elimite, a water/binder ratio of 0.78 is needed (Bernardo et al., 2006). Even self-desiccation can occur in such cements at lower water/binder ratios than that needed for ettringite formation and its bound water content (Glasser and Zhang, 2001). Water demand for such clinkers is mostly affected by the added gypsum amount and reaches its maximum when the added gypsum amount is about 30 % (replacement of cement). Still, it is recommended that the calcium sulfate amount be adjusted so as to remain a bit lower than the theoretical need to obtain a dimensionally stable mortar or concrete (Glasser and Zhang, 2001). The reactivity of gypsum also affects the properties of C$\bar{S}$A cement (Sahu et al., 1991; Winnefeld and Lothenbach, 2010; Winnefeld and Barlag, 2010; Winnefeld et al., 2017). Mate et al. (2015) investigated the effects of three different types of added calcium sulfate (anhydrite, hemihydrate and dihydrate) on the properties of C$\bar{S}$A cement pastes prepared by combining 75 % C$\bar{S}$A clinker and 25 % calcium sulfate by weight. They concluded that for early strength development, gypsum (dihydrate) is the best choice whereas anhydrite prevails for ultimate strength gain and hemihydrate (bassanite) was not recommended due to its fast dissolution rate with sharply reduced setting time of the cement paste. They could not obtain workable pastes when bassanite was added despite using a polycarboxylate-based superplasticizer.

In light of the great importance of sulfate content for C$\bar{S}$A cement mentioned above, Zhang (2000) proposed Equation (22) to find the optimum level:

$$C_T = 0.13*M*(A/\bar{S}) \quad (22)$$

where C_T is the ratio of gypsum to clinker, A is the weight % of ye'elimite in the clinker, $\bar{S}$ is the weight % of SO_3 in the gypsum, M is the molar ratio of gypsum to ye'elimite and 0.13 is a coefficient related with the changes among mass and molar values. M also indicates the type of cement produced; whether it is rapid-hardening

(M = 0-1.5), expansive (M = 1.5-2.5) or self-stressing (M = 2.5-6) properties. Also, Chen (2009) introduced Equation (23) for C$\bar{S}$A cements based on ettringite formation from the hydration of ye'elimite and ferrite phases (Eqn. (10), (16) and (17)) to find the optimal value of gypsum to be added:

$$126.45 \times [0.4461(C_4A_3\bar{S}\ \%) + 0.8403(C_4AF\ \%) - 1.000(C\bar{S}\ \%)] / \{100 + 1.2645 \times [0.4461(C_4A_3\bar{S}\ \%) + 0.8403(C_4AF\ \%) - 1.000(C\bar{S}\ \%)] \quad (23)$$

Figure 2.1 shows how the hydrated phase distribution of a C$\bar{S}$A cement is affected by the added gypsum content (Glasser and Zhang, 2001) and Figure 2.2 exemplifies the hydrate phase formation of a C$\bar{S}$A cement (Winnefeld and Lothenbach, 2010):

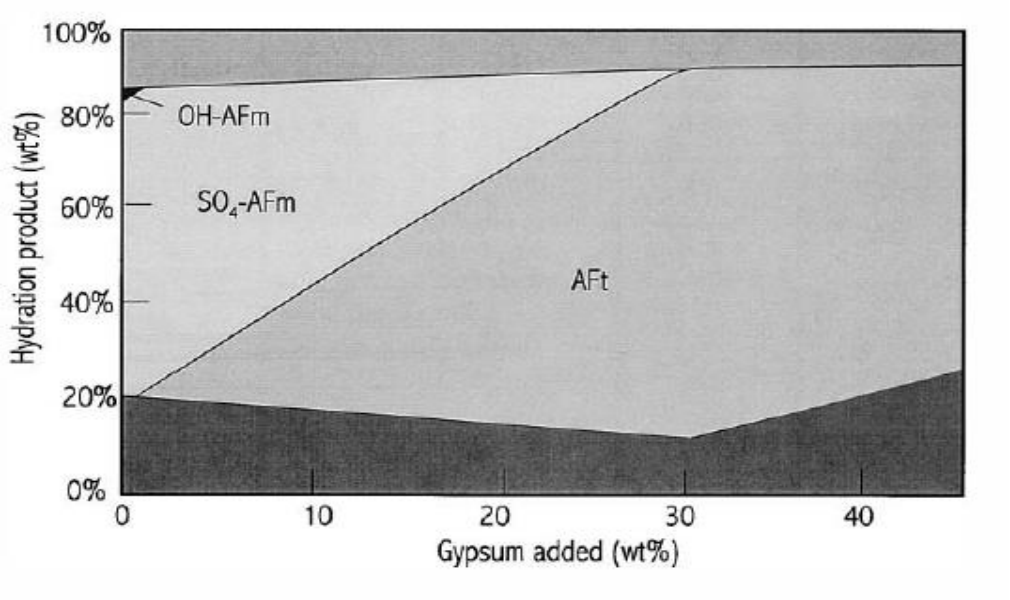

Figure 2.1 Calculated hydrate phase composition of a C$\bar{S}$A cement varying by added gypsum amount (Glasser and Zhang, 2001)

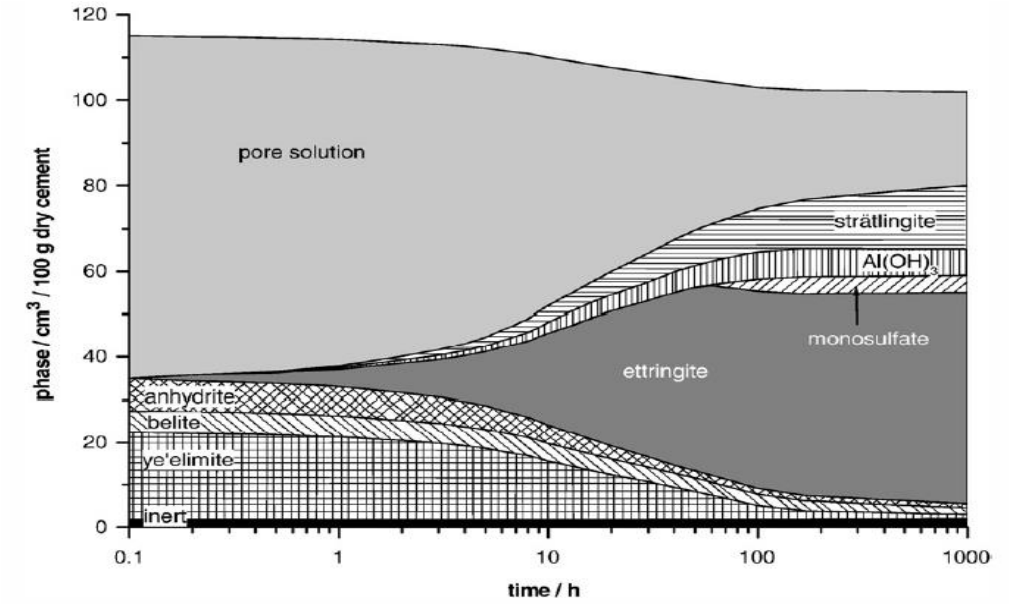

Figure 2.2 Modelled phase formation of a C$\bar{S}$A cement with water/cement = 0.8 (Winnefeld and Lothenbach, 2010)

It can be clearly seen in figures (2.1) and (2.2) that ettringite is the preponderant hydration product for C$\bar{S}$A cement. Also, its amount can be increased by adding up to 30 % gypsum until 4 days.

C$\bar{S}$A cement is known to have lower pH values than OPC (Wang et al., 1992; Sharp et al., 1999; Winnefeld and Lothenbach, 2010). Andac and Glasser (1999) investigated the pore solution composition of a commercial C$\bar{S}$A clinker without adding calcium sulfate. They prepared cement pastes with water-to-cement ratio of 0.8 and cured them at 20 °C with 98-100 % humidity up to 60 days. They found that the pH of the pore solution decreased from 13.1 to 12.9 within 60 days. The alkalis in the C$\bar{S}$A clinker were easily released and the pore solution was dominated by K and Al with low contents of Na, Ca, Cl, Br and SO_4^{-2}. Also, a sharp decrease of K after 3 days indicated possible stratlingite formation as a sink for potassium. On the other hand, Winnefeld and Lothenbach (2010) found an increase of pH from 10.9 to 12.8 up to 28 days which was related with the increasing alkalis due to the hydrate phase formation after the gypsum has been consumed. Also, potassium decreased after 7 days of hydration due to stratlingite formation, compatible with the findings of Andac and Glasser (1999).

For C$\bar{S}$A cement, a major part of the heat evolution takes place in the first day of hydration due to the rapid formation of ettringite from the hydration of ye'elimite (Zhang and Glasser, 2002; Chen, 2009; Winnefeld and Lothenbach, 2010). A rapid

initial exothermic peak followed by the decreased peak(s) after a short dormant period, related with possible monosulfate formation (AFm) in addition to ettringite, describes the typical heat flow curve of C$\bar{S}$A cement. ~120 J/g to ~400 J/g overall heat evolution was reported in the literature depending on the phase formation (Zhang and Glasser, 2002; Martin-Sedeňo et al., 2010; Winnefeld and Lothenbach, 2010).

Mercury intrusion porosimetry (MIP) studies for C$\bar{S}$A cements reveal that less cumulative Hg volume (~120 mm^3/g) is intruded at early ages than in PC (~160 mm^3/g) because of the rapid formation of hydration products, thereafter total porosity does not vary much between the two cements at later ages. However, C$\bar{S}$A cement shows a multimodal distribution of pore structure from the beginning of hydration with a typical first critical (threshold) pore radius of ~200 nm and second critical pore radius of ~25 nm, whereas OPC has a unimodal distribution of pores at early ages indicating a continuous network between pores with the critical pore radius up to ~650 nm. OPC also shows a multimodal pore size distribution at later ages (Bernardo et al., 2006; Telesca et al., 2014).

According to the literature, setting times of C$\bar{S}$A cements range between 30 minutes and 4 hours depending on the ye'elimite and gypsum contents, as well as their reactivities (Glasser and Zhang, 2001; Winnefeld and Lothenbach, 2010; Juenger et al., 2011). In order to extend the workable time during placement, retarders can be used for concretes made of C$\bar{S}$A cements (Quillin, 2001).

2.4 Strength Development

Strength development of a C$\bar{S}$A cement depends on its phase composition and gypsum content (Odler, 2000). Table 2.5 shows how the phase composition of ye'elimite-containing cements affect their compressive strength development (Mehta, 1980).

Table 2.5 Effects of phase content on the compressive strength development of various ye'elimite bearing cements (Mehta, 1980)

Compound	**Rapid**	**Rapid**	**Normal**	**Slow**	**Slow**
C_2S	25	30	45	50	65
$C_4A_3\bar{S}$	20	20	20	10	10
C_4AF	40	30	15	30	15
$\bar{S}$	15	20	20	10	10
Compressive strength (MPa)					
8 h	-	15.6	-	-	-
1 d	34.8	28.3	9.5	5.6	5.2
3 d	36.9	33.8	19.3	7.6	8.9
7 d	37.4	37.7	27.4	11.7	12.4
28 d	-	-	49.8	14.1	14.5
90 d	-	-	-	21.4	22.4
120 d	51.8	53.8	86.2	-	-

Péra and Ambroise (2004) prepared 5 different self-leveling topping mortars by combining a sulfoaluminate clinker containing 66 % ye'elimite and phosphogypsum, at different ratios. The clinker-to-phosphogypsum ratio ranged from 90:10 to 70:30. Mortar samples exceeded 35 MPa and 50 MPa at 1 day and 28 days of hydration, respectively. Winnefeld et al. (2017) prepared mortar samples by using a water-to-binder ratio of 0.74, cured at 20 °C with 95 % relative humidity. The added calcium sulfate content was determined based on the $CaSO_4/C_4A_3\bar{S}$ (M-value) and fixed to 0.8. When anhydrite was added to the $C\bar{S}A$ clinker with 68.1 % ye' elimite, compressive strengths of ~12 MPa and ~28.3 MPa were achieved at 1 day and 28 days, respectively. When gypsum was added instead of anhydrite compressive strength reached ~25 MPa and ~32 MPa at 1 day and 28 days, respectively, which indicates the beneficial effect of gypsum addition compared to anhydrite. Quillin (2001) demonstrated the effect of curing conditions on compressive strength development of $C\bar{S}A$ cement. 100-mm concrete cubes made of $C\bar{S}A$ cement were prepared with a water-to-cement ratio of 0.563 and cured the samples in either water or air, at different ambient temperatures. Air-stored samples gained 45 MPa compressive strength at 28 days followed by a decrease to 38.5 MPa at 720 days whereas the water-stored samples increased their strength from 44 MPa to 59 MPa at 720 days. Chen (2009) prepared mortar cubes according to ASTM C 109 by using three different synthesized $C\bar{S}A$ cements. The ye'elimite content of clinkers were 65.3 %, 42 % and 15.4 %, and these clinkers were abbreviated as HS, MS and LS, respectively. Added gypsum amounts were calculated

according to Equation (23). Compressive strengths of all synthetic C$\bar{S}$A cements were less than that of the reference ASTM Type I/II Portland cement at every curing age. HS and MS cements reached about ~13 MPa compressive strength at 1 day whereas LS gained only about ~6 MPa. Until 28 days, MS increased its strength to ~40 MPa while HS and LS could not exceed ~33 MPa and ~20 MPa, respectively.

It can be clearly deduced from the aforementioned studies that strength development of C$\bar{S}$A cements can vary significantly since it is affected by many factors like phase composition, sulfate content and curing conditions. Also, it must be taken into account that various methods to measure the compressive strength of C$\bar{S}$A cements are present in the literature. Higher compressive strength can be obtained by using paste samples whereas mortar samples obtain lower compressive strength than pastes since the water-to-binder ratio needed can be significantly higher for mortars.

2.5 Utilization of wastes within the C$\bar{S}$A system

Various industrial wastes are used as raw materials in the production of C$\bar{S}$A clinker such as; coal combustion residuals, phosphogypsum, galvanic sludge, red mud, marble sludge waste, etc (Singh et al., 1996; Zivica, 2000; Li et al., 2007; Luz et al., 2009; Wu et al., 2011; Chen and Juenger, 2012; El-Alfi and Gado, 2016; Huang et al., 2017). El-Alfi and Gado (2016) produced C$\bar{S}$A clinker by combining marble sludge waste, kaolin and gypsum in different proportions. Paste samples from clinker containing 55 wt.% marble sludge gained 35 MPa compressive strength at 28 days when a water-to-cement ratio of 0.5 was used. Huang et al. (2017) demonstrated the possible utilization of phosphogypsum as an added agent for the C$\bar{S}$A cement if H_3PO_4 can be eliminated from its chemical composition. Singh and Pradip (2008) produced C$\bar{S}$A cement containing 70 wt.% phosphochalk waste from fertilizer plants as a raw material in addition to bauxite and minor amounts of fly ash. It is highlighted that C$\bar{S}$A cement is not affected by P_2O_5 and Fluorine impurities in phosphochalk waste. A 28-day compressive strength of ~46 MPa at 28 days was obtained. Luz et al. (2009) replaced C$\bar{S}$A cement consisting of 20 wt.% phosphogypsum and 80 wt.% C$\bar{S}$A clinker, with 25 wt.% galvanic sludge and prepared mortar samples according to EN 196-1. ~20 MPa and ~33 MPa compressive strengths were reached at 1 and 3 days, respectively. Also, it was observed that ettringite formed can accommodate chromium (Cr) ions by replacing sulfate ions. Duvallet and Robl (2013) showed the possible production of a

hybrid cement containing both alite and ye'elimite by using CaF_2 as a mineralizer. The raw materials also included some industrial wastes such as bottom ash, red mud and blast furnace slag fines. Singh et al. (1996) prepared different batches of C$\bar{S}$A cements with varying amounts of limestone, red mud, fly ash, bauxite and gypsum. They observed that cements containing red mud can gain compressive strength comparable to OPC whereas fly ash could not be incorporated as an alternative to bauxite since it leads to degradation. Zivica (2000) replaced sulfoaluminate belite cement (SAB) with different pozzolans such as silica fume, slag and fly ash with 5 wt.%, 15 wt.% and 30 wt.%. Since the pozzolans used were siliceous materials and demand portlandite to yield C-S-H, optimal amounts of pozzolans to be replaced with SAB cement were observed to be lower than OPC, in terms of compressive strength. This is related with the low amount of portlandite content in hydrated SAB cement as it only comes from the belite phase unlike in OPC which has both alite and belite as sources of portlandite.

2.6 Influence of Retarders on the Hydration of C$\bar{S}$A Cement

Rapid setting of C$\bar{S}$A cements can induce poor workability, therefore use of special admixtures like retarders or superplasticizers are essential for such systems (Zhang et al., 1999; Glasser and Zhang, 2001; Quillin, 2001). Sugars and citric, gluconic or tartaric acids are known as strong retarders for high-aluminate and C$\bar{S}$A cements (Taylor, 1990).

Zhang et al. (2016) investigated the effects of three different types of superplasticizers such as β-naphthalenelfonic acid-based superplasticizer (BNS), liquid aminosulfonic acid-based superplasticizer (AS), liquid polycarboxylate acid-based superplasticizer (PC) and different combinations of such superplasticizers with retarders such as citric acid (CA) and sodium gluconate (SG) on the fluidity and compressive strength of C$\bar{S}$A cement pastes. They concluded that there was an optimal amount for the retarder to attain better fluidity and compressive strength otherwise hydration products may be negatively affected. A decline in the intensity of ettringite in the XRD pattern was observed with an increasing dosage of retarder. However, they did not examine the influence of such retarders by using them separately (not mixed with superplasticizers). Pelletier et al. (2010) used citric acid as 0.27 % by weight of the binder within a ternary blend system consisting of OPC, C$\bar{S}$A and C$\bar{S}$ with different proportions. It was observed that ettringite formed from the hydration process may be

reduced with citric acid addition to some extent but when the citrate ions have been complexed, ettringite formation can be accelerated. Velazco et al. (2014) studied the influence of citric acid amount as 0 % and 0.5 % by weight of the binder, on the properties of C$\bar{S}$A cement made of synthetic ye'elimite and bassanite. They found that samples containing citric acid gained higher compressive strength than samples without added citric acid due to the more compact pore structure and better distribution of ettringite needles as demonstrated in SEM graphs. Also, citric acid addition caused a decrease in total heat evolution. On the contrary, Burris and Kurtis (2018) did not encounter a reduction in total heat release in the presence of citric acid. But, they also found that compressive strength of C$\bar{S}$A cement can be increased with optimum amount of citric acid.

2.7 Durability

Durability studies demand large amounts of cement therefore studies assessing the durability of C$\bar{S}$A cements are scarce and generally limited with laboratory-produced samples.

The fire resistance of C$\bar{S}$A cements is a major concern for the potential thermal dissociation of its hydrate phases at elevated temperatures (> 500 °C) accompanied with strength loss up to 70 % (Su et al., 1997). Ettringite decomposition which is the dominant hydration product of such cements is the basic reason for the strength loss since it is only stable up to 110 °C. Also, it has a tendency toward carbonation (Glasser and Zhang, 2001). Through the following reaction it may form aluminum hydroxide, calcium sulfate and calcite (Beretka et al., 1992, 1997; Sherman et al., 1995):

$$C_6A\bar{S}_3H_{32} + 3\hat{C} \rightarrow 3C\hat{C} + 3C\bar{S}H_2 + AH_3 + 23H \quad (24)$$

Quillin (2001) stated that concretes made of C$\bar{S}$A cement carbonate faster than those made of OPC. Reinforcement corrosion may also take place in such concretes due to the reduced alkalinity. In a recent study, Hargis et al. (2017) found that the carbonation resistance of C$\bar{S}$A cements increases with reducing water-to-cement ratio (w/c) and increasing anhydrite content. In addition, strength loss was observed for C$\bar{S}$A mortars with higher w/c after carbonation due to the shrinking of solid volume which led to higher porosity whereas mortars with lower w/c gained compressive strength after carbonation because of the densification of the hydrated cement paste.

Since C$\bar{S}$A clinker does not contain C_3A and its major phases are fully sulfated, it can exhibit high sulfate resistance (Malami et al., 1996; Glasser and Zhang, 2001). The lower alkalinity of C$\bar{S}$A clinker can help to prevent alkali-aggregate reaction (Zhang et al., 1999; Juenger et al., 2011). Glasser and Zhang (2001) examined a concrete pipe made of C$\bar{S}$A cement which had been in service for 14 years and found that steel reinforcement remained uncorroded due to the realized self-desiccation because of the higher water demand of such cements.

CHAPTER 3

EXPERIMENTAL PROCEDURE

3.1 Materials

3.1.1 Natural Materials

Limestone, bauxite and gypsum rock were used as natural raw materials in this study. Limestone and gypsum rock were obtained from Votorantim Hasanoğlan cement plant. Bauxite was obtained from Seydişehir Eti Aluminum plant. Natural materials were air dried and ground in a laboratory mill until > 90 % passed the 150-μm sieve. Chemical compositions of the natural raw materials were determined using X-ray fluorescence spectroscopy (XRF) and are shown in Table 3.1.

Table 3.1 Oxide composition of the natural raw materials used

Oxide (%)	Limestone	Bauxite	Gypsum
SiO_2	2.96	12.06	4.55
Al_2O_3	1.44	51.14	1.64
Fe_2O_3	0.61	17.53	1.07
CaO	49.86	1.10	34.86
MgO	0.73	0.33	0.33
SO_3	0.16	0.44	42.18
K_2O	0.17	0.31	0.26
TiO_2	-	2.68	0.13
Na_2O	-	-	-
L.O.I (%)	44	14	15
Density (g/cm^3)	2.69	3.15	2.51
Fineness (cm^2/g)	-	-	8300

Finenesses (Blaine) of limestone and bauxite were not determined since they were used only in the clinker raw meal, unlike gypsum. The XRD patterns and minerals identified in the natural raw materials are given in Figure 3.1.

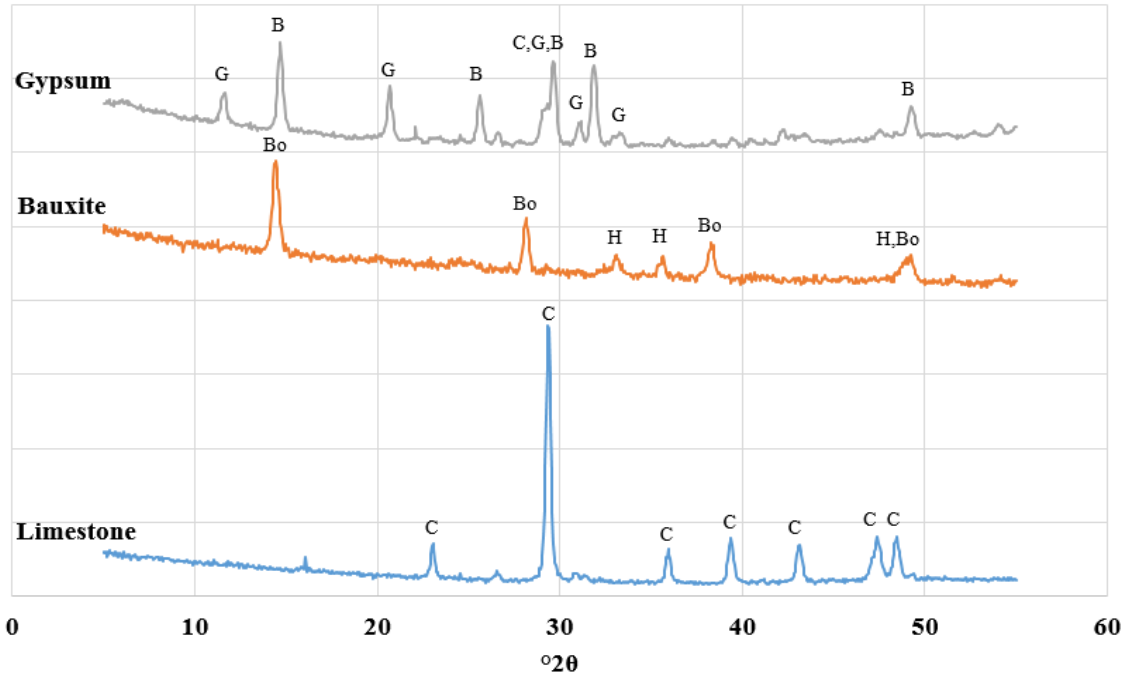

Figure 3.1 X-ray diffractograms for the natural raw materials used (Legend: B – Bassanite; Bo – Boehmite; C – Calcite; G – Gypsum; H – Hematite)

The mineral composition of gypsum can affect the water demand of CS̄A cement, regardless of the properties of clinker, because of its use as an added agent. Therefore, phases in gypsum were investigated with XRD quantitative analysis using the Rietveld refinement method. Results are given in Table 3.2. The amounts of anhydrite, bassanite and dihydrate in the gypsum can influence the water need and overall properties of mixtures it is used in.

Table 3.2 Mineral composition of gypsum used, with agreement factors (R_{wp}) from XRD quantitative analysis

Mineral	**Amount (%)**
Calcite	5.4
Bassanite	63.0
Dihydrate	28.6
Quartz	3.0
R_{wp}/%	8.5

3.1.2 Waste Materials

One of the main objectives of this study was the accommodation of wastes into CS̄A clinker. In accordance, red mud, desulfogypsum and fly ash were used as the industrial wastes from local sources. Red mud was obtained from Seydişehir Eti Aluminum

plant. Fly ash and desulfogypsum were obtained from Afşin Elbistan thermal power plant. Waste materials were air-dried and ground in a laboratory mill until > 90 % passed the 150-µm sieve. The oxide compositions of wastes were determined with X-ray fluorescence spectroscopy (XRF) and are shown in Table 3.3. Finenesses (Blaine) of fly ash and red mud were not determined since they were not used as the added agents unlike desulfogypsum. The XRD patterns and minerals identified in the waste raw materials are shown in Figure 3.2

Table 3.3 Oxide composition of the waste materials

Oxide (%)	Fly Ash	Red Mud	Desulfogypsum
SiO_2	28.25	15.12	0.39
Al_2O_3	13.06	19.88	0.16
Fe_2O_3	7.99	33.27	0.15
CaO	29.17	2.48	37.66
MgO	2.23	0.27	0.14
SO_3	13.46	0.21	44.63
K_2O	0.99	0.50	0.01
TiO_2	0.81	4.90	-
Na_2O	0.23	11.34	0.05
L.O.I (%)	3.1	11	16.7
Density (g/cm^3)	2.43	3.00	2.67
Fineness (cm^2/g)	-	-	10000

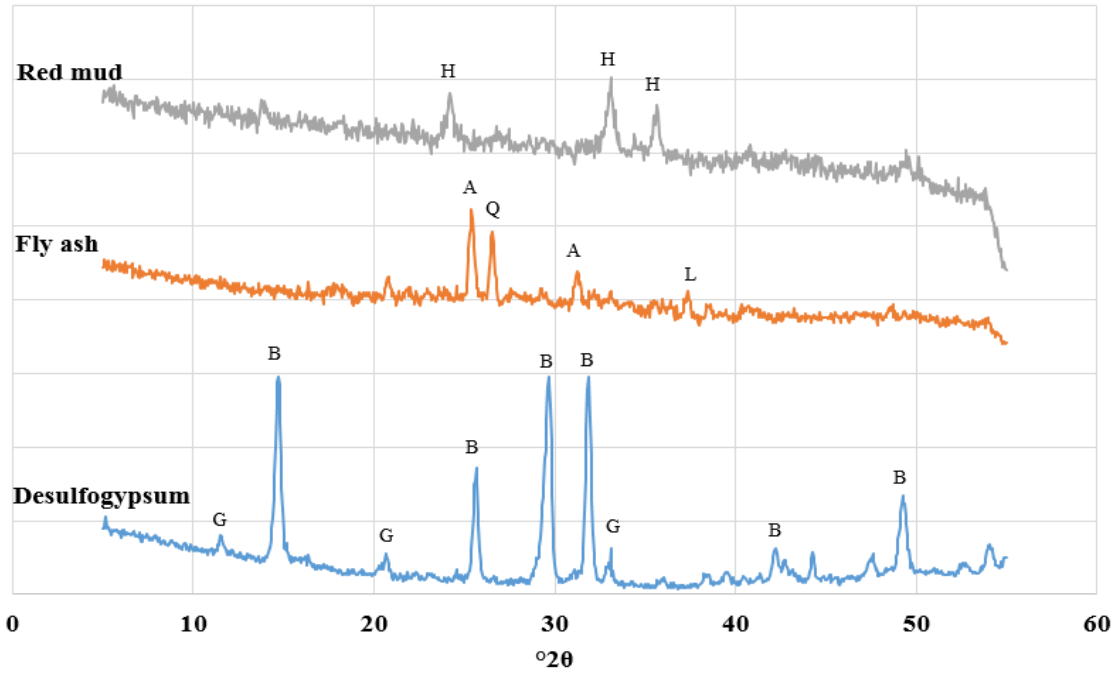

Figure 3.2 X-ray diffractograms for the waste materials used (Legend: A – Anhydrite; B – Bassanite; G – Gypsum; H – Hematite; L – Lime; Q - Quartz)

Fly ash is a by-product of the coal combustion process of thermal power plants and it can be used in cementitious systems depending on its chemical properties. Fly ash from Afşin-Elbistan thermal power plant does not fulfill the requirements of ASTM C 618 to be used in blended cements because of its high sulfate content and is mostly landfilled (> 3 million tons per year) (Mahyar and Erdoğan, 2015). The reason for using Afşin-Elbistan fly ash in this research was its potential to form ye'elimite because of its high CaO, Al_2O_3 and SO_3 contents. Therefore, it may partially replace limestone, bauxite and gypsum rock in C$\bar{S}$A clinker production.

Red mud is a waste material that is produced during alumina extraction from bauxite ore through the Bayer process and approximately 1.5 t of red mud is generated per ton of alumina produced (Brunori et al., 2004). It is mostly landfilled and causes environmental problems mainly because of its high alkalinity and iron content. Seydişehir Eti Aluminum plant is the only source of red mud in Turkey and generates 200000 t of red mud annually. Since the red mud used contains medium amounts of alumina, it can partially replace bauxite. Also, the higher amounts of hematite and alkalis it contains may be beneficial for C$\bar{S}$A clinker production and clinker performance.

Desulfogypsum is a synthetic product derived from thermal power plants as a result of the flue gas desulfurization process used to reduce SO_2 emissions. As much expected, the oxide composition of desulfogypsum is very similar to that of gypsum albeit it contains some minor constituents different than gypsum. However, desulfogypsum can contribute $\bar{S}$ and C for further phase formation. Also, it can be used to replace the gypsum added to C$\bar{S}$A clinker to promote ettringite formation. Mineral composition of the desulfogypsum used was obtained through Rietveld refinement with XRD quantitative analysis and is given in Table 3.4.

Table 3.4 Mineral composition of desulfogypsum used, with agreement factors (R_{wp}) from XRD quantitative analysis

Mineral	**Amount (%)**
Calcite	8.2
Bassanite	88.0
Dihydrate	3.3
Quartz	0.5
R_{wp}/%	11.4

It is observed that the bassanite content of the desulfogypsum is significantly higher than that of the natural gypsum.

3.1.3 Supplementary Materials

3.1.3.1 Citric Acid

The citric acid used was obtained from BDH Laboratory Supplies in Turkey as a white colored powder. It has the chemical formula of $C_6H_8O_7.H_2O$ and a molecular weight of 210.14 g/mol.

3.2 Methods

3.2.1 Clinker Production

In order to produce C$\bar{S}$A clinker, pastes with calculated proportions of raw materials were mixed at approximately W/B = 0.25 according to ASTM C 305 (2014) and shaped on a refractory plate prior to burning in the furnace to allow uniform clinkering as shown in Figure 3.3. A PROTHERM MoS-B 160/8 furnace, shown in Figure 3.4, was used. Properties of the furnace and refractory plates used permitted the production of about 1 kg of clinker per trial and the production process was completed within a day considering the heating, dwelling and cooling times of the furnace.

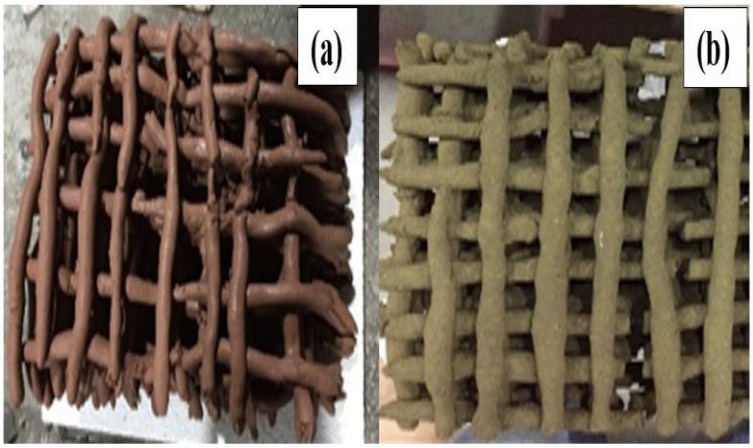

Figure 3.3 C$\bar{S}$A clinker production: (a) Paste mixture before burning; (b) C$\bar{S}$A clinker produced after burning

Figure 3.4 Front view of the furnace used

3.2.2 Determination of Clinker Raw Mixture Proportioning

Based on the oxide compositions of the raw materials, a "reference clinker" was prepared by combining 40 % limestone, 40 % bauxite and 20 % gypsum. Kiln temperature and residence time were determined as 1300 °C and 120 minutes, respectively, to minimize the formation of free lime and the decomposition of ye'elimite (Puertas et al., 1995; Sharp et al., 1999; Liu and Li, 2005). Minimizing the free lime in all produced clinkers (< 1 %) was targeted since it can cause durability problems. The amount of gypsum to be added to the clinker was determined as 19 % by weight of cement for the reference clinker, using Equation (22) to achieve the ideal gypsum-to-ye'elimite ratio of 2 from Equation (10). While determining the optimum added gypsum content for the reference clinker, the anhydrite content of the clinker itself was taken as zero since the XRD quantitative analysis found only minor amounts, despite expectations based on the modified Bogue' s equations (~9 %). Hence, a reference cement with the reference clinker-to-added gypsum ratio of 81:19 was produced.

Other than the reference, one other clinker made only of natural materials was produced by combining 45 % limestone, 45 % bauxite and 10 % gypsum (wt.% of clinker) while keeping the calcination parameters constant. Maximizing the ye'elimite content according to the modified Bogue's equations was the target for this clinker. It must be noted that this clinker would not be preferable because of its increased limestone and bauxite contents.

While determining the raw mixture proportioning of CS̄A clinkers containing industrial wastes, minimizing the bauxite content using various wastes was the main objective since bauxite increases the cost of CS̄A cement. Although the incorporation of industrial wastes in the clinker raw mixture is important, it was limited due to the oxide compositions of materials used. Ye'elimite cannot be formed and free lime may exist at undesirable levels if industrial wastes are used higher than appropriate amounts. All CS̄A clinkers were sieved through a 1-mm sieve after grinding. Table 3.5 summarizes all produced clinkers within the scope of the research.

Table 3.5 Raw mixture proportions, burning parameters and naming of the produced clinkers

Raw Mixture (wt.%)					**Burning Parameters**	**Abbreviation**
Natural Materials			**Wastes**			
Limestone	**Bauxite**	**Gypsum**	**Red Mud**	**Fly Ash**		
40	40	20	-	-	1300 °C / 90 min.	N1
40	40	20	-	-	1300 °C / 120 min.	N2*
40	40	20	-	-	1300 °C / 150 min.	N3
40	40	20	-	-	1250 °C / 120 min.	N4
40	40	20	-	-	1350 °C / 120 min.	N5
45	45	10	-	-	1300 °C / 120 min.	N6
40	35	5	-	5	1250 °C / 90 min.	W5FA
40	30	20	10	-	1250 °C / 90 min.	W10RM
40	25	20	15	-	1250 °C / 90 min.	W15RM
40	20	20	15	5	1250 °C / 90 min.	W15RM5FA
40	20	16.5	10	13.5	1250 °C / 90 min.	W10RM13.5FA
40	20	20	20	-	1250 °C / 90 min.	W20RM
40	10	5	-	45	1250 °C / 90 min.	W45FA
42	10	-	-	48	1250 °C / 90 min.	W48FA

*Clinker N2 is the "reference clinker".

3.2.3 Investigation of the Influence of Clinker Fineness and W/C Used on the Strength Gain of CS̄A cement

In order to find the optimal w/c and to investigate the influence of clinker fineness on strength gain of CS̄A cement, 5 different CS̄A mortar samples were produced with w/c of 0.6, 0.65, 0.7, 0.75 and 0.8 using two reference CS̄A clinkers (N2) which were ground to 6000 ± 100 cm^2/g and 3000 ± 100 cm^2/g fineness (Blaine) respectively. Amount of added gypsum was kept constant as 19 %. The importance of clinker fineness was examined only from the compressive strength point of view. Mixture design for investigating the influence of clinker fineness on strength gain is given in Table 3.6.

Table 3.6 Mixture design for the investigation of the effects of clinker fineness and w/c on the strength gain of CS̄A cement

Clinker ID	Clinker Fineness (cm^2/g)	Added Gypsum (wt.% of cement)	W/C	Compressive Strength (days)
N2	6000	19	0.6, 0.65, 0.7, 0.75, 0.8	1, 7, 28
N2	3000	19	0.6, 0.65, 0.7, 0.75, 0.8	1, 7, 28

3.2.4 Investigation of the Influence of Calcination Parameters on the Properties of CS̄A Cement

Clinkers made with natural raw materials only were used to study the effects of calcination parameters on the properties of CS̄A clinker. For this purpose, clinkers were produced at different kiln temperatures with different dwelling times. To illustrate, when studying the kiln temperature effect on the properties of CS̄A clinker, dwelling time in the kiln was kept constant and same method was applied for investigating the dwelling time. While determining the different calcination parameters, kiln temperatures of 1250 °C and 1350 °C were chosen as higher and lower temperatures than that of the reference clinker (1300 °C) also dwelling times of 90 minutes and 150 minutes were selected as higher and lower durations than that of the reference clinker (120 minutes). All clinkers were ground to 4000 ±100 cm^2/g fineness (Blaine). XRD, thermal analysis and heat evolution tests were conducted in

addition to the determination of compressive strength. Mixture design for determining the compressive strength of various mortars made with different clinkers, is shown in Table 3.7.

Table 3.7 Mixture design for the investigation of the effects of calcination parameters on the strength gain of C$\bar{S}$A cement

Clinker ID	Clinker Fineness (cm^2/g)	Added Gypsum (wt.% of cement)	W/C	Compressive Strength (days)
N1	4000	19	0.7	1, 3, 7, 28
N2	4000	19	0.7	1, 3, 7, 28
N3	4000	19	0.7	1, 3, 7, 28
N4	4000	19	0.7	1, 3, 7, 28

3.2.5 Investigation of the Influence of Clinker Raw Mixture Proportioning Using Only Natural Materials and Added Gypsum Amount on the Properties of C$\bar{S}$A Cement

Two different C$\bar{S}$A clinkers (N2 and N6) were produced using only natural materials, as mentioned in Section 3.2.2. Calcination conditions were kept constant during the production of N2 and N6 to compare their strength gain, heat evolution and hydration product development. Effect of the added gypsum amount on the properties of such clinkers was investigated separately.

Mainly, the amount of gypsum to be added to the system was determined from the ye'elimite content in C$\bar{S}$A clinker. However, all of the aluminate phases including ferrite phase (brownmillerite) and other minor phases can yield ettringite like ye'elimite, through a reaction with calcium sulfate. Also, the reactivities of clinker phases are important for these calcium sulfate-consuming reactions. Therefore, calculation of the optimum amount of gypsum to be added is not straightforward and needs to be investigated experimentally. In this study, 14 % and 24 % (wt.% of cement) calcium sulfate were selected as low and high amounts compared with the amount considered to be the optimum (19 %). Compressive strengths of C$\bar{S}$A cements incorporating different amounts of gypsum were determined. Also, XRD, thermal analysis and heat evolution test were conducted. Mixture design for determining the

compressive strength of different C$\bar{S}$A mortars prepared with different amounts of gypsum, is given in Table 3.8.

Table 3.8 Mixture design for the investigation of the effects of added gypsum amount on the strength gain of C$\bar{S}$A cement

Clinker ID	Clinker Fineness (cm^2/g)	Added Gypsum (wt.% of cement)	W/C	Compressive Strength (days)
N2	4000	14	0.7	1, 3, 7, 28
N2	4000	19	0.7	1, 3, 7, 28
N2	4000	24	0.7	1, 3, 7, 28
N6	2800	14	0.7	1, 3, 7, 28
N6	2800	19	0.7	1, 3, 7, 28
N6	2800	24	0.7	1, 3, 7, 28

3.2.6 Investigation of the Influence of Clinker Raw Mixtures Containing Various Industrial Wastes on the Properties of C$\bar{S}$A cement

Various C$\bar{S}$A cements were produced from clinkers containing industrial wastes to investigate the possibility of waste material incorporation into the clinker raw mixture. Red mud and fly ash were added to the raw mixture both separately and in combination. Total amount of waste incorporation ranges between 5 % and 48 % and bauxite use was as low as 10 % in sum of the clinker raw mixtures.

Desulfogypsum was also used while preparing C$\bar{S}$A cements. Mineral composition of desulfogypsum (Table 3.4) differs from that of the natural gypsum used and can be considered as a source of bassanite. The great water demand of bassanite hindered the use of desulfogypsum in the clinker raw mixture because it led to the clinker raw mixture hardening very rapidly and made the clinker paste unable to be shaped upon mixing with water. However, it was added to the cement paste only with citric acid and could be compared with gypsum in terms of strength gain. In order to demonstrate the competition between gypsum and desulfogypsum, various C$\bar{S}$A cements were produced with constant amounts of added gypsum or desulfogypsum. Amount of calcium sulfate added to the system was not determined separately for such cements and kept constant for comparison (19 % or 24 % wt. of cement). Therefore, this section can also be considered as a study on the effect of different calcium sulfates on the properties of C$\bar{S}$A cements.

Compressive strength was determined for all of these cements. Use of a retarder was necessary for CS̄A mortars consisting of CS̄A clinkers named W5FA, W10RM, W15RM, W15RM5FA and W20RM because of their rapid hardening could not be overcomed with remixing. These mixtures showed great heat liberation within the first minutes of mixing when prepared without retarder. Also, hydration product development was investigated through XRD with thermal analysis and heat evolution was investigated through isothermal calorimetry for the selected cements. CS̄A cements with the added calcium sulfate source which gave highest 28-day strength were selected for each CS̄A clinker produced using waste materials. Mixture parameters for determining the compressive strength of CS̄A cements including gypsum and desulfogypsum, is given in Table 3.9.

Table 3.9 Mixture design for the investigation of the effects of added calcium sulfate and clinker raw mix proportioning on strength gain of various CS̄A cements incorporated with waste materials

Clinker ID	**Added desulfogypsum (wt.% of cement)**	**Added gypsum (wt.% of cement)**	**Added Citric Acid (wt.% of cement)**	**W/C**	**Compressive Strength (days)**
W5FA	-	19	0.5	0.6	1, 3, 7, 28
	19	-			1, 3, 7, 28
	24	-			1, 3, 7, 28
W10RM	-	19	0.5	0.6	1, 3, 7, 28
	19	-			1, 3, 7, 28
W15RM	-	19	0.5	0.6	1, 3, 7, 28
	19	-			1, 3, 7, 28
W15RM5FA	-	19	0.5	0.6	1, 3, 7, 28
	19	-			1, 3, 7, 28
W10RM13.5FA	-	19	-	0.7	1, 3, 7, 28
	-	19	0.5	0.6	1, 3, 7, 28
	19	-			1, 3, 7, 28
W20RM	-	19	0.5	0.6	1, 3, 7, 28
	19	-			1, 3, 7, 28
W45FA	-	19	-	0.7	1, 3, 7, 28
	19	-	0.5	0.6	1, 3, 7, 28
	24	-			1, 3, 7, 28
W48FA	-	19	-	0.7	1, 3, 7, 28
	19	-	0.5	0.6	1, 3, 7, 28
	24	-			1, 3, 7, 28

3.3 Tests Performed on the CS̄A Cements and Raw Materials

3.3.1 Physical Properties

Density was determined according to ASTM C 188 (2016) and fineness (Blaine) was determined following ASTM C 204 (2016), for clinkers and raw materials used. A laboratory ball mill in the Materials of Construction Laboratory of Middle East Technical University was used for grinding. Flow of cement mortars was determined through ASTM C 1437 (2015). Loss on ignition (L.O.I) of materials was determined at 1050 °C for 2 hours in the kiln.

3.3.2 Strength

In order to determine compressive and flexural strength, 4x4x16 cm^3 prism samples were cast according to EN 196-1 (2005) with the exceptions that w/c was not 0.5 but higher (0.6 or 0.7) because of the higher water demand of CS̄A clinkers, and the sand-to-cement ratio was 2.75 instead of 3. In order to prevent rapid setting, 0.5 % (wt.% of cement) citric acid was added to samples and correspondingly w/c was reduced from 0.7 to 0.6. Prepared mortars were cured at room temperature at a relative humidity > 80 %. Compressive and flexural strength were determined at 1, 3, 7 and 28 days with the average of three samples at each curing time for compressive strength. One exception is that while investigating the effects of clinker fineness and w/c on the strength gain of CS̄A cements, the average of two samples was taken and 3-day strength was not determined.

3.3.3 X-ray Diffraction (XRD)

Qualitative information about the minerals in all clinkers and raw materials were obtained using an Olympus BTX-II XRD analyzer with a scanning range between 5-55 °2θ, and with a resolution of 0.25 °2θ. This device uses 30 kV tube voltage and 330 μA tube current at CuKα radiation. ~15 mg of crushed powder was sieved to < 150 μm and loaded into the device chamber. Peaks within the observed patterns were matched with diffraction peaks for known minerals using the American Mineralogist Crystal Structure Database (AMCSD) and PDF-2 database (2010) of International Centre for Diffraction Data (ICDD) (Scrivener et al., 2016b). In order to observe hydration development and products, cement pastes were prepared with w/b = 0.4.

Quantitative analysis of clinkers and raw materials was performed with the Materials Analysis Using Diffraction (MAUD) software (Lutterotti et al., 1999). This process basically matches the X-ray diffraction image (spectrum) of the specimen with diffractograms of expected phases obtained from databases and applies the Rietveld refinement method (Rietveld, 1969). Quantitative analysis was performed on the ground C$\bar{S}$A clinkers and calcium sulfates used. In quantitative analysis, an agreement index, R_{wp}, was also provided. This index is generally utilized to interpret fitting between simulated and experimental patterns. R_{wp} is known as numerical criterion of fitting and analyses with $R_{wp} < 15$ % are generally considered as accurate (Jansen et al., 1994; Scrivener et al., 1996b; Chang et al., 2017). AMCSD codes of minerals, used for XRD quantitative analyses, are provided in Table 3.10.

Table 3.10 Phases and AMCSD codes used for XRD quantitative analyses (Scrivener et al., 2016b)

Phase	**AMCSD Codes**
Anhydrite	0005117
Bassanite	0006909
Belite	0012179
Brownmillerite	0003433
Calcite	0000098
Dolomite	0000904
Gehlenite	0007694
Gypsum	0017897
Lime	0017989
Merwinite	0000294
Periclase	0000501
Perovskite	0005501
Quartz	0017992
Tricalcium aluminate	0017746
Ye'elimite	0014178

3.3.4 X-ray Fluorescence (XRF) Spectroscopy

A Rigaku XRF device at METU Central Laboratory was used. Samples were dried at 105 °C for 2 hours and tested over the boron-to-uranium elemental spectrum. Results were collected as metal and oxide compositions.

3.3.5 Isothermal Calorimetry

Heat of hydration of samples was measured using a "TAM Air Isothermal Calorimeter" with eight channels. ~10 g pastes with w/b = 0.4 were prepared and hydrated in small glass ampoules and subsequently placed inside the calorimeter operating at a temperature of 20 °C. Rate of heat evolution and cumulative heat were recorded in W/g and J/g, respectively, up to 2 or 3 days of hydration. Results were normalized using the binder (dry powder mass) content within the pastes. Heat evolution in the first 30 minutes was discarded due to the disturbance and thermal instability caused by the placement of the samples into the calorimeter measurement channels.

In calorimeter tests, for pastes containing citric acid, ~0.034 g citric acid has to be added to ~2.724 g water. Considering the difficulty of working with such a small quantity, 0.5 g of citric acid was dissolved in 40 g of water and 2.724 g of the citric acid-water solution was used to prepare pastes.

3.3.6 Thermal Analysis

Differential thermal analysis/thermogravimetric analysis (DTA/TGA) were performed to investigate the nature of reaction products in the hydrated pastes. These tests were performed in the METU Central Laboratory. Pastes hydrated at w/b = 0.4 and cured for 3 days and 28 days, were investigated. Samples were heated in a N_2 environment until 1100 °C at a rate of 20 °C/min. Small (100 µl) corundum crucibles were used. The same procedure followed to prepare samples containing citric acid for the calorimeter tests was also applied for thermal analysis.

3.3.7 Scanning Electron Microscopy (SEM)

Scanning electron microscopy was performed on the hydrated C$\bar{S}$A cement pastes to observe their microstructure which shows clinker phases and hydration products formed. Clinkers named N2 and N6 were selected to investigate the microstructure of C$\bar{S}$A cements produced using only natural materials. Also, clinkers named W15RM, W10RM13.5FA and W45FA were selected to examine the microstructure of C$\bar{S}$A cements incorporated waste materials. For these cement pastes, samples prepared at w/b = 0.4 and cured for 3 days. Energy-dispersive X-ray spectroscopy (EDX) which

is an analytical technique used to identify elements and their relative proportions from a chosen region within the sample, was also performed. A QUANTA 400F with a resolution of 1.2 nm, was used for both SEM and EDX analyses at METU Central Laboratory. Samples were oven dried and gold-palladium coated prior to testing.

CHAPTER 4

RESULTS AND DISCUSSION

4.1 Properties of Clinkers Produced Using Only Natural Materials

4.1.1 Physical Properties

In order to study the physical properties of the C$\bar{S}$A clinkers produced, their density, fineness and grindability characteristics were investigated. Densities of ground C$\bar{S}$A clinkers produced using only natural materials, are shown in Table 4.1.

Table 4.1 Density of clinkers produced using only natural raw materials

Clinker ID*	Density (g/cm^3)
N1	3.00
N2	3.00
N3	3.03
N4	3.02
N6	3.06

*Density of N5 could not be determined since its amount was limited.

Table 4.1 shows that calcination parameters did not have a large effect on the density of C$\bar{S}$A clinkers. A slight difference between the density of N6 and those of others is expected since it had different raw mixture.

To investigate the grindability, correlation between the fineness and grinding duration was compared for all clinkers. Table 4.2 demonstrates the time of grinding and finenesses achieved of the reference C$\bar{S}$A clinker (N2) and the clinker with a different raw mixture (N6).

Table 4.2 Grinding duration and fineness of clinkers produced with varying raw mixtures under constant calcination parameters, using only natural materials

Clinker ID	Weight of Batch (kg)	Time of Grinding (minutes)	Fineness Achieved (cm^2/g)
N2	3	300	6000
N2	3	60	4000
N2	5	60	3000
N6	5	60	2800

It is observed that there was not any significant difference between the fineness of clinkers produced with different raw mixtures if other parameters were kept constant. The slightly different finenesses of N2 and N6 clinkers may be related with the higher bauxite content in the raw mixture of N6 than in N2, also meaning more ferrite in the clinker, which probably caused a harder clinker.

Table 4.3 shows the finenesses and required duration of grinding for C$\bar{S}$A clinkers produced with same raw mixture but varying kiln temperature and residence time. It can be clearly seen in Table 4.3 that grindability of clinkers was not affected from the calcination parameters while using the same raw mixture.

Table 4.3 Grinding duration and fineness of C$\bar{S}$A clinkers produced with the same raw mixture under varying calcination parameters, using only natural materials

Clinker ID	Weight of Batch (kg)	Time of Grinding (minutes)	Fineness Achieved (cm^2/g)
N1	2	30	4000
N3	2	30	4000
N4	2	30	4000

4.1.2 Chemical Properties

Chemical compositions of clinkers produced using only natural materials are given in Table 4.4. Major differences between the oxide compositions of clinkers was not observed in Table 4.4 except for Al_2O_3 and SO_3 since the limestone and bauxite contents in N6 were 5 % higher than in the other clinkers (N1, N2, N3, N4, N5).

Table 4.4 Chemical composition of C$\bar{S}$A clinkers from only natural materials

Oxide (%)	Clinker ID					
	N1	**N2**	**N3**	**N4**	**N5**	**N6**
SiO_2	8.80	8.45	8.71	8.71	8.62	9.23
Al_2O_3	25.20	24.19	24.95	24.95	24.70	28.11
Fe_2O_3	8.68	8.33	8.59	8.59	8.51	9.61
CaO	44.33	42.56	43.89	43.89	43.44	44.74
MgO	0.75	0.72	0.74	0.74	0.74	0.80
SO_3	10.25	9.84	10.15	10.15	9.95	5.33
K_2O	0.33	0.32	0.33	0.33	0.32	0.33
TiO_2	1.28	1.23	1.27	1.27	1.24	1.42
Na_2O	0	0	0	0	0	-
L.O.I (%)	0	4	1	1	2	0

4.1.3 Phase Composition

Phase composition of C$\bar{S}$A clinkers can be significantly affected by the calcination parameters and the raw mixture proportioning therefore, effects of these parameters on the phase composition of clinkers were investigated with qualitative and quantitative XRD analyses.

4.1.3.1 Effect of Kiln Temperature on the Phase Composition of C$\bar{S}$A Clinkers

XRD patterns of C$\bar{S}$A clinkers produced at different kiln temperatures using only natural materials, are shown in Figure 4.1. Also, quantitative analysis of such clinkers is given in Table 4.5 with the theoretical amounts of phases expected from Bogue calculations.

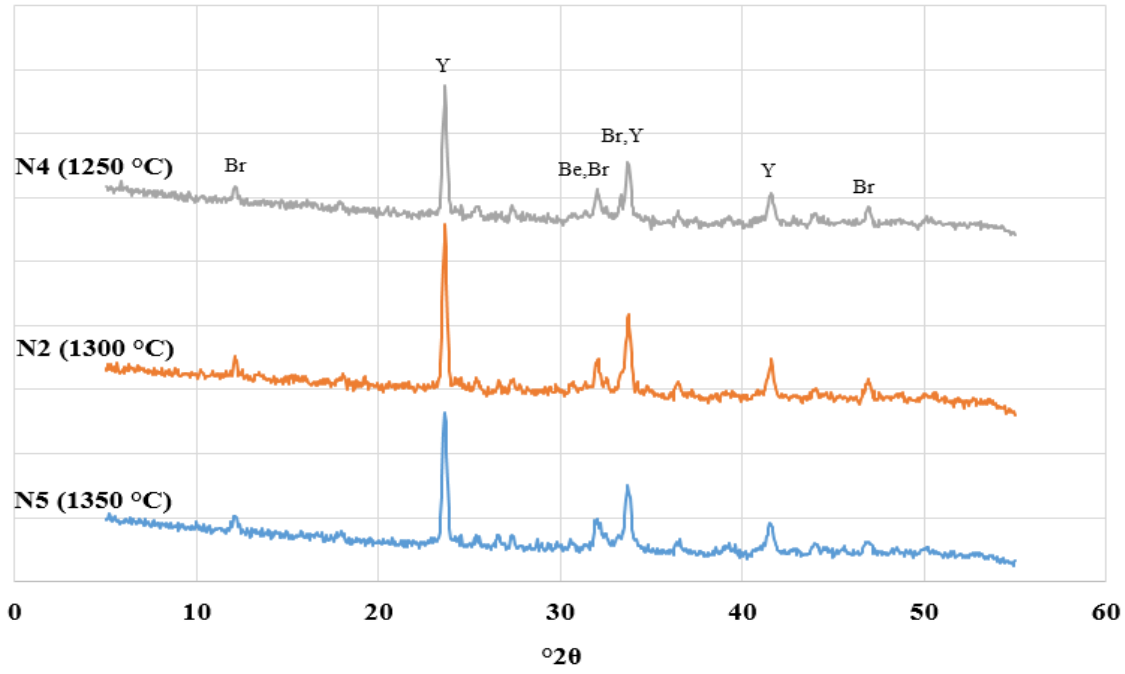

Figure 4.1 X-ray diffractograms for CS̄A clinkers produced under different kiln temperatures using only natural materials (Legend: Be – Belite; Br – Brownmillerite; Y – Ye'elimite)

Figure 4.1 proves that the minerals formed in N2, N4 and N5 were similar. However, in Bogue calculations (Table 4.5), anhydrite content in each clinker was expected as ~9 % but quantitative analysis did not indicate any. It was also found that increasing kiln temperature from 1250 °C to 1300 °C caused lower anhydrite and higher ye'elimite amounts. Martín-Sedeño et al. (2010) also encountered lower ye'elimite in CS̄A clinker produced at 1250 °C than in CS̄A clinkers produced at higher temperatures. This phenomenon indicates the ye'elimite formation via anhydrite consumption. Unlike brownmillerite, less belite seems to be formed than excepted. The reason might be the depletion of calcium ions for ye'elimite or brownmillerite formation. Minor amounts of free lime also show the thorough clinkering for each clinker. The XRD patterns also support the absence of free lime, as it could not be identified. It was also observed that, at 1350 °C, the clinker (N5) fused and stuck to the surface of the refractory plate so the quantity recovered was limited, enough only for XRD, heat evolution and thermal analyses. Compressive strength samples could not be prepared for this clinker. Singh et al. (1996) also reported the same problem. Besides, some other phases like perovskite and gehlenite were identified which can be considered as hydraulically inactive (Juenger et al., 2011).

Table 4.5 Phase composition of C$\bar{S}$A clinkers produced under different kiln temperatures using only natural materials, with agreement factors (R_{wp}) from XRD quantitative analysis

Phase		**Amount (%)**		
		1250 °C (N4)	**1300 °C (N2)**	**1350 °C (N5)**
Belite	Bogue	25.2	25.2	25.2
	Calculated	16.0	14.6	19.5
Brownmillerite (C_4(A,F))	Bogue	26.4	26.4	26.4
	Calculated	28.6	29.2	27.5
Ye'elimite	Bogue	39.2	39.2	39.2
	Calculated	41.8	49.1	45.5
Anhydrite	Bogue	8.7	8.7	8.7
	Calculated	3.7	1.4	2.0
Periclase	Bogue	0.7	0.7	0.7
	Calculated	0.8	0.6	0.1
Free Lime	Bogue	0	0	0
	Calculated	0.2	0.3	1.1
Gehlenite	Calculated	2.1	1.7	0
Perovskite	Calculated	1.9	0.4	0.8
Dolomite	Calculated	1.4	1.5	0.2
Tricalcium aluminate	Calculated	0.6	0.2	2.3
Merwinite	Calculated	3.0	1.1	1.0
R_{wp}/%	Calculated	7.7	8.5	8.1

4.1.3.2 Effect of Kiln Residence Time on the Phase Composition of C$\bar{S}$A Clinkers

The XRD patterns and the phase composition of C$\bar{S}$A clinkers produced at different kiln residence durations using only natural materials are given in Figure 4.2 and Table 4.6, respectively.

Major changes in the amounts of main phases were not observed with varied kiln residence durations, (from 90 minutes to 150 minutes) as well as the minerals formed (Figure 4.2). Therefore, it can be said that 90 minutes of dwelling duration is enough also regarding the energy and fuel consumption of the kiln. One interesting point is that, increased kiln residence times also caused limited increase for ye'elimite formation in exchange for anhydrite reduction which corresponded to the further reaction of anhydrite to form ye'elimite (Table 4.6).

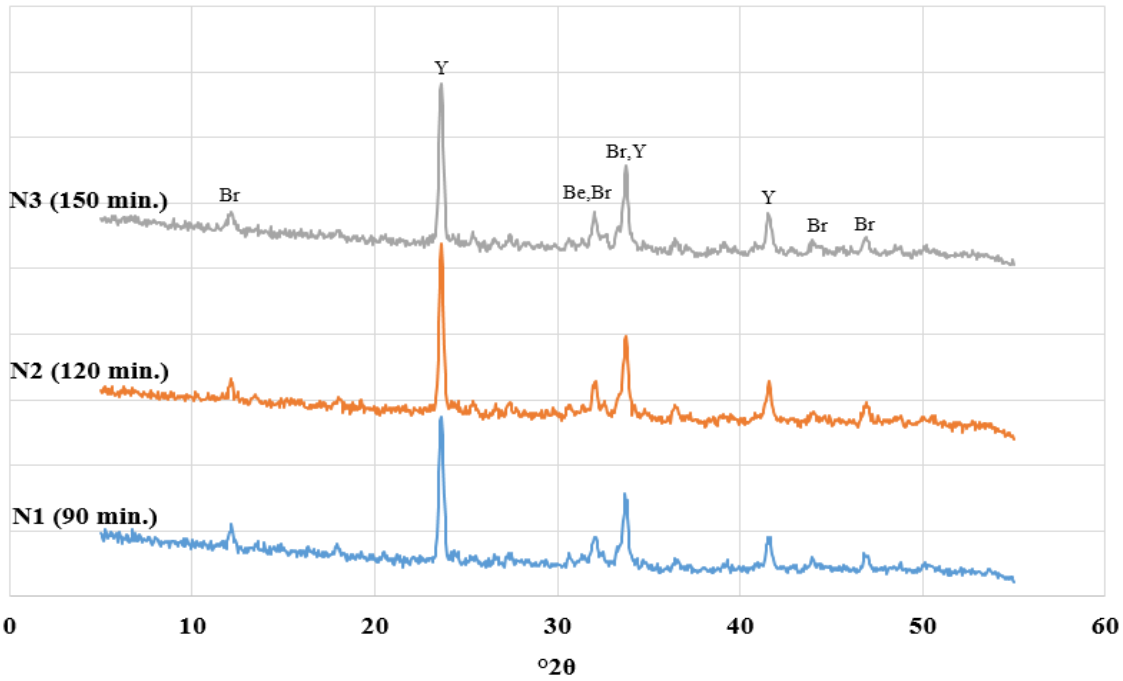

Figure 4.2 X-ray diffractograms for CS̄A clinkers produced under different kiln residence durations using only natural materials (Legend: Be – Belite; Br – Brownmillerite; Y – Ye'elimite)

Table 4.6 Phase composition of CS̄A clinkers produced under different kiln residence durations using only natural materials, with agreement factors (R_{wp}) from XRD quantitative analysis

Phase		**Amount (%)**		
		90 min. (N1)	**120 min. (N2)**	**150 min. (N3)**
Belite	Bogue	25.2	25.2	25.2
	Calculated	15.6	14.6	16.7
Brownmillerite ($C_4(A,F)$)	Bogue	26.4	26.4	26.4
	Calculated	29.0	29.2	25.5
Ye'elimite	Bogue	39.2	39.2	39.2
	Calculated	48.2	49.1	50.6
Anhydrite	Bogue	8.7	8.7	8.7
	Calculated	1.8	1.4	1.0
Periclase	Bogue	0.7	0.7	0.7
	Calculated	0	0.6	1.0
Free Lime	Bogue	0	0	0
	Calculated	0	0.3	0
Gehlenite	Calculated	3.2	1.7	1.1
Perovskite	Calculated	0.1	0.4	0.1
Dolomite	Calculated	1.6	1.5	0.5
Tricalcium aluminate	Calculated	0.1	0.2	0
Merwinite	Calculated	0	1.1	3.5
R_{wp}/%	Calculated	7.7	8.5	8.7

4.1.3.3 Effect of Raw Mixture Proportioning on the Phase Composition of CS̄A Clinkers

In this study, two different clinker raw mixtures were prepared with only natural materials, as mentioned in Section 3.3.1. The XRD patterns and the phase compositions of such clinkers were introduced in Figure 4.3 and Table 4.7, respectively. Reference clinker (N2) was used in the figure (4.3) and table (4.7) for the purpose of comparison with other clinker (N6) regarding to their same calcination conditions.

Qualitative analysis indicates the same minerals formed in N2 and N6 (Figure 4.3). According to the quantitative analysis, N6 had lower ye'elimite content (~10 %) than N2, contrary to the expected phase amounts from Bogue calculations (Table 4.7). On the other hand, the sum of brownmillerite and ye'elimite content of each clinker were approximately same. The higher bauxite and lower gypsum contents of N6 than those of N2 might be the reason for this since the bauxite used also contains medium amounts of iron oxide (~17 %). Increased limestone content might be favored the further complexing of ferric ions with calcium to yield more ferrite phase (brownmillerite) instead of ye'elimite, in the absence of sulfate ions. It can be concluded that, N6 is not preferable due to the increased limestone and bauxite content in its raw meal and has less promising phase composition in terms of strength gain.

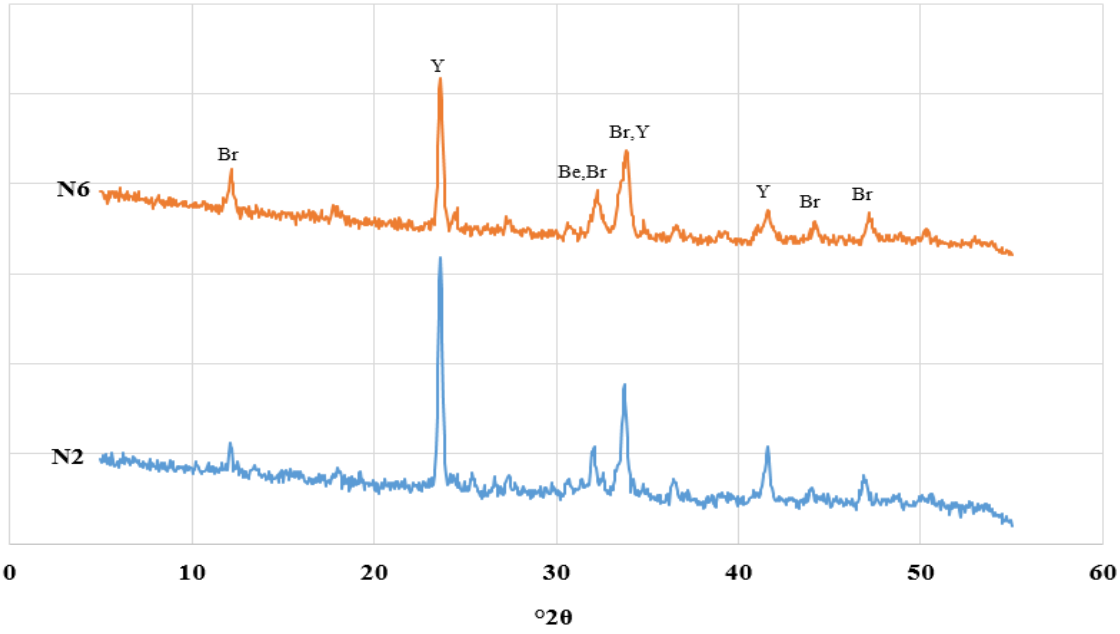

Figure 4.3 X-ray diffractograms for CS̄A clinkers produced by combining only natural materials at different ratios (Legend: Be – Belite; Br – Brownmillerite; Y – Ye'elimite)

Table 4.7 Phase composition of CS̄A clinkers produced by combining only natural materials at different proportions, with agreement factors (R_{wp}) from XRD quantitative analysis

Phase		Amount (%)	
		N2	**N6**
Belite	Bogue	25.2	26.4
	Calculated	14.6	15.4
Brownmillerite ($C_4(A,F)$)	Bogue	26.4	29.2
	Calculated	29.2	39.5
Ye'elimite	Bogue	39.2	43.8
	Calculated	49.1	40.5
Anhydrite	Bogue	8.7	0
	Calculated	1.4	0
Periclase	Bogue	0.7	0.8
	Calculated	0.6	0.4
Free Lime	Bogue	0	0
	Calculated	0.3	0.3
Gehlenite	Calculated	1.7	0.8
Perovskite	Calculated	0.4	1.4
Dolomite	Calculated	1.5	0
Tricalcium aluminate	Calculated	0.2	0
Merwinite	Calculated	1.1	1.9
R_{wp}/%	Calculated	8.5	7.2

4.2 Properties of Clinkers Incorporated with Waste Materials

4.2.1 Physical Properties

Density, fineness and grindability characteristics were investigated for CS̄A clinkers incorporated with waste materials. Table 4.8 gives the densities of these clinkers.

Table 4.8 Density of clinkers incorporated with waste materials

Clinker ID	Density (g/cm^3)
W5FA	3.03
W10RM	3.09
W15RM	3.14
W15RM5FA	3.18
W10RM13.5FA	3.15
W20RM	3.17
W45FA	3.12
W48FA	3.20

It is observed from Table 4.8 that densities of CS̄A clinkers produced with waste materials were higher than the clinkers produced using only natural materials (Table 4.1). Also, increasing waste content in clinker raw meal, especially red mud, corresponded to higher densities. Table 4.9 shows the time of grinding and finenesses achieved for such clinkers.

Table 4.9 Grinding duration and fineness of CS̄A clinkers incorporated with waste materials

Clinker ID	**Weight of Batch (kg)**	**Time of Grinding (minutes)**	**Fineness Achieved (cm^2/g)**
W5FA	3	30	3400
W10RM	3	30	4200
W15RM	3	30	4200
W15RM5FA	3	30	4200
W10RM13.5FA	3	30	4200
W20RM	3	30	4200
W45FA	3	30	3400
W48FA	3	30	3400

From Table 4.9, it can be said that grindability of CS̄A clinkers containing red mud does not change with increasing wastes content in clinker raw mixture. Furthermore, raw mixture proportioning of W5FA slightly differs from that of the reference clinker (Table 4.2), as a result, grindability of such clinkers were estimated to be constant as observed. On the other hand, achieved finenesses of W45FA and W48FA were lower than expected despite their bauxite content being the lowest among all produced clinkers. This is in contrast with the other findings which indicates easier grindability with decreasing bauxite content in the clinker raw mixture.

4.2.2 Chemical Properties

Chemical compositions of CS̄A clinkers containing waste materials is shown in Table 4.10 and Table 4.11 (Two tables were used to demonstrate the results clearly).

Table 4.10 Chemical composition of clinkers incorporated with waste materials (1)

Oxide (%)	Clinker ID			
	W5FA	**W10RM**	**W15RM**	**W15RM5FA**
SiO_2	9.47	9.04	9.19	9.91
Al_2O_3	22.72	21.38	19.53	17.19
Fe_2O_3	8.02	10.33	11.17	10.54
CaO	45.4	44.26	44.34	45.62
MgO	0.84	0.74	0.74	0.83
SO_3	10.82	10.17	10.16	10.78
K_2O	0.36	0.35	0.36	0.39
TiO_2	1.15	1.51	1.63	1.51
Na_2O	0.01	1.26	1.90	1.90
L.O.I (%)	0.8	0.5	0.5	0.8

Table 4.11 Chemical composition of clinkers incorporated with waste materials (2)

Oxide (%)	Clinker ID			
	W10RM13.5FA	**W20RM**	**W45FA**	**W48FA**
SiO_2	11.29	9.32	16.88	17.50
Al_2O_3	17.08	17.65	13.12	13.41
Fe_2O_3	9.30	12.00	6.08	6.25
CaO	46.41	44.32	51.31	51.68
MgO	0.99	0.73	1.61	1.68
SO_3	10.18	10.12	8.89	6.80
K_2O	0.43	0.37	0.63	0.65
TiO_2	1.29	1.75	0.70	0.71
Na_2O	1.29	2.53	0.11	0.11
L.O.I (%)	1.2	0.7	0	0.5

It can be inferred from Table 4.10 and Table 4.11 that, decreasing bauxite content in clinker raw meal resulted in lower Al_2O_3 as expected. Increasing red mud content corresponded to increase in Fe_2O_3. Also, SiO_2 and CaO amounts for such clinkers remained similar except for W45FA and W48FA since the fly ash used has medium amounts of SiO_2 and CaO (~29 %). Alkali content also increased with increasing red mud and fly ash incorporation in clinker raw mixture.

4.2.3 Phase Composition

Calcination parameters (1250 °C / 90 min.) were kept constant during the production of clinkers containing industrial wastes therefore raw mixture proportioning was the only parameter to alter the phase composition of such clinkers. Figure 4.4 and Figure

4.5 present the XRD patterns. Also, Table 4.12 and Table 4.13 give the phase composition of clinkers incorporated with waste materials (Two tables and two figures were used to demonstrate the results clearly).

It was observed from Table 4.12 and Table 4.13 that ye'elimite formed more than expected for all clinkers produced using waste materials. This phenomenon may be related with the incorporation of calcium and sulfate ions, which were expected to form anhydrite (Bogue calculations), with aluminum to yield ye'elimite. Increasing red mud content also increased brownmillerite amount and corresponded to decrease in ye'elimite content which may be promising to compare these phases based on the strength gain of such clinkers (W10RM, W15RM, W20RM). Raw mixture proportions of W45FA and W48FA differed only slightly but the resultant phase composition of such clinkers demonstrated major differences between them. Although, W48FA had slightly higher SiO_2 and CaO amounts than in W45FA, belite content of W45FA was ~5 % higher than W48FA. Silica in W48FA observed to be incorporated for gehlenite formation, in addition to belite. Approximately 5 % gehlenite in W48FA indicated the absence of sulfate ions to form ye'elimite. Free lime looked to be minimized in all clinkers which was an indicator of successful clinkering. Other phases like periclase, perovskite and dolomite were found at minor amounts, but they could not be identified in the XRD patterns.

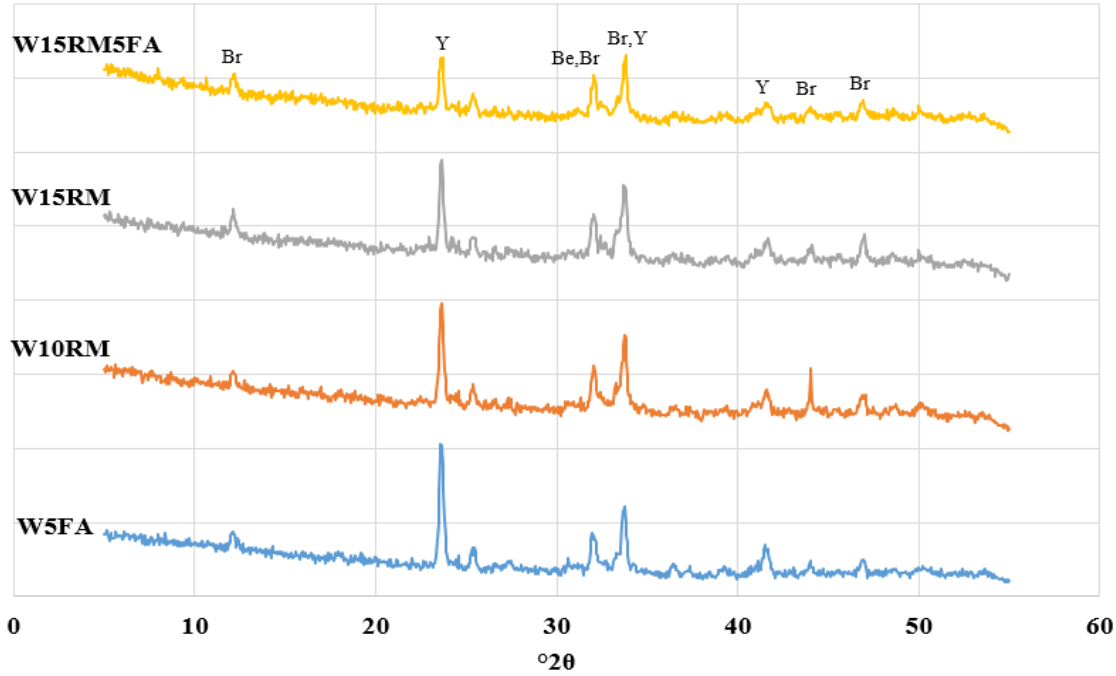

Figure 4.4 X-ray diffractograms for CS̄A clinkers incorporated with waste materials (1) (Legend: Be – Belite; Br – Brownmillerite; Y – Ye'elimite)

Table 4.12 Phase composition of CS̄A clinkers incorporated with waste materials (1), with agreement factors (R_{wp}) from XRD quantitative analysis

Phase		**Amount (%)**			
		W5FA	**W10RM**	**W15RM**	**W15RM5FA**
Belite	Bogue	27.4	26.1	26.5	28.7
	Calculated	21.3	22.5	22.1	29.3
Brownmillerite ($C_4(A,F)$)	Bogue	24.6	31.6	34.2	32.3
	Calculated	27.1	33.7	35.8	33.4
Ye'elimite	Bogue	35.4	29.7	24.9	21.0
	Calculated	41.4	36.5	32.9	28.0
Anhydrite	Bogue	10.7	10.8	11.8	13.8
	Calculated	5.4	1.4	6.2	1.7
Periclase	Bogue	0.9	0.7	0.7	0.8
	Calculated	0.2	0	1.3	1.2
Free Lime	Bogue	0	0	0	0
	Calculated	0.9	0	0	0.4
Gehlenite	Calculated	0	0.9	0.1	1.9
Perovskite	Calculated	0	0.5	0.6	0.7
Dolomite	Calculated	1.8	1.6	0.8	2.9
Tricalcium aluminate	Calculated	0.7	0	0	0.1
Merwinite	Calculated	1.3	3.0	0	0.5
R_{wp}/%	Calculated	8.4	8.2	7.5	7.9

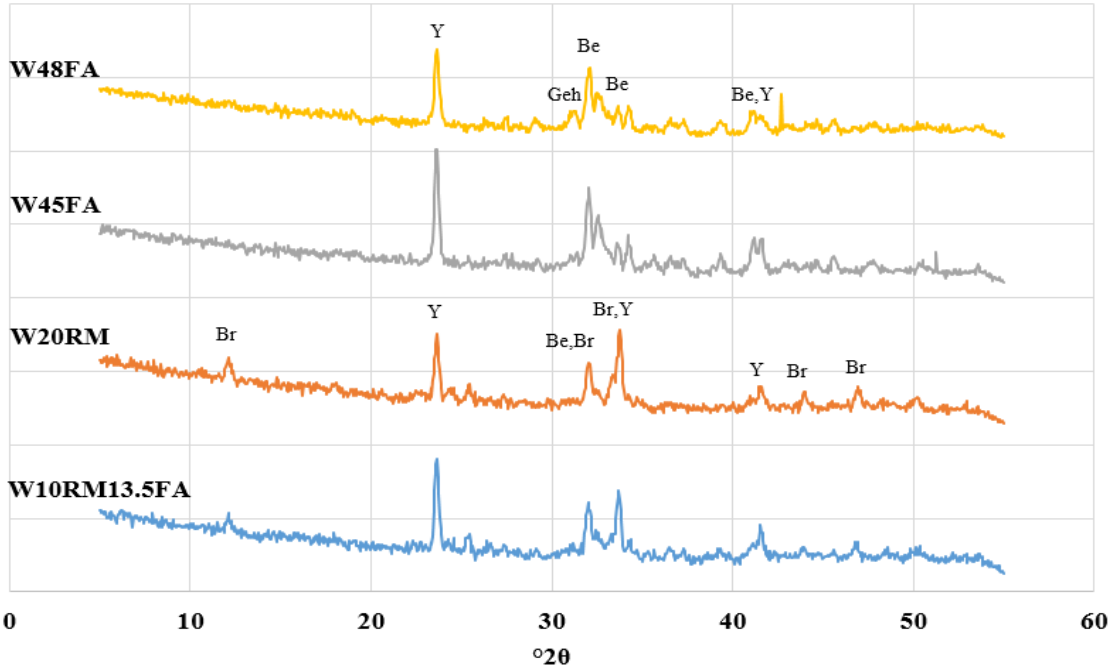

Figure 4.5 X-ray diffractograms for CS̄A clinkers incorporated with waste materials (2) (Legend: Be – Belite; Br – Brownmillerite; Geh – Gehlenite; Y – Ye'elimite)

Table 4.13 Phase composition of CS̄A clinkers incorporated with waste materials (2), with agreement factors (R_{wp}) from XRD quantitative analysis

Phase		Amount (%)			
		W10RM13.5FA	**W20RM**	**W45FA**	**W48FA**
Belite	Bogue	32.8	26.9	48.4	50.4
	Calculated	32.8	20.4	61.3	56.8
Brownmillerite ($C_4(A,F)$)	Bogue	28.6	36.8	18.5	19.1
	Calculated	25.3	42.7	1.7	5.4
Ye'elimite	Bogue	22.5	20.1	18.4	18.9
	Calculated	30.2	24.3	28.2	23.9
Anhydrite	Bogue	12.5	12.9	11.0	7.4
	Calculated	4.2	4.8	1.0	0
Periclase	Bogue	1.0	0.7	1.6	1.7
	Calculated	0.9	0.4	0	0.4
Free Lime	Bogue	0	0	0	0.3
	Calculated	0	0.3	0	0.4
Gehlenite	Calculated	1.0	0	1.3	4.8
Perovskite	Calculated	2.3	0.8	2.9	0.6
Dolomite	Calculated	1.9	1.3	2.3	4.5
Tricalcium aluminate	Calculated	0.8	0.2	1.2	3.0
Merwinite	Calculated	0.9	4.9	0.1	0.3
R_{wp}/%	Calculated	8.0	6.5	8.6	8.8

4.3 Influence of Fineness and Used W/C on the Strength Development of CS̄A cements

Table 4.14 and Table 4.15 show the strength gain of CS̄A cements with two different finenesses prepared with different w/c. Flow of cement mortars is also provided.

Table 4.14 Compressive and flexural strength of mortars containing finer CS̄A clinker (6000 cm^2/g), and gypsum with clinker-to-gypsum ratio of 81:19, at different w/c ratios

W/C	Flexural Strength (MPa)			Compressive Strength (MPa)			Flow (%)
	1 day	7 days	28 days	1 day	7 days	28 days	
0.6	1.5	2.2	1.9	5.8	10.3	12.0	10
0.65	2.3	2.8	2.1	13.4	12.7	19.0	20
0.7	3.5	5.1	4.6	17.8	22.5	28.1	35
0.75	3.4	3.8	3.3	15.9	20.1	24.7	60
0.8	3.1	3.7	3.1	15.6	19.2	22.6	75

Table 4.15 Compressive and flexural strength of mortars containing coarser CS̄A clinker (3000 cm^2/g), and gypsum with clinker-to-gypsum ratio of 81:19, at different w/c ratios

W/C	Flexural Strength (MPa)			Compressive Strength (MPa)			Flow (%)
	1 day	7 days	28 days	1 day	7 days	28 days	
0.6	2.2	3.3	1.9	8.5	15.7	10.8	20
0.65	2.6	3.7	2.1	15.0	23	25.8	35
0.7	3.8	4.3	4.6	17.3	23.5	20.2	55
0.75	3.4	4.0	3.3	16.5	21.1	21.5	80
0.8	3.1	3.6	3.1	13.4	19.3	19.8	95

The great water demand of CS̄A clinker, mainly due to ettringite formation, leads to flow and compaction problems. The optimum flow of 110 ± 5 % as stated in ASTM C 109 (2016), could not be reached even when a w/c of 0.8 was used, as shown in Table 4.14 and Table 4.15. Regarding the maximum 28-day compressive strengths achieved for two CS̄A cements with different finenesses, the main strength gain was achieved in the first 7 days. However, finer CS̄A cement gained its ~80 % of compressive strength at 7 days (22.5 MPa-of-28.1 MPa) which was approximately 8 % lower than that of coarser cement (23 MPa-of-25.8 MPa) and the same trend was

effective for every w/c used. This is related with the longer hydration period of the finer clinker and its better strength performance than the coarser CS̄A clinker in terms of strength gain. However, producing CS̄A clinker with high fineness demands longer grinding durations and greater energy expenditure and cost. Also, difference between the highest 28-day compressive strengths of the two clinkers was not great. It can be concluded that, clinker fineness was not a significant parameter and other parameters that may affect strength gain need to be investigated. In further investigations, a w/c of 0.7 was constantly used when citric acid was not added into clinker paste, to achieve adequate flow while also considering strength gain at the same time.

4.4 Influence of Calcination Parameters on the Properties of CS̄A Cement

4.4.1 Strength Development

Mixture parameters used for this study was given at Table 3.7. Table 4.16 gives the strength development of CS̄A cements produced at different kiln temperatures but with constant residence times.

Although XRD quantitative analysis indicates lower ye'elimite content for N4 (Table 4.5), the strength gains of N2 and N4 were similar. This may be related with the same amount of gypsum having been added to each clinker, to consume ye'elimite in the course of the ettringite formation. Also, the flows of the cement mortars were similar (~65 %), therefore it cannot be considered as a critical parameter for the strength development of these cements.

Table 4.16 Compressive and flexural strength of CS̄A cement mortars made of clinkers produced at different kiln temperatures with a clinker-to gypsum ratio of 81:19

Clinker	Flexural Strength (MPa)				Compressive Strength (MPa)			
	1 day	3 days	7 days	28 days	1 day	3 days	7 days	28 days
N2	4.5	4.7	4.9	5.9	18.6	21.2	21.8	23.2
N4	4.2	4.5	4.9	5.0	18.3	20.1	20.8	23.1

Table 4.17 shows the strength development of CS̄A cements produced at constant kiln temperature but with different residence times.

N1 gained the highest compressive strength at 28 days even though they had similar phase composition (Table 4.6) and almost identical ye'elimite content. The difference between the strengths of cements may be related to the varied reactivities of clinker phases, especially ye'elimite. Also, the flows of cement mortars were close to each other (~65 %) due to the constant amount of gypsum added to the system (19 %).

Table 4.17 Compressive and flexural strength of CS̄A cement mortars made of clinkers produced at various kiln residence times with a clinker-to gypsum ratio of 81:19

Clinker	**Flexural Strength (MPa)**				**Compressive Strength (MPa)**			
	1 day	**3 days**	**7 days**	**28 days**	**1 day**	**3 days**	**7 days**	**28 days**
N1	4.2	4.3	5.3	4.9	20.5	20.7	24.6	27.4
N2	4.5	4.7	4.9	5.9	18.6	21.2	21.8	23.2
N3	4	4.8	4.5	5.8	19.7	22.5	24.0	25.6

Figure 4.6 demonstrates the compressive strength development of CS̄A cements containing same amount of gypsum (19 %) but produced under different calcination conditions.

It can be seen in Figure 4.6 that any significant difference between compressive strengths of these cements was not observed at early ages. However, N1 gained 2-4 MPa higher 28-day compressive strength than the others. Still, compressive strengths were lower when compared to the other studies (Quillin, 2001; Glasser and Zhang, 2001; Pera and Ambroise, 2004), probably due to the high w/c used. It can be concluded that clinker production at 1250 °C for 90 minutes can be preferable for the further clinker productions regarding the environmental and economic considerations.

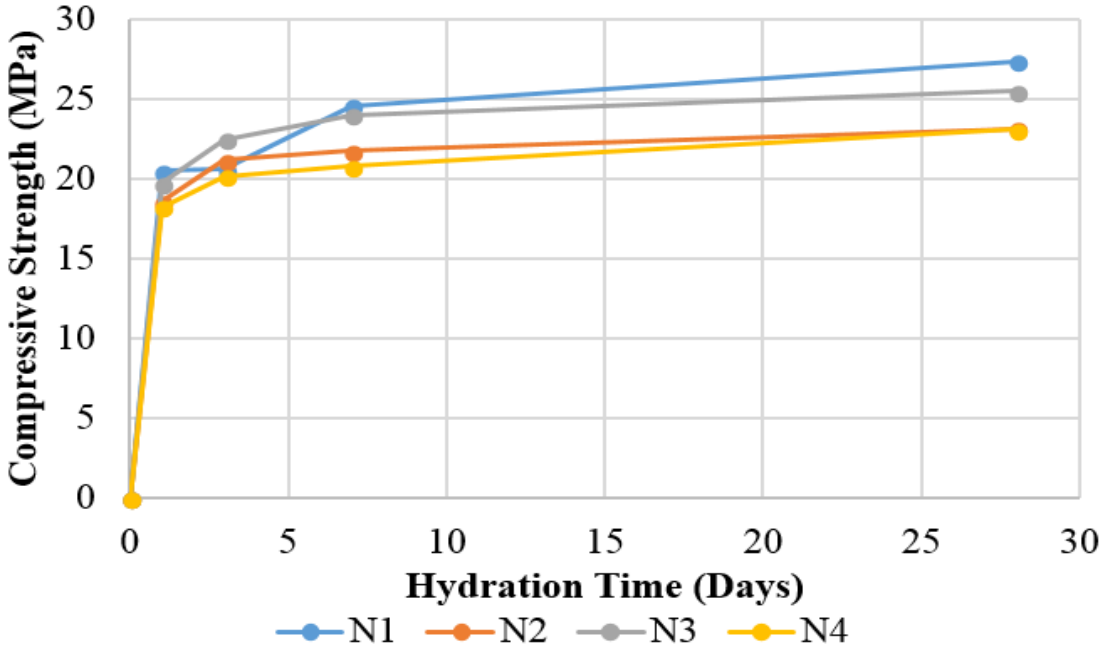

Figure 4.6 Compressive strength development of CS̄A cement mortars made of clinkers produced at different kiln temperatures and residence times with clinker-to gypsum ratio of 81:19

4.4.2 X-ray diffraction

Figure 4.7 displays the XRD pattern of the reference cement paste containing 19 % added gypsum, at various hydration times.

It is observed in Figure 4.7 that, the main minerals formed during the hydration of the reference CS̄A cement were ettringite and gypsum. Most of the ye'elimite consumption (~65 %) and ettringite formation occurred up to 3 days which was also compatible with the strength development of this cement. Contrary to the results of Glasser and Zhang (2001), gypsum was detected even after 28 days of hydration. This observation may be related with the formation of amorphous AH_3 which is able to coat the surfaces of clinker and to impede the hydration of cement (Chang et al., 2017), or the hindered mobility of ions within the system (Hargis et al., 2014). Particle size of the clinker and the low reactivity of gypsum used might be the other reasons. Furthermore, the presence of gypsum at later ages is a potential durability problem such as delayed ettringite formation occurred from the reaction of gypsum with monosulfate phase. However, monosulfate cannot be identified in the XRD patterns due to its poorly crystalline form. Nevertheless, monosulfate can be identified with

calorimetry and thermal analyses if it formed during the hydration of reference cement. Also, belite and brownmillerite were observed not to react until 28 days of hydration.

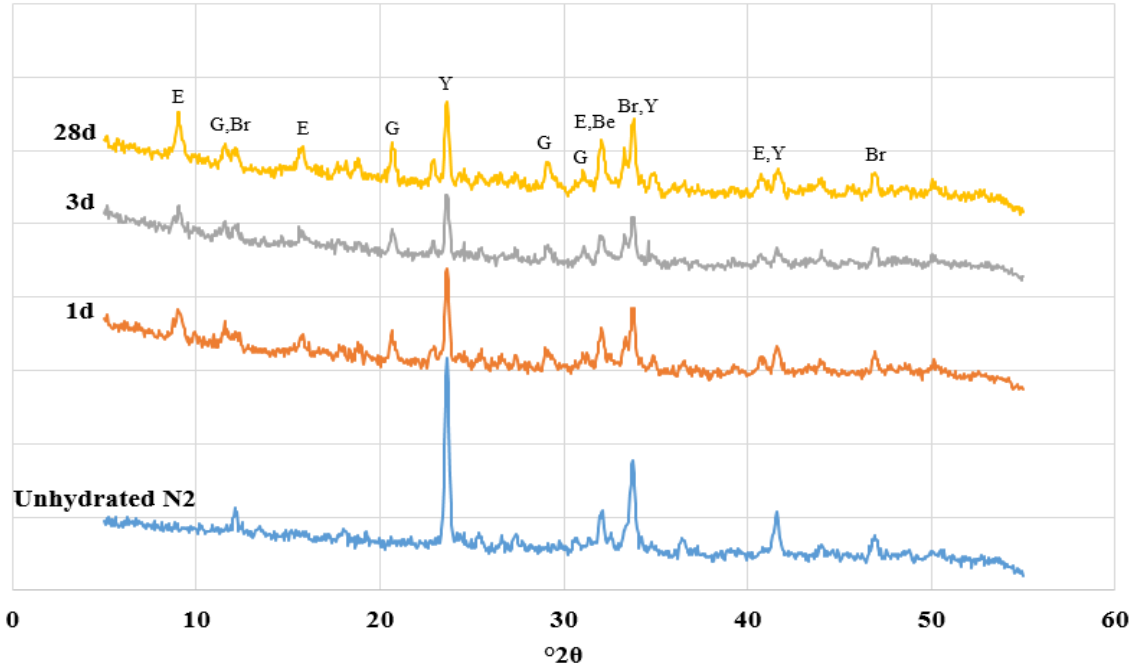

Figure 4.7 XRD patterns of reference cement paste with clinker-to-gypsum ratio of 81:19, at 1, 3 and 28 days of hydration (Legend: Be – Belite; Br – Brownmillerite; E – Ettringite; G – Gypsum; Y – Ye'elimite)

Minerals to be formed from the hydration reactions were expected to be similar among CS̄A cements produced under different calcination conditions using same raw mixture proportioning. Yet, hydration product development of such pastes at various hydration times, was investigated in Figure 4.8 to observe any difference. The XRD pattern of the unhydrated reference clinker (N2) is also shown in Figure 4.8 to compare the changes of the peak intensities of minerals, during the hydration.

As expected, no difference was observed between the minerals formed from the hydration of these CS̄A pastes. Also, most of the ettringite formation, which is the strength giving phase of CS̄A cements, was realized up to 3 days of hydration for each clinker and was compatible with their strength development except for N5 whose strength gain could not be determined as mentioned in Section 4.1.3.1.

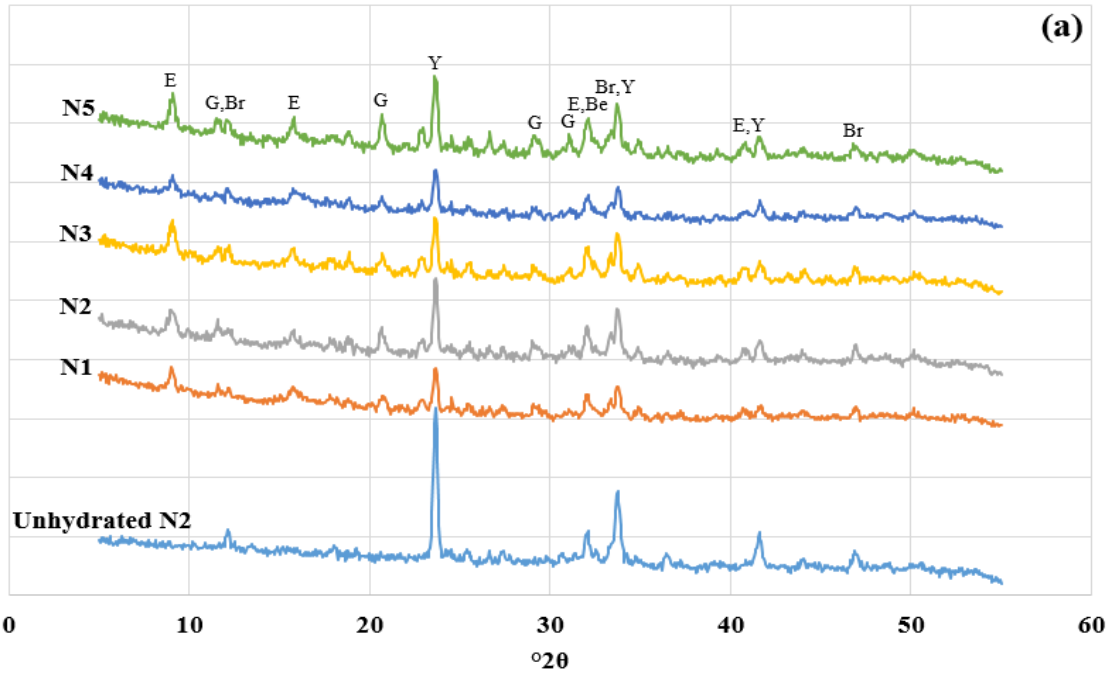
(a)
E
G,Br
E
G
Y
G
G
E,Be
Br,Y
E,Y
Br
N5
N4
N3
N2
N1
Unhydrated N2
0
10
20
30
40
50
60
°2θ

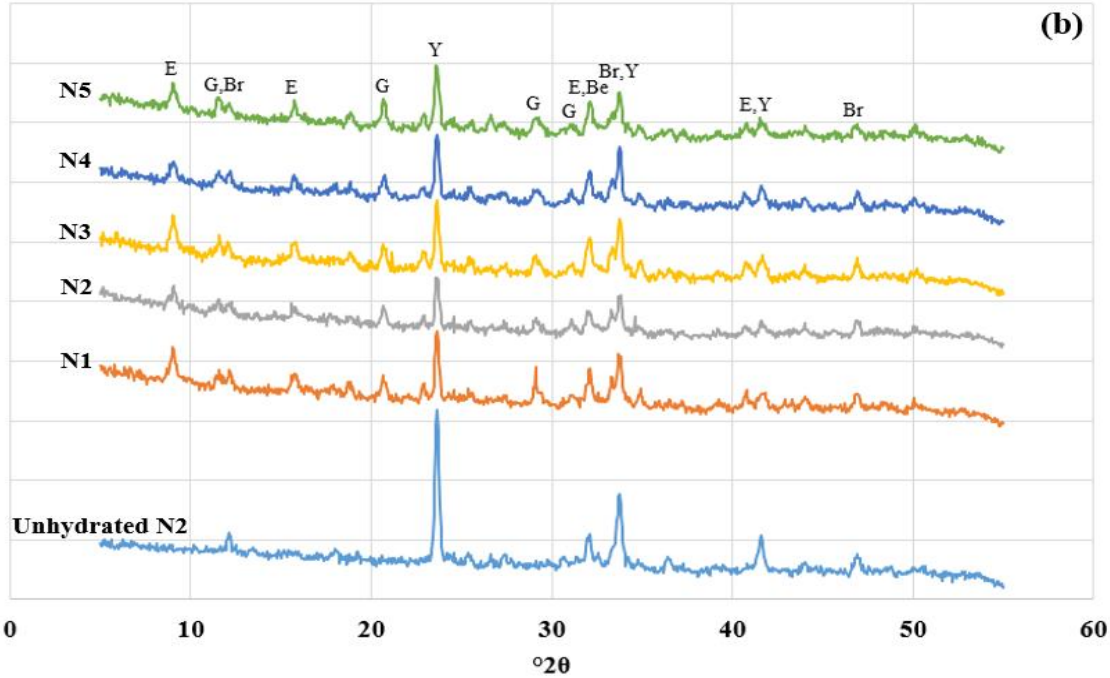
(b)
E
G,Br
E
G
Y
G
G
E,Be
Br,Y
E,Y
Br
N5
N4
N3
N2
N1
Unhydrated N2
0
10
20
30
40
50
60
°2θ

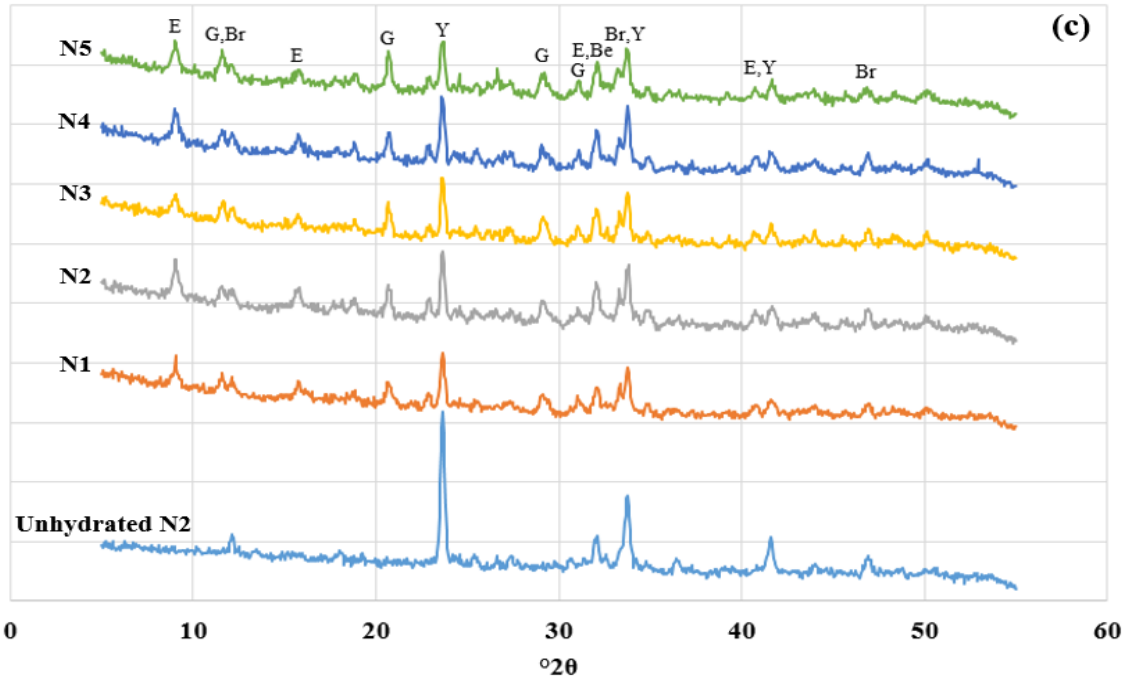

Figure 4.8 XRD patterns of cement pastes containing CS̄A clinkers, produced under different calcination conditions, and gypsum with clinker-to-gypsum ratio of 81:19, a) 1 d; b) 3 d; c) 28 d (Legend: Be – Belite; Br – Brownmillerite; E – Ettringite; G – Gypsum; Y – Ye'elimite)

4.4.3 Isothermal Calorimetry

Rate of heat evolution and cumulative heat release of the CS̄A cement pastes consisting of clinkers produced at different kiln conditions are shown in Figure 4.9 and Figure 4.10, respectively.

Figure 4.9 indicates very short induction periods (~1h). The first peak of all pastes comes from the initial wetting and early reactions such as the conversion of hemihydrate to dihydrate. The second peak after the dormant period shows the ettringite formation from the reaction of ye'elimite and calcium sulfate (Eqn. 10). Total heat productions of these CS̄A cements were lower than that of typical OPC (300-400 J/g). Strength gain of pastes (Figure 4.6) are compatible with their cumulative heat evolution (Figure 4.10). N1 and N3 which have similar compressive strengths also have closer total heat evolved. Furthermore, N2 and N4 which exhibited almost same strength gain, but lower strengths than that of others (N1 and N3), also evolved lower total heat. On the other hand, clinker produced at 1350 °C (N5) evolved the highest cumulative heat among others. Therefore, it can be inferred that if

sufficient amounts of N5 could be produced to observe its strength gain, N5 could yield the highest compressive strength among others, at 28 days.

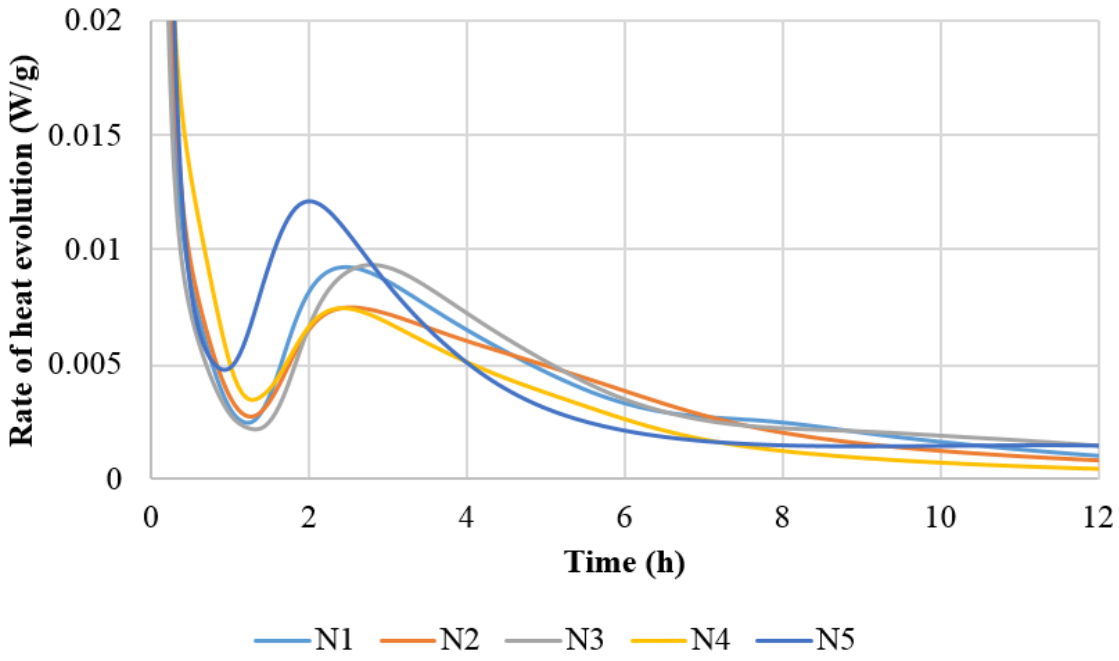

Figure 4.9 Rate of heat evolution for cement pastes containing CS̄A clinkers, produced under different calcination conditions, and gypsum with clinker-to-gypsum ratio of 81:19

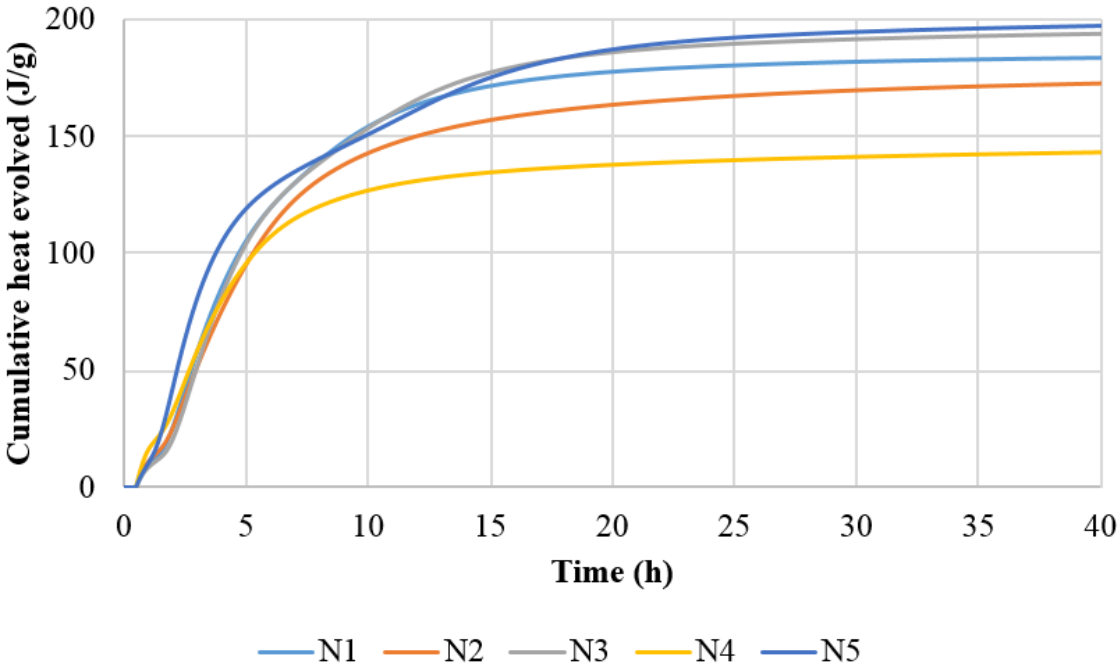

Figure 4.10 Cumulative heat evolved for cement pastes containing CS̄A clinkers, produced under different calcination conditions, and gypsum with clinker-to-gypsum ratio of 81:19

4.4.4 Thermal Analysis

Figure 4.11 and Figure 4.12 displays the thermal analyses of the reference cement paste at 3 and 28 days of hydration.

Weight loss between 80-150 °C can be attributed to the decomposition of ettringite. Decomposition of gypsum to anhydrite occured at 100-160 °C (Winnefeld and Barlag, 2010; Hargis et al., 2014). Also, AH_3 phase which was expected to form simultaneously with ettringite (Eqn. (10), (12), (13), (14), (15), (17)) but not observed in XRD patterns mainly due to its amorphous form, is identified at the weight loss between 250-280 °C (Winnefeld and Lothenbach, 2010; Winnefeld and Barlag, 2010; Hargis et al., 2014). As expected, traces of portlandite, which has a characteristic weight loss at around 450 °C (Scrievener et al., 2016b), could not be found in the TGA analyses. Continuous weight loss up to 600 °C can also be related with some amorphous hydration products and C-S-H formed (Nedeljkovic et al., 2016; Scrivener et al., 2016b). These hydration products could not be identified with XRD analyses probably due to their amorphous nature or their too low quantities to be detected. Absence of portlandite may stem from the relatively slow hydration of belite. Weight loss at around 700 °C indicates the presence of calcite in the cement paste. However, calcite could not be clearly detected by XRD as its main peak may be overlapped with one of gypsum (29-30 °2θ). It was also observed that with ongoing hydration, the amount of ettringite decreased while the amounts of gypsum, AH_3 and calcite increased in the reference cement paste even though such reduction for ettringite content was not observed at the XRD patterns. This phenomenon indicates the carbonation of ettringite via the Equation (24) resulting in the formation of calcium carbonate, calcium sulfate and aluminum hydroxide.

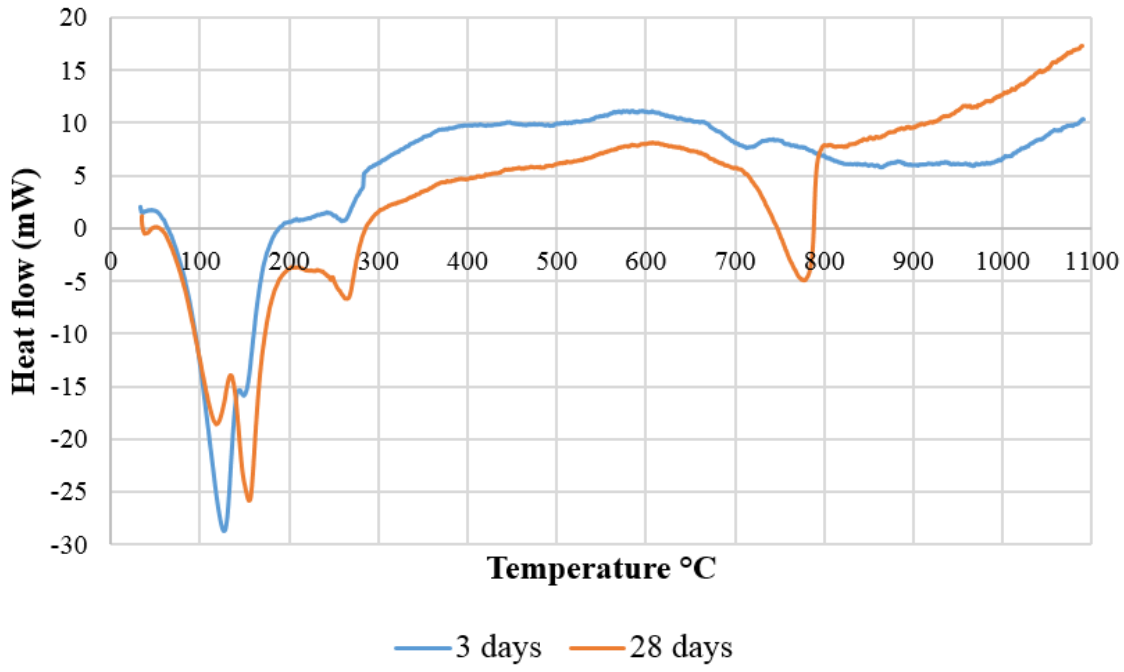

Figure 4.11 Heat flow of reference cement paste at 3 and 28 days of hydration

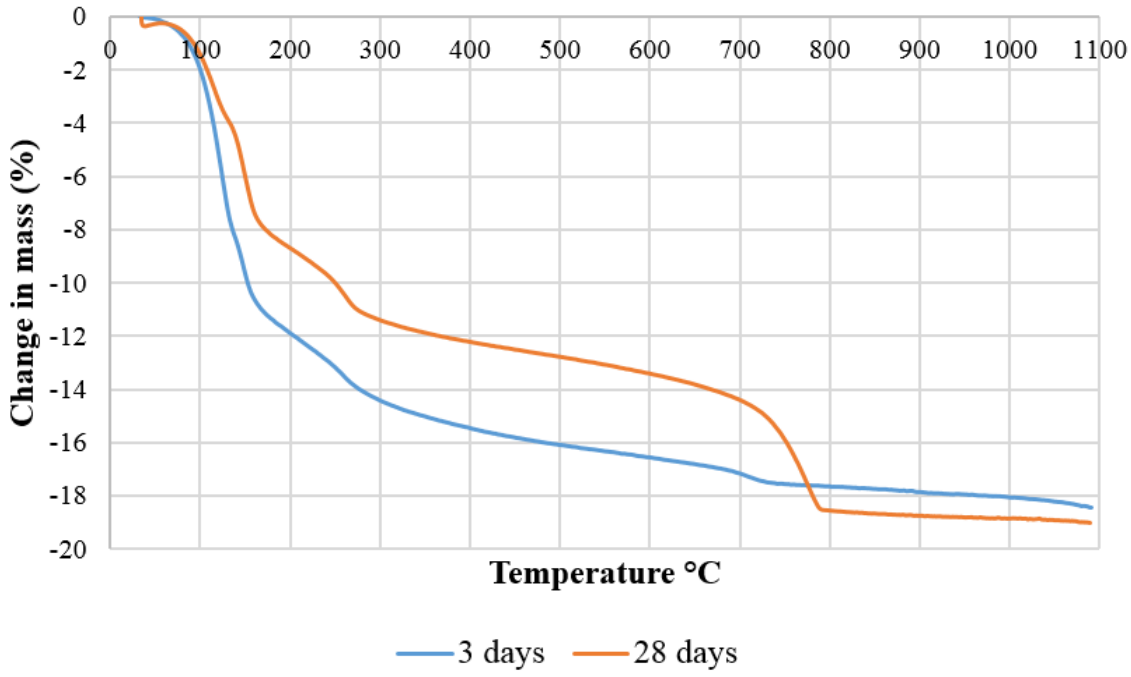

Figure 4.12 Mass loss of reference cement paste at 3 and 28 days of hydration

Figure 4.13 and Figure 4.14 comparatively shows the heat flow and mass loss of pastes containing CS̄A clinkers produced under different calcination conditions, and gypsum with constant clinker-to-gypsum ratio of 81:19, at 3 and 28 days of hydration, respectively.

Minerals formed within such pastes were similar and these main hydration products were, ettringite (weight loss between 80-150 °C), gypsum (weight loss between 100-160 °C), AH_3 (weight loss between 250-280 °C) and calcite (weight loss at around 700 °C). However, amount of ettringite formed in N1 was higher than in others at 28 days according to Figure 4.13 and Figure 4.14. It was observed that mass loss up to 150 °C for N1 corresponded to ~40 % of its total mass loss while other pastes underwent ~25 % mass loss within the same temperature range (Figure 4.14b). This observation is a good indicator of the difference between the amount of ettringite formed in such pastes therefore the differences between their strength developments which was provided in Figure 4.6 showing that N1 gained the highest compressive strength among others at 28 days. On the other hand, carbonation of ettringite for all pastes was also observed which corresponded to the increasing amounts of AH_3, gypsum and calcite. Shifting of the calcite peak (s) from 700 °C to 800 °C during hydration (Figure 4.13) can be related with its increasing amount (Scrivener et al., 2016b).

Mass loss from bound water in cement pastes is generally realized up to 600 °C whereas mass loss between 600-1100 °C is associated with the decarbonation of minerals present while the pore water is evaporating below 105 °C (Scrivener et al., 2016b). However, in hydrated C$\bar{S}$A cements, mass loss below <105 °C cannot be ascribed only to pore water since ettringite, C-S-H, monosulfate and gypsum may start losing their bonded water below 105 °C. Also, it should be emphasized that bound water in C$\bar{S}$A systems is mainly attributed to the formation of ettringite which can bind 32 moles of water. Therefore, demonstrating the mass loss of C$\bar{S}$A pastes separately, as loss of water (H_2O) and loss of CO_2 could be useful to predict bound water in phases formed and to observe the changes (relative proportions by mass) of hydration products with ongoing hydration.

Table 4.18 shows the relative proportions of loss of water, up to 600 °C, and loss of CO_2, between 600-1100 °C, in total mass loss of C$\bar{S}$A cement pastes whose clinkers produced under different calcination conditions but blending with the constant amount of gypsum (19 %), at 3 and 28 days of hydration. Considering the difference of mass loss from pore water (up to 105 °C) was not great for these pastes, results given in Table 4.18 could be useful to evaluate the changing in relative proportions of the hydrated phases to the carbonated ones.

Although any comments about the quantities of hydration products formed cannot be made directly from Table 4.18, it was clearly observed that for all cement pastes, the relative proportion of the hydrate phases in the cement matrix decreased while the carbonated hydration products, mainly calcite, increased with ongoing hydration. However, strength development of mortars consisting of these cement pastes (Figure 4.6) was not affected from such phenomenon as they gained strength up to 28 days. Yet, reinforcement corrosion in concretes consisting of such cements could occur because of the reduced pH in cement matrix, the investigation of which was not a part of this study.

Table 4.18 Calculated loss of water and CO_2 for cement pastes containing $C\bar{S}A$ clinkers, produced under different calcination conditions, and gypsum with clinker-to-gypsum ratio of 81:19, at 3 and 28 days of hydration, as % of their total mass loss

Clinker ID	**Loss of H_2O (%)**		**Loss of CO_2 (%)**	
	3 days	**28 days**	**3 days**	**28 days**
N1	91.4	78.1	8.6	21.9
N2	89.8	70.5	10.2	29.5
N3	91.4	67.3	8.6	32.7
N4	79.7	69.1	20.3	30.9
N5	87.2	67.5	12.8	32.5

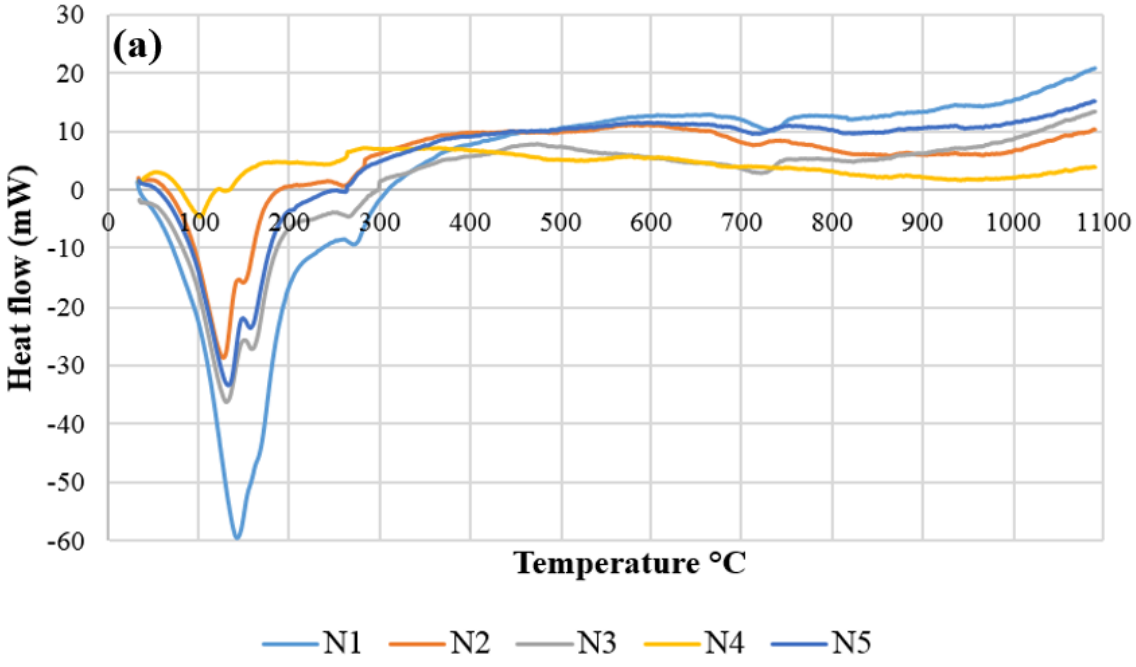

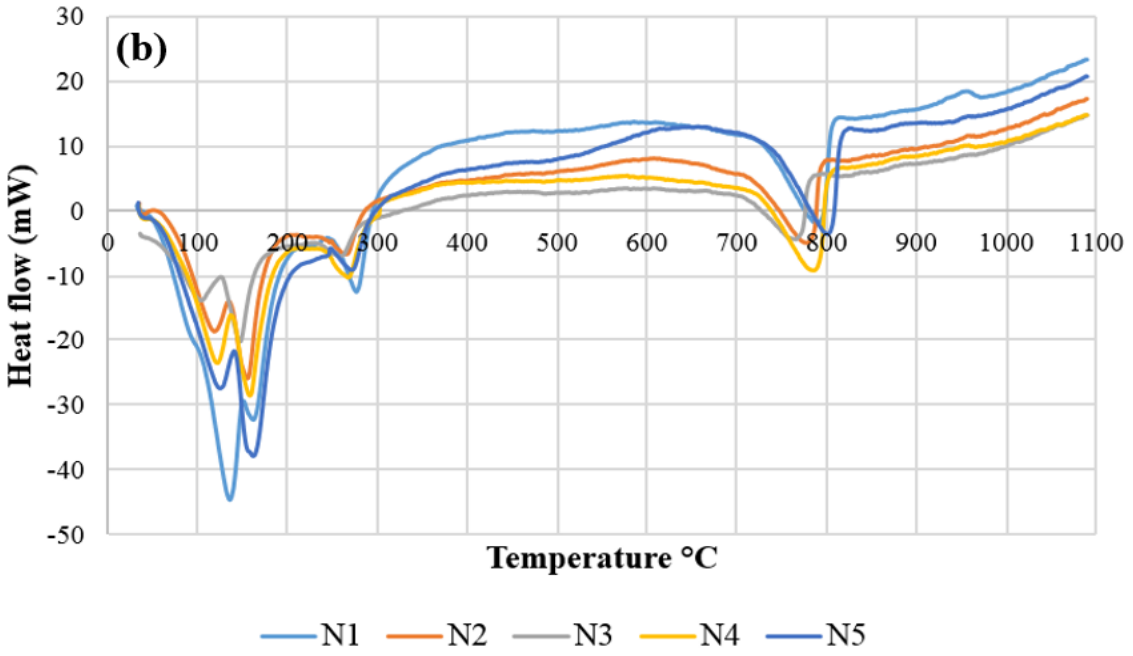

Figure 4.13 Heat flow of cement pastes containing CS̄A clinkers, produced under different calcination conditions, and gypsum with clinker-to-gypsum ratio of 81:19, a) 3 days of hydration; b) 28 days of hydration

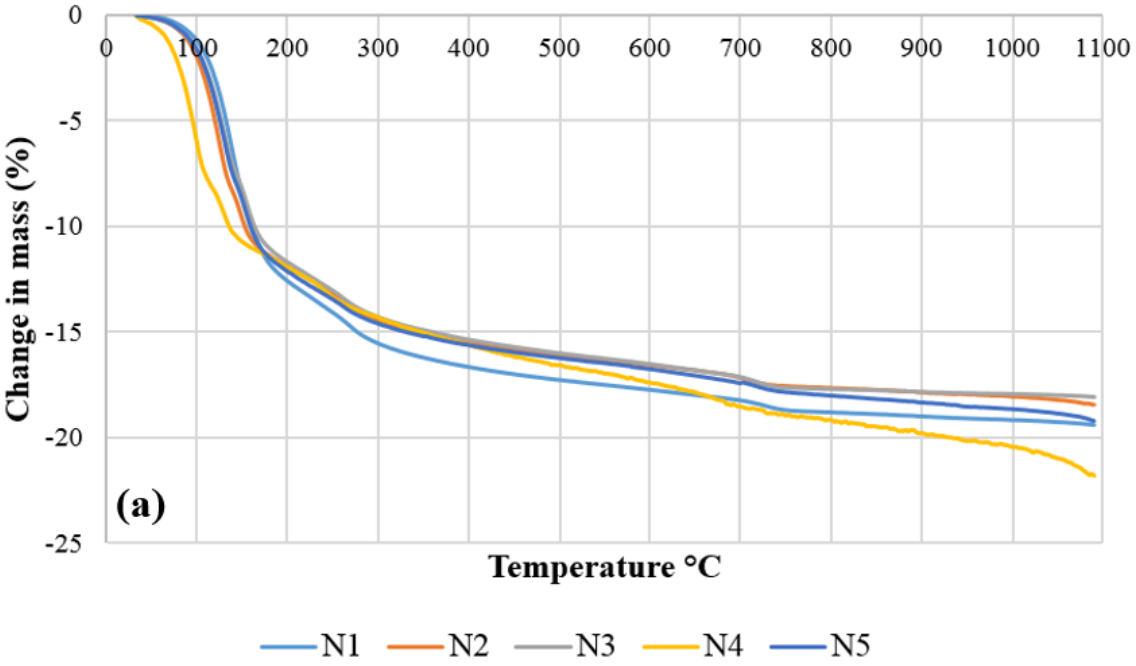

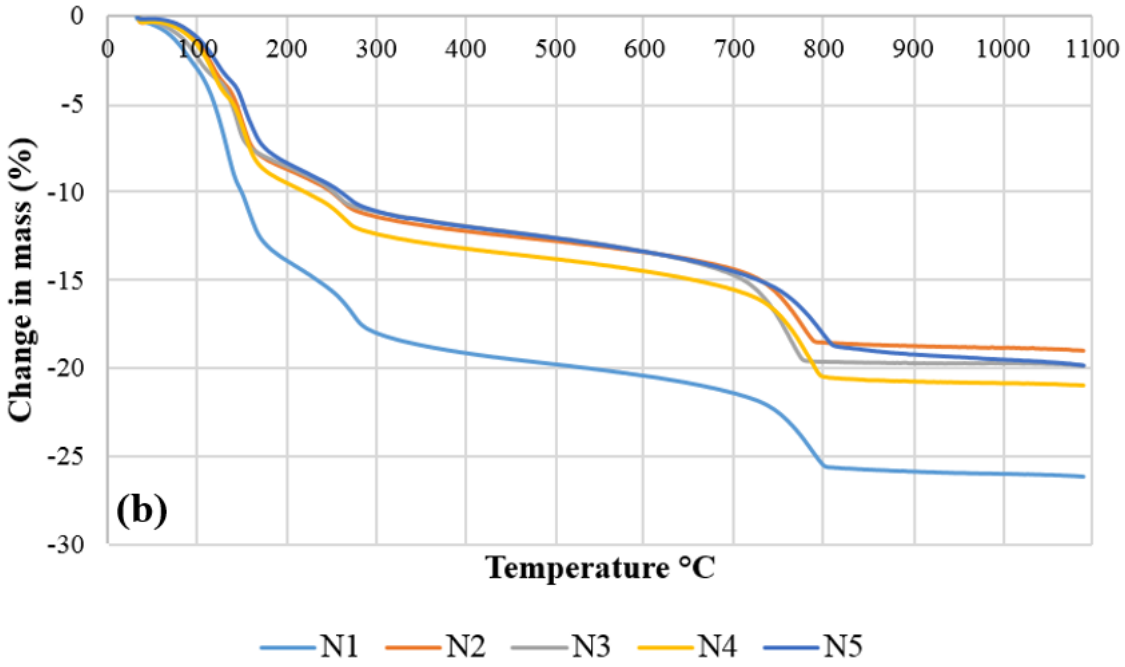

Figure 4.14 Mass loss of cement pastes containing C$\bar{S}$A clinkers, produced under different calcination conditions, and gypsum with clinker-to-gypsum ratio of 81:19, a) 3 days of hydration; b) 28 days of hydration

4.5 Influence of Clinker Raw Mixture Proportioning Using Only Natural Materials and Added Gypsum Amount on the Properties of C$\bar{S}$A Cement

4.5.1 Strength Development

Table 3.8 shows the mixture design for the investigation of added gypsum amount on the strength gain of N2 and N6. Table 4.19 and Table 4.20 introduces the strength results for N2 and N6 with different amounts of added gypsum, respectively. Also, Table 4.21 shows the flow of cement mortars for such.

Both Table 4.19 and Table 4.20 shows that maximum compressive strength at 28 days was achieved for the mixtures containing highest amount of gypsum (24 %) and major part of the strength was achieved up to 3 days (> 80 %). High gypsum content in the cements is also preferable in terms of economic and ecological considerations since it reduces the amount of clinkers in the system. However, Table 4.19 and Table 4.20 also shows that C$\bar{S}$A cement containing the lowest amount of added gypsum (14 %) gained higher compressive strength at 28 days than the cement containing 19 % added gypsum. The reason for this might be that the highest flow was attained for mortars

containing the lowest amount of gypsum (Table 4.21), which indicates that improvement for the compaction of mortars may outweigh the chemical parameters to impact strength gain of CS̄A cements, to some extent. Therefore, increasing gypsum content to greater than 24 % in CS̄A cements was not considered due to the flow concerns.

Table 4.19 Strength development of CS̄A cement mortars consisting of N2 and different amounts of added gypsum with clinker-to-gypsum ratios of 86:14, 81:19, 76:24

Added Gypsum Amount (%)	Flexural Strength (MPa)				Compressive Strength (MPa)			
	1 day	3 days	7 days	28 days	1 day	3 days	7 days	28 days
14	4.8	5.1	4.9	4.5	17.9	21.1	21.7	25.4
19	4.5	4.7	4.9	5.9	18.6	21.2	21.8	23.2
24	3.7	4.8	4.8	5.2	19.0	26.9	27.6	30.9

Table 4.20 Strength development of CS̄A cement mortars consisting of N6 and different amounts of added gypsum with clinker-to-gypsum ratios of 86:14, 81:19, 76:24

Added Gypsum Amount (%)	Flexural Strength (MPa)				Compressive Strength (MPa)			
	1 day	3 days	7 days	28 days	1 day	3 days	7 days	28 days
14	3.2	4.2	4.5	6.3	15.3	18.1	21.1	24.4
19	3.2	4.1	4.8	4.7	15.5	20.3	20.7	21.8
24	3.4	4.9	4.6	6.2	18.8	24.1	20.8	29.3

Table 4.21 Flow of CS̄A cement mortars consisting of clinkers named N6 and N2 and different amounts of added gypsum with clinker-to-gypsum ratios of 86:14, 81:19, 76:24

Added Gypsum Amount (%)	Flow (%)	
	N2	N6
14	93	90
19	65	80
24	55	50

Figure 4.15 comparatively demonstrates the compressive development of CS̄A cement mortars consisting of clinkers N2 and N6, with different amounts of added gypsum. The higher ye'elimite content in N2 (~10 %) than in N6, may have resulted the

difference between 1-day compressive strengths of N2 and N6 even though both clinkers achieved closer 28-day compressive strengths.

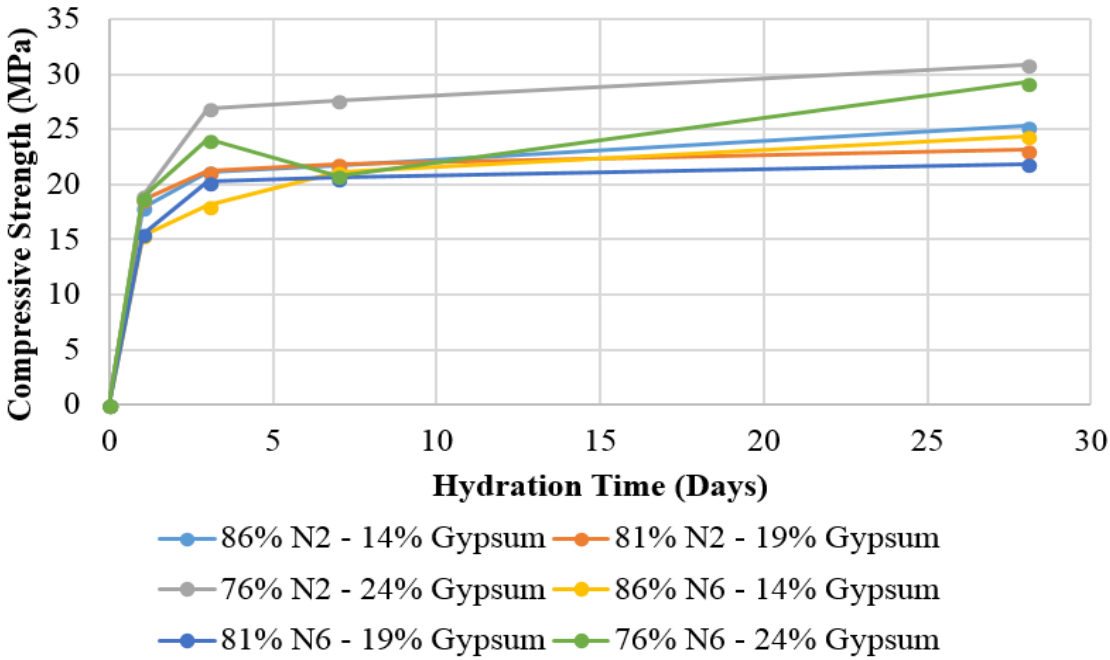

Figure 4.15 Compressive strength development of CS̄A cement mortars made of clinkers, N2 and N6, and gypsum with clinker-to gypsum ratios of 86:14, 81:19, 76:24

4.5.2 X-ray diffraction

Figure 4.16 and Figure 4.17 demonstrate the hydration product development of N2 and N6 with different amounts of added gypsum at 28 days, respectively.

It was observed from both figures that the peak intensities of the remaining gypsum increased with increasing added gypsum (14 % to 24 %). Also, for N2 (Figure 4.16), amount of the ettringite (main peak at ~9.1 °2θ) decreased with increasing gypsum (19 % to 24 %) which may be related with the dilution of CS̄A clinker in cement paste. Further studies like TGA can elucidate such phenomenon. However, such a decrease is not coherent with the strength development of N2 since ettringite is the strength-giving phase and is expected to be present at maximum amount for 24 % mass of gypsum added system. On the other hand, reduction for ettringite content with increasing amounts of added gypsum like N2, was not observed at the XRD patterns of N6 (Figure 4.17). However, minerals formed during the hydration were same (gypsum and ettringite) for both clinkers as expected. Also, belite and brownmillerite

were not reacting up to 28 days and not effected from the different amounts of added gypsum in clinker pastes.

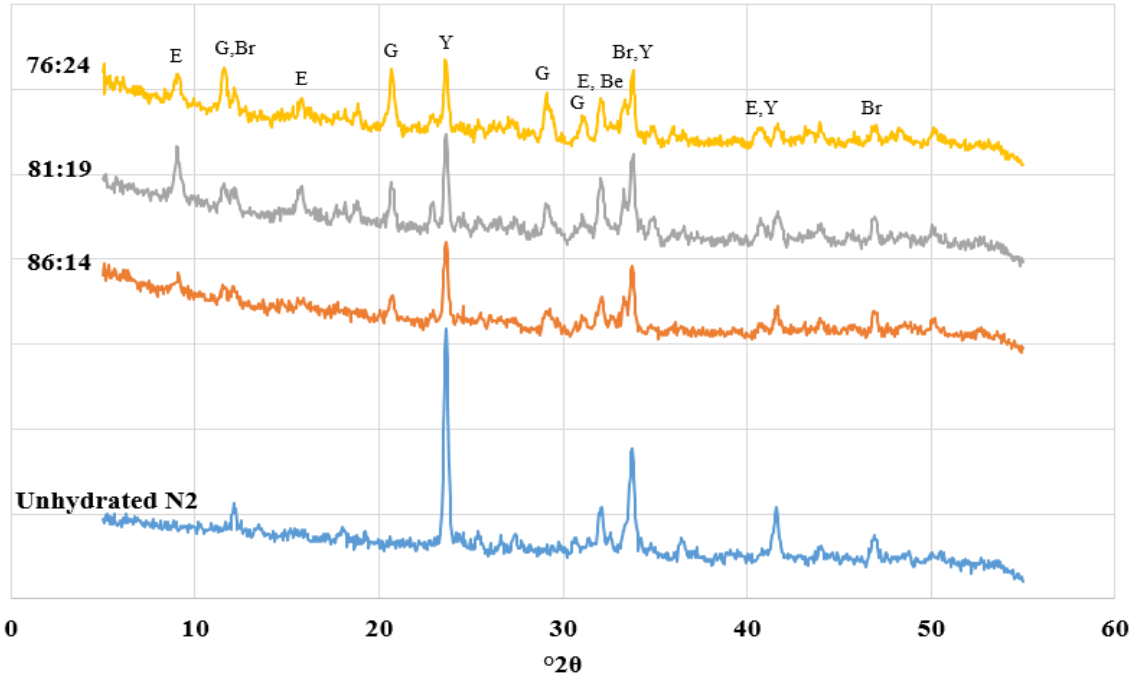

Figure 4.16 XRD patterns of cement pastes containing N2 and gypsum with clinker-to-gypsum ratios of 86:14, 81:19, 76:24 at 28 days of hydration (Legend: Be – Belite; Br – Brownmillerite; E – Ettringite; G – Gypsum; Y – Ye'elimite)

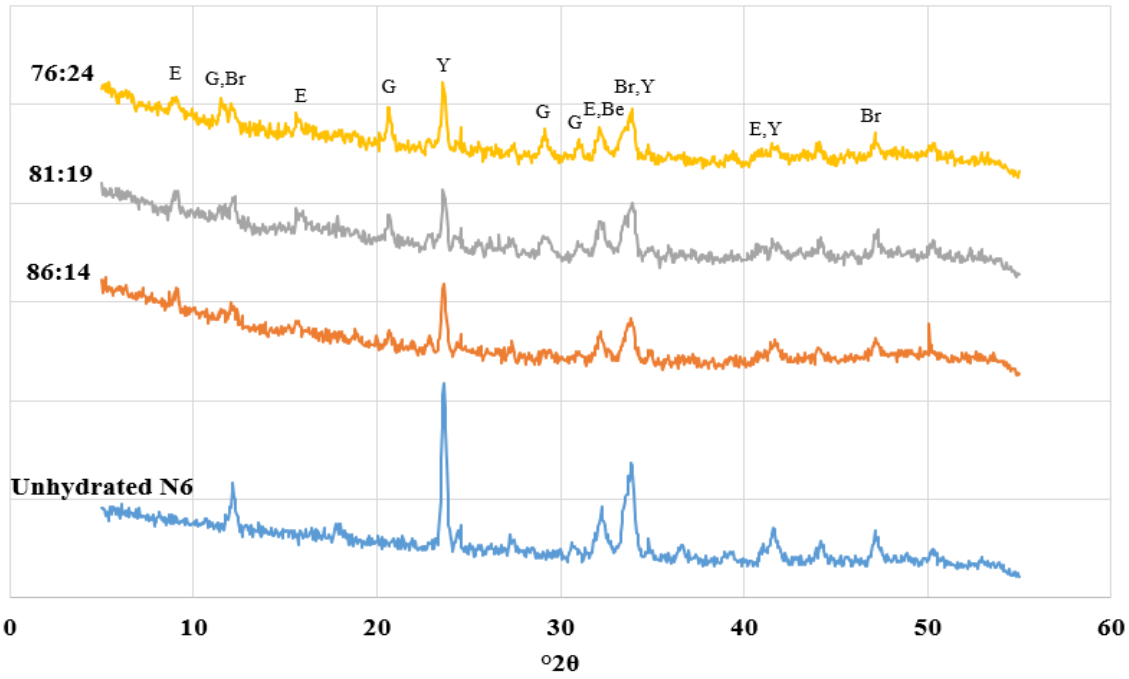

Figure 4.17 XRD patterns of cement pastes containing N6 and gypsum with clinker-to-gypsum ratios of 86:14, 81:19, 76:24 at 28 days of hydration (Legend: Be – Belite; Br – Brownmillerite; E – Ettringite; G – Gypsum; Y – Ye'elimite)

4.5.3 Isothermal Calorimetry

Figure 4.18 and Figure 4.19 shows the rate of heat evolution and cumulative heat evolution of N2 with different amounts of added gypsum, respectively.

The long induction period (~10h) of pure N2 (100:0) is compatible with the findings of Winnefeld and Barlag (2010) which was attributed to the coating of clinker particles by the rapidly forming hydration products. The peak after the dormant period of pure N2 can be referred to ettringite formation from below equation (25):

$$4C_4A_3\bar{S} + 80H \rightarrow C_6A\bar{S}_3H_{32} + C_4A\bar{S}H_{12} + 2C_3AH_6 + 8AH_3 \quad (25)$$

Furthermore, replacement of gypsum with the C$\bar{S}$A clinker caused a significant decrease for the induction period, from ~10h to ~1h. It is generally accepted that, the first peak after the dormant period corresponds to ettringite and AH_3 formation (Eqn. 10) and the second maximum or shoulder indicates the formation of monosulfate (Eqn. (12) and (13)), from the consumption of gypsum (Martin-Sedeňo et al., 2010; Winnefeld and Barlag, 2010; Chen and Juenger, 2012). Only the clinker paste containing 14 % gypsum showed a secondary peak after the main heat evolution which could indicate the possible monosulfate formation that could not be identified with XRD analysis (Figure 4.16). Pure clinker paste demonstrated the highest cumulative heat evolved which was approximately 250 J/g. However, dilution of C$\bar{S}$A clinker with gypsum reduced the cumulative heat evolution between the range of 70-80 J/g for such pastes. Clinker paste containing 24 % gypsum produced approximately 15 J/g more heat than other pastes containing 14 % and 19 % gypsum which could favor its strength gain. It was also observed that such pastes evolved similar cumulative heat up to 20 hours thereafter cement paste containing 24 % gypsum kept evolving heat while others could not evolve much, possibly from the relatively prolonged hydration with increasing added gypsum amount in the system.

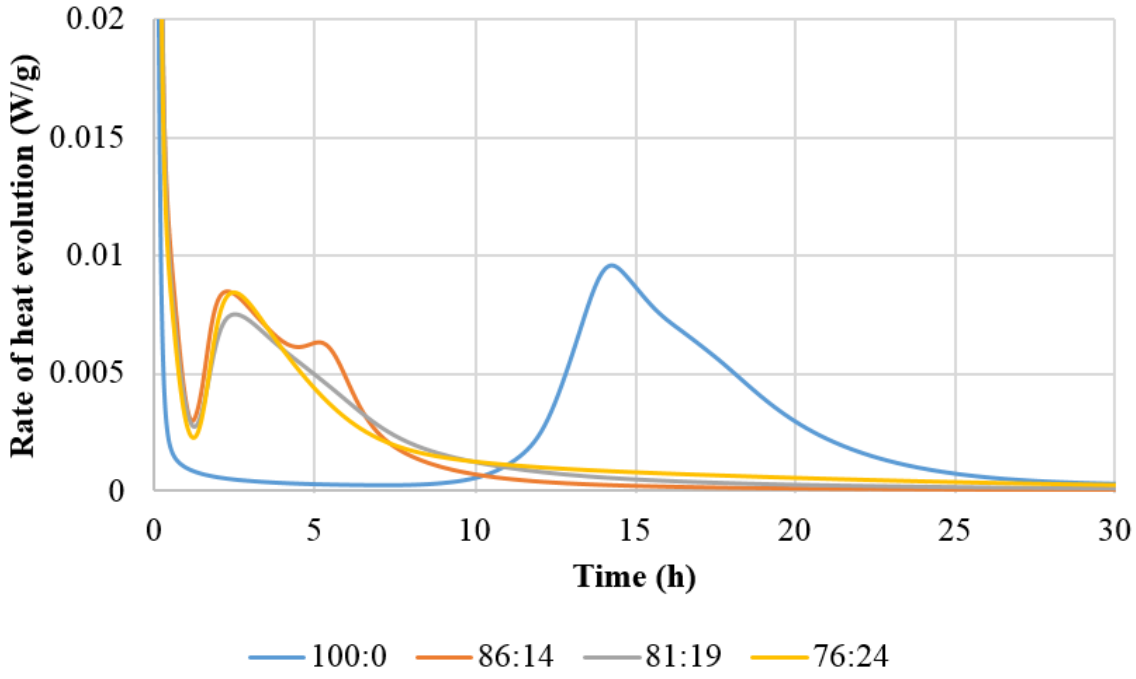

Figure 4.18 Rate of heat evolution for cement pastes containing N2 and gypsum with clinker-to-gypsum ratios of 100:0, 86:14, 81:19, 76:24

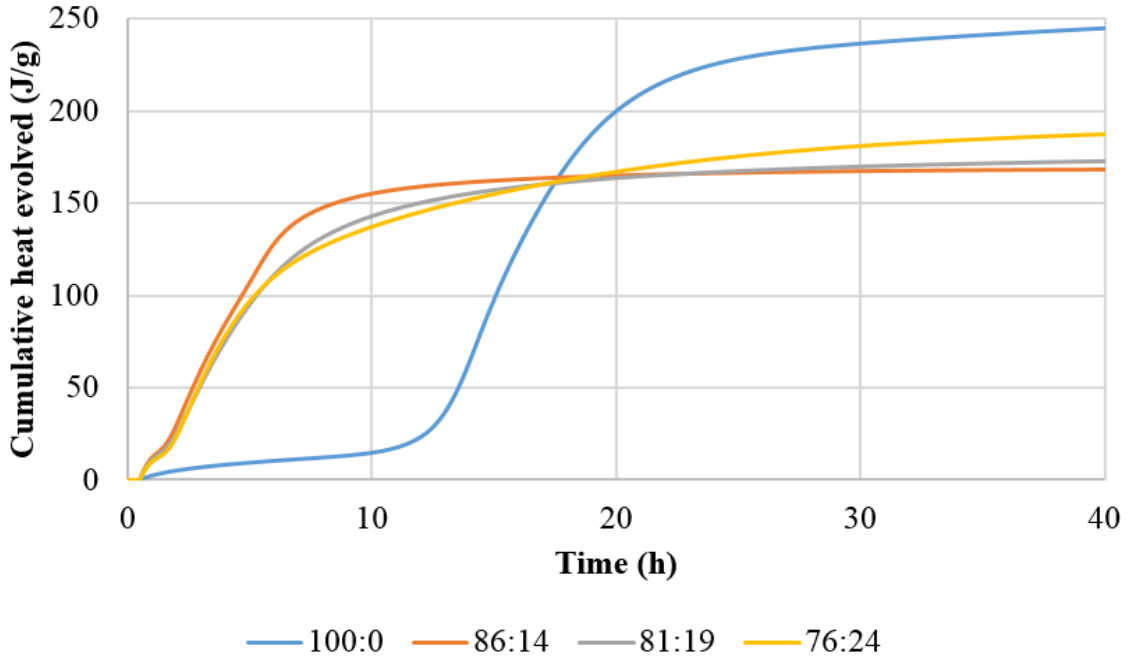

Figure 4.19 Cumulative heat evolved for cement pastes containing N2 and gypsum with clinker-to-gypsum ratios of 100:0, 86:14, 81:19, 76:24

Figure 4.20 and Figure 4.21 shows the rate of heat evolution and cumulative heat evolution of N6 with different amounts of added gypsum, respectively.

Induction period of pure N6 (100:0) was similar to those of pastes containing gypsum (~2h). This is in contrast with the findings of pure N2 which had 10 hours of induction period. Also, N6 did not show shortening in induction period with the addition of gypsum unlike N2 (Figure 4.20). The main peak of pure N6 could indicate the possible ettringite formation from Equation (25). Also, ongoing heat evolution between 5 and 25 hours shows the prolonged hydration period of pure N6. Pastes containing 14 % and 19 % had secondary peak after their induction periods which shows monosulfate formation from depletion of gypsum. Even though compressive strengths of N6 were slightly lower than that of N2, cumulative heat production of pastes containing N6 and gypsum were higher (20-30 J/g) than that of pastes with N2 (Figure 4.21).

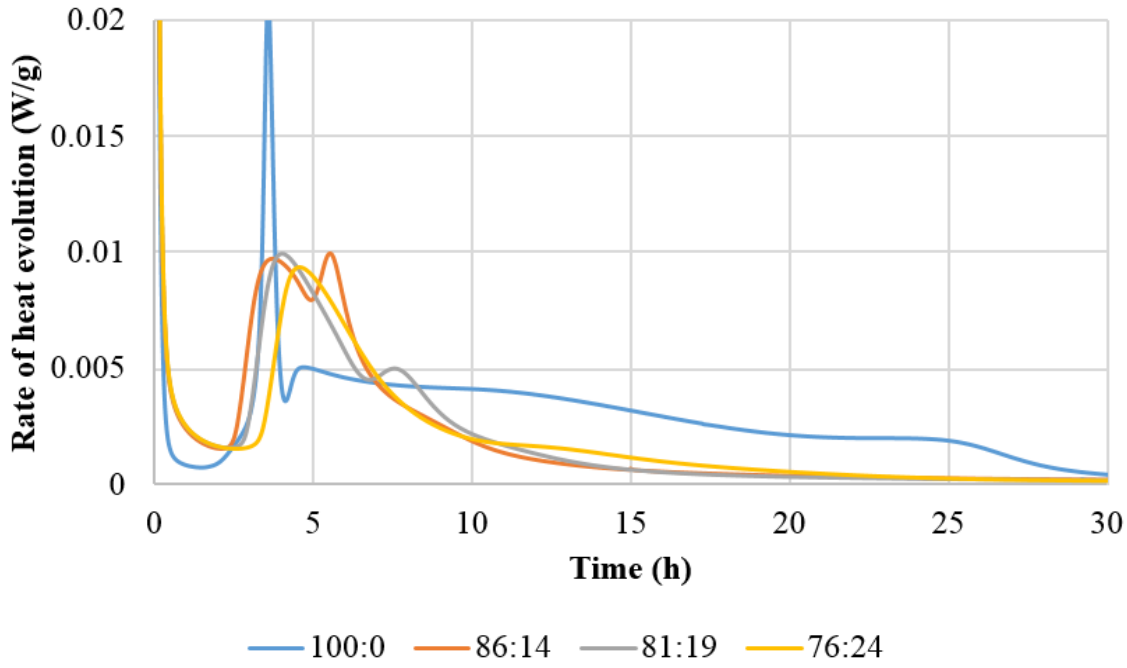

Figure 4.20 Rate of heat evolution for cement pastes containing N6 and gypsum with clinker-to-gypsum ratios of 100:0, 86:14, 81:19, 76:24

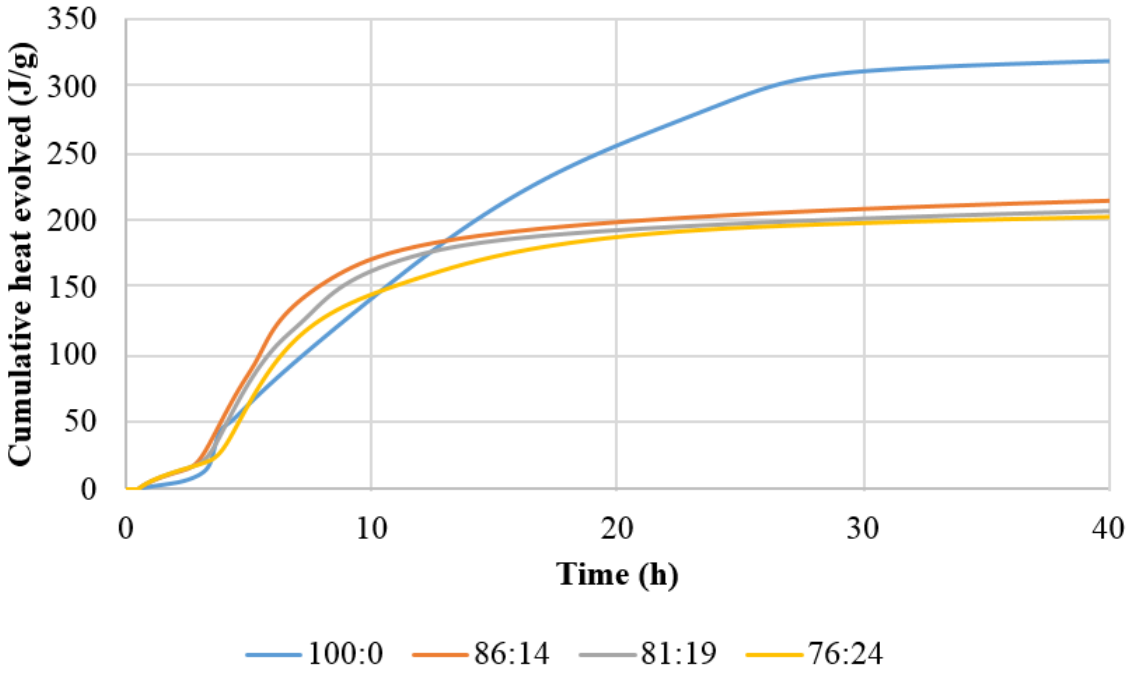

Figure 4.21 Cumulative heat evolved for cement pastes containing N6 and gypsum with clinker-to-gypsum ratios of 100:0, 86:14, 81:19, 76:24

4.5.4 Thermal Analysis

Figure 4.22 and Figure 4.23 comparatively shows the influence of added gypsum amount on the heat flow and mass loss of cement pastes containing N2 at various hydration times, respectively. Table 4.22 shows the relative proportions of loss of water and loss of CO_2 in total mass loss of C$\bar{S}$A cement pastes consisting of N2 and gypsum at 3 and 28 days of hydration.

Minerals formed within such pastes were similar but present at different quantities as cement paste containing 24 % gypsum shows slightly more ettringite content than others at 28 days (Figure 4.23b) which was expected from the difference between the strength gain of such cement pastes. All minerals formed were: ettringite (weight loss between 80-150 °C), gypsum (weight loss between 100-160 °C), AH_3 (weight loss between 250-280 °C) and calcite (weight loss at around 700 °C). Weight loss at around 190 °C indicates the formation of monosulfate (Hargis et al., 2014; Song et al., 2015) which was expected from calorimetry results. However, monosulfate could not be detected in figure (4.22) as its peak might be overlapped with the ones of ettringite and gypsum (Winnefeld and Barlag, 2010). Carbonation of ettringite in such pastes

was observed as the amounts of calcite, AH_3 and gypsum were increasing with corresponding decrease for ettringite.

It can be seen that mass loss until 105 °C was almost same for such pastes. A relatively sharp change in proportions of hydration products containing water or CO_2 was observed for the 14 % gypsum added cement paste (Table 4.22). This difference is coherent with Figure 4.16 showing that ettringite in 14 % gypsum paste was at the lowest amount among others even though main calcite peak, expected from the carbonation of ettringite, could not be detected probably due to overlapping with the one of gypsum (29-30 °2θ). Carbonation rates of $C\bar{S}A$ cement mortars containing various amounts of calcium sulfate (maximum carbonation with lowest anhydrite content) was also demonstrated by Hargis et al. (2017).

Table 4.22 Calculated loss of water and CO_2 for cement pastes containing N2 and gypsum with clinker-to-gypsum ratios of 86:14, 81:19, 76:24, at 3 and 28 days of hydration, as % of their total mass loss

Added Gypsum Amount (%)	**Loss of H_2O (%)**		**Loss of CO_2 (%)**	
	3 days	**28 days**	**3 days**	**28 days**
14	90.6	63.2	9.4	36.8
19	89.8	70.5	10.2	29.5
24	89.9	68.9	10.1	31.1

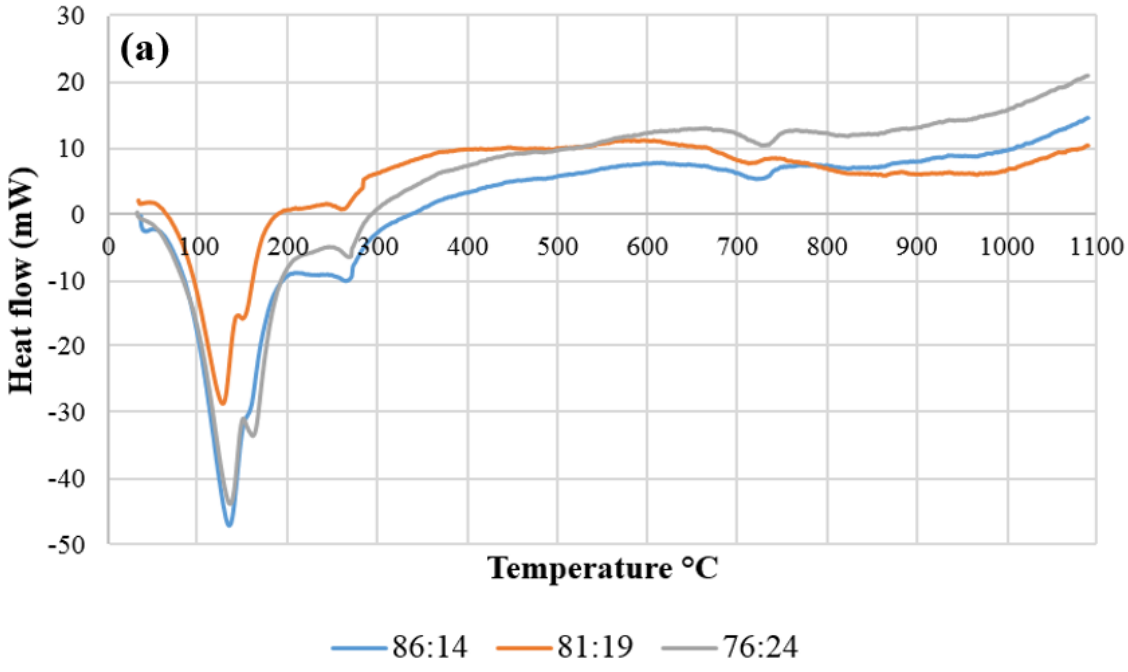

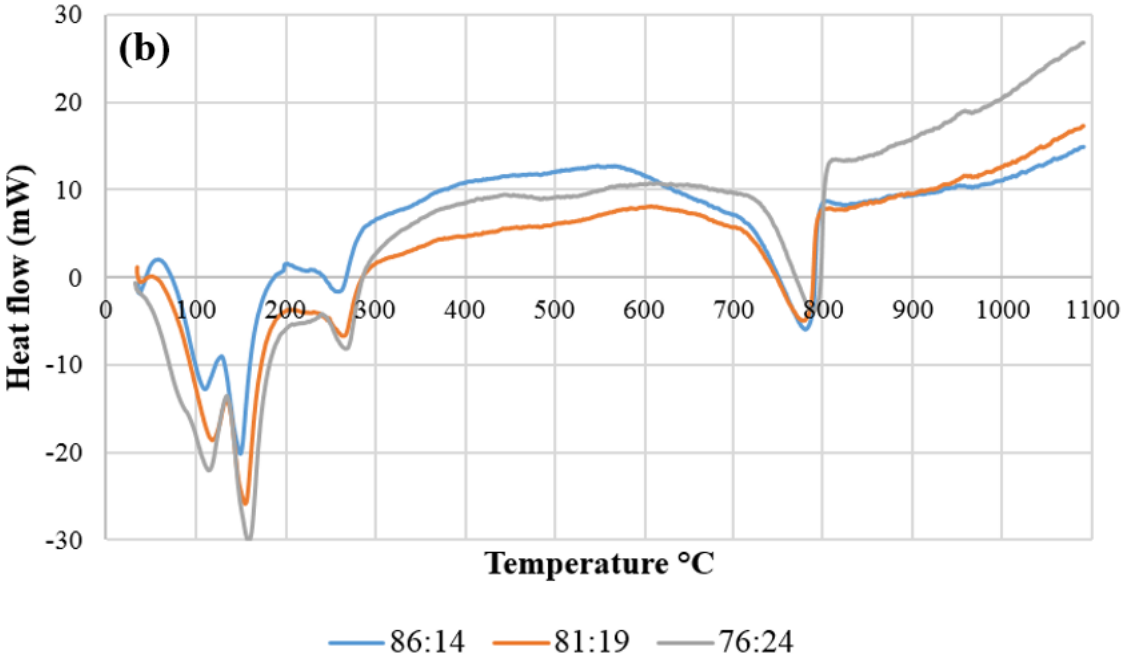

Figure 4.22 Heat flow of cement pastes containing N2 and gypsum with clinker-to-gypsum ratios of 86:14, 81:19, 76:24, a) 3 days of hydration; b) 28 days of hydration

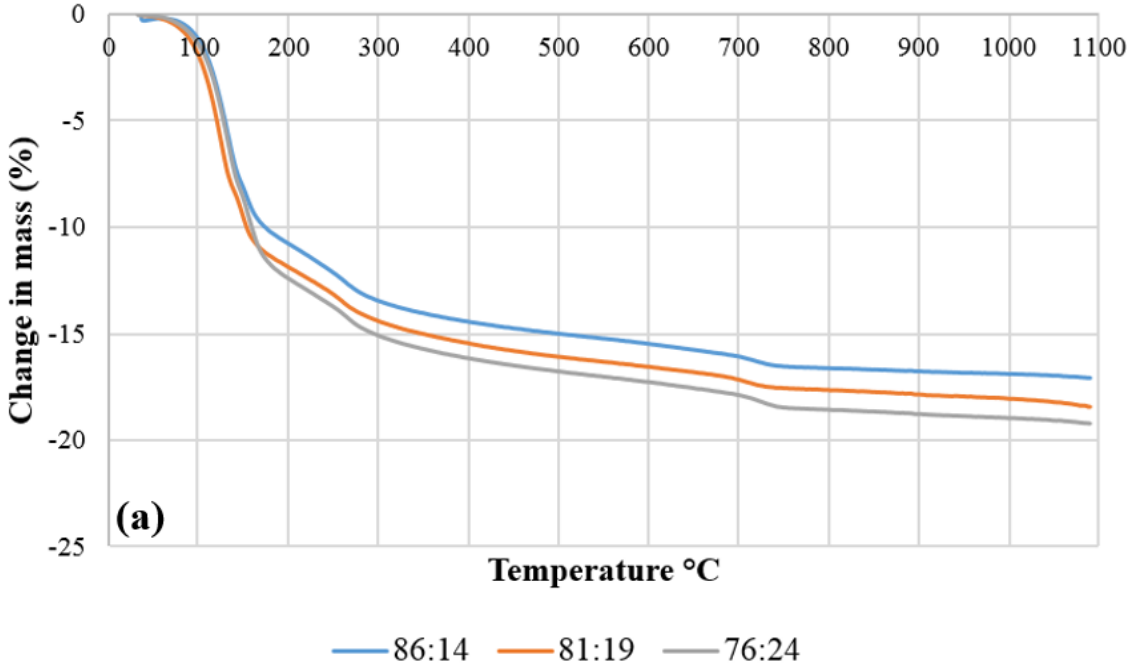

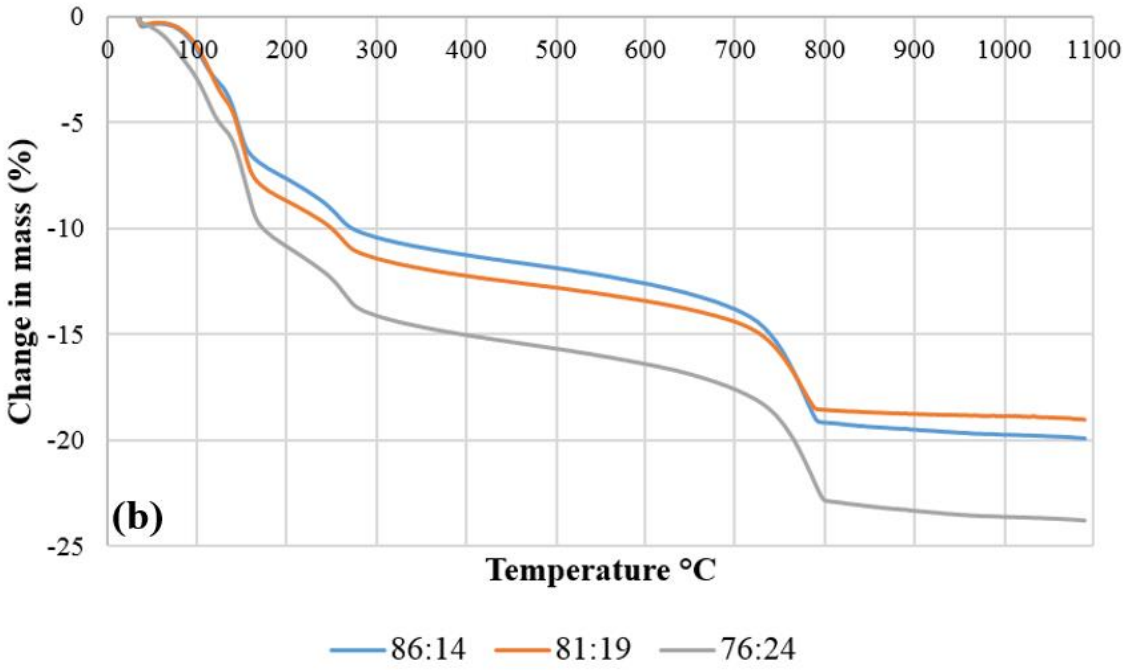

Figure 4.23 Mass loss of cement pastes containing N2 and gypsum with clinker-to-gypsum ratios of 86:14, 81:19, 76:24, a) 3 days of hydration; b) 28 days of hydration

Figure 4.24 and Figure 4.25 comparatively shows the influence of added gypsum amount on the heat flow and mass loss of pastes containing N6 at various hydration times, respectively. Table 4.23 shows the relative proportions of loss of water and loss of CO_2 in total mass loss of $C\bar{S}A$ cement pastes consisting of N6 and gypsum at 3 and 28 days of hydration.

Ettringite, gypsum, AH_3 and calcite were identified as hydration products of cement pastes containing N6 and different amounts of added gypsum at 3 and 28 days of hydration. In conjunction with the results of N2 (Table 4.22), N6 also realized most change in phase proportions when 14 % gypsum was added to the cement paste which indicates the elevated carbonation of cement pastes containing 14 % added gypsum, during the hydration (Table 4.23). However, Figure 4.15 demonstrates for both N2 and N6, continuous strength gains up to 28 days for mortars containing 14 % added gypsum.

Table 4.23 Calculated loss of water and CO_2 for cement pastes containing N6 and gypsum with clinker-to-gypsum ratios of 86:14, 81:19, 76:24, at 3 and 28 days of hydration, as % of their total mass loss

Added Gypsum Amount (%)	Loss of H_2O (%)		Loss of CO_2 (%)	
	3 days	28 days	3 days	28 days
14	89.1	57.9	10.9	42.1
19	85.8	72.5	14.2	27.5
24	81.5	66.0	18.5	34.0

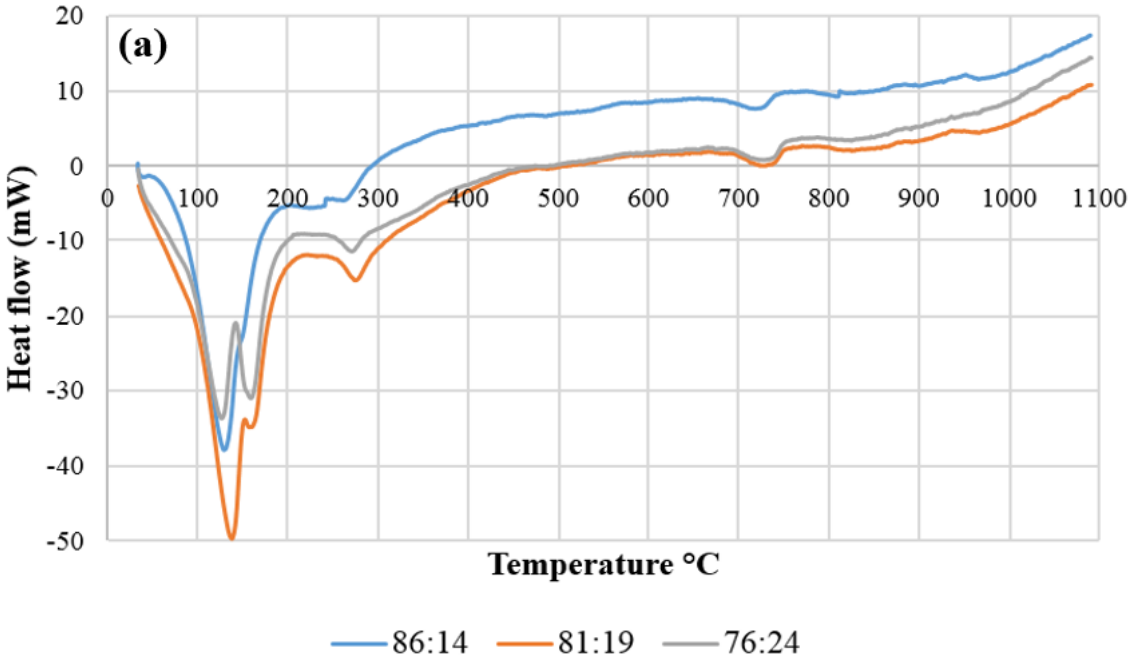

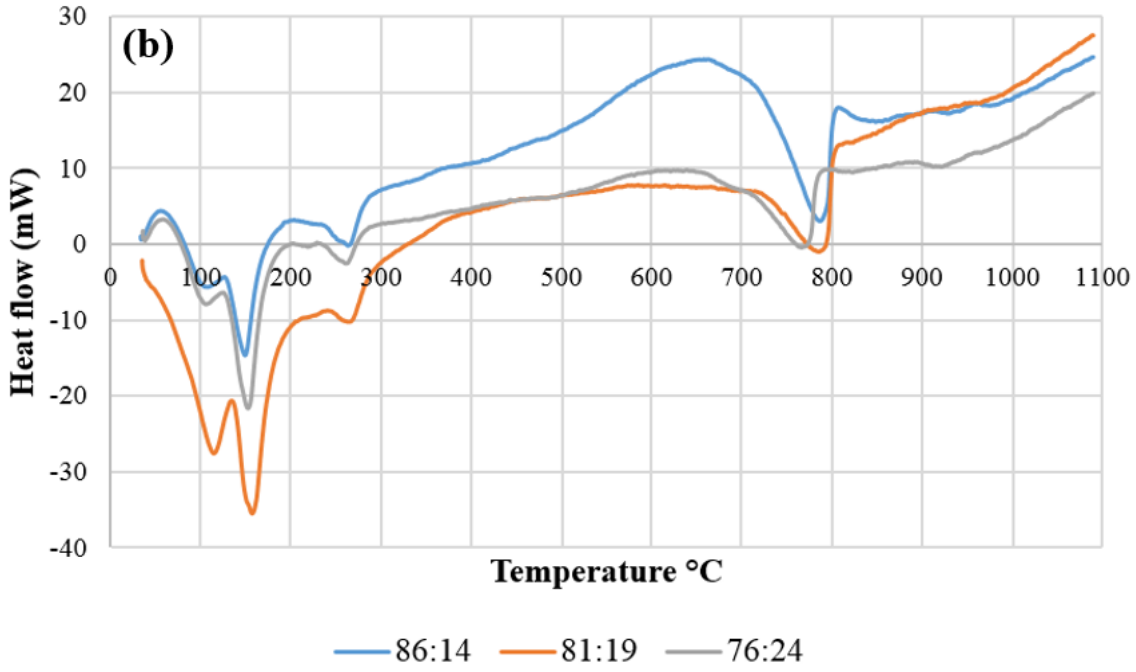

Figure 4.24 Heat flow of cement pastes containing N6 and gypsum with clinker-to-gypsum ratios of 86:14, 81:19, 76:24, a) 3 days of hydration; b) 28 days of hydration

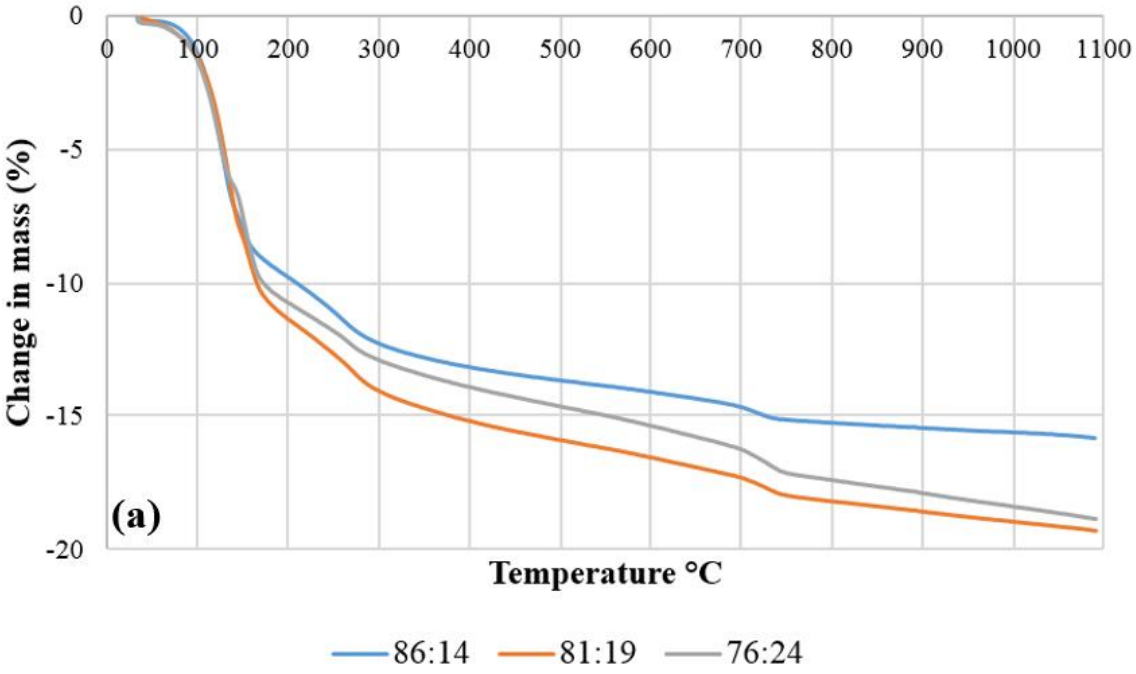

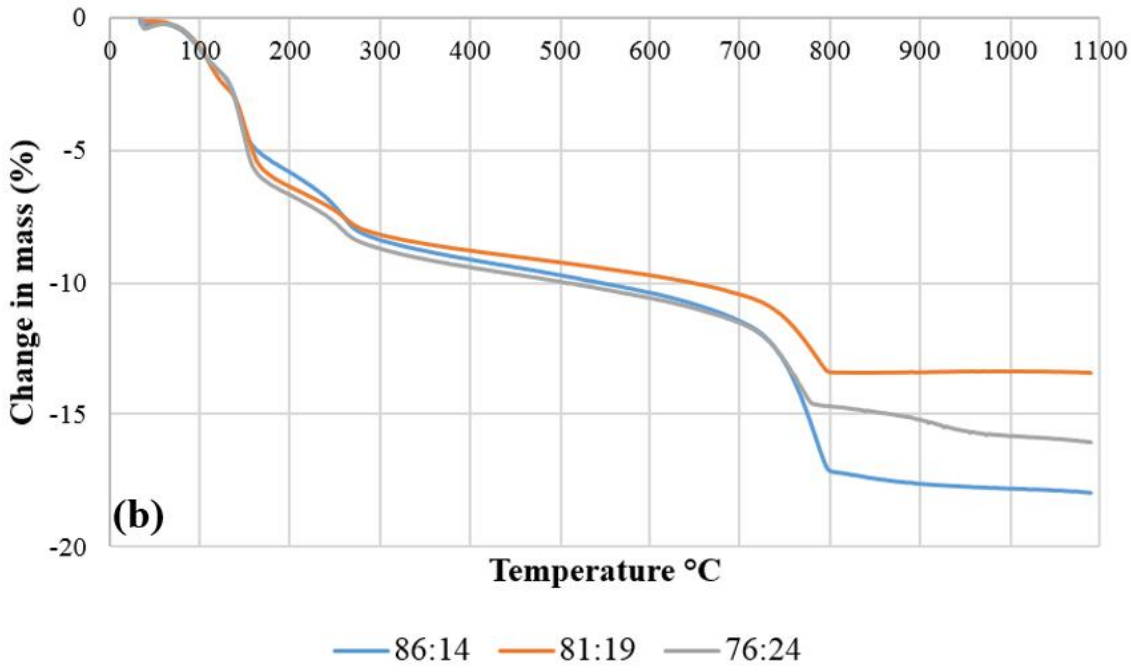

Figure 4.25 Mass loss of cement pastes containing N6 and gypsum with clinker-to-gypsum ratios of 86:14, 81:19, 76:24, a) 3 days of hydration; b) 28 days of hydration

4.6 Influence of Clinker Raw Mixtures Containing Various Industrial Wastes on the Properties of CS̄A cement

In this section, results of each test were separated into 3 groups as CS̄A clinkers containing red mud only as a waste material (W10RM, W15RM, W20RM), CS̄A clinkers containing red mud and fly ash as waste materials (W15RM5FA, W10RM13.5FA) and CS̄A clinkers containing fly ash only as a waste material (W5FA, W45FA, W48FA), respectively. The reader is referred to Section 3.2.6 and Table 3.9 for mixture ingredients and proportions.

4.6.1 Strength Development

Mostly, amount of citric acid added and w/c ratio for mortars prepared from CS̄A cements incorporating waste materials, were 0.5 % (wt.% of cement) and 0.6, respectively. Cement pastes not containing citric acid were the pastes which could be prepared without rapid hardening or lots of heat liberation. These pastes were also prepared at a w/c ratio of 0.7 because of the great water demand of such clinkers as well as direct comparison. However, all mortars containing desulfogypsum were in need of a retarder as the reason was mentioned in Section 3.2.6. The exceptions about

the amount of citric acid added and the w/c ratio used that were different from 0.5 % (wt. % of cement) and 0.6, respectively, were provided under the below tables. Flow of hydraulic cement mortars containing citric could not be determined because of the very runny pastes.

Compressive and flexural strengths of C$\bar{S}$A cements consisting of clinkers named W10RM, W15RM and W20RM and added gypsum or desulfogypsum are given in Table 4.24 and Table 4.25, respectively.

It can be seen in Table 4.24 and Table 4.25 that increasing red mud content in the clinker raw mixture reduced the compressive strength of mortars. However, they all achieved medium compressive strength at 28 days (>20 MPa) which was more than double their 1-day compressive strengths. Considering the direct bauxite replacement by red mud, these strengths were important. Also, desulfogypsum was observed to be more beneficial than gypsum to be added to clinker paste.

Table 4.24 Strength development of C$\bar{S}$A cement mortars consisting of clinkers produced using red mud only as a waste material and gypsum with clinker-to-gypsum ratio of 81:19

Clinker ID	**Flexural Strength (MPa)**				**Compressive Strength (MPa)**			
	1 day	**3 days**	**7 days**	**28 days**	**1 day**	**3 days**	**7 days**	**28 days**
W10RM	4.7	5.5	6.5	7.2	20.6	23.9	34.3	45.5
W15RM	3.1	4.4	5.8	4.5	12.0	16.0	23.2	27.9
W20RM	1.7	3.4	3.7	2.7	6.2	12.2	15.5	22.4

Table 4.25 Strength development of C$\bar{S}$A cement mortars consisting of clinkers produced using red mud only as a waste material and desulfogypsum with clinker-to-desulfogypsum ratio of 81:19

Clinker ID	**Flexural Strength (MPa)**				**Compressive Strength (MPa)**			
	1 day	**3 days**	**7 days**	**28 days**	**1 day**	**3 days**	**7 days**	**28 days**
W10RM	4.6	5.3	5.7	7.3	20.3	23.0	33.6	47.8
W15RM	3.1	3.3	4.6	3.5	13.1	17.1	26.6	34.2
W20RM	2.2	2.7	3.8	2.7	6.7	10.8	16.7	24.7

Figure 4.26 shows the strength development of C$\bar{S}$A cements containing red mud at different levels, as a percentage of their 28-day strength. Results of desulfogypsum

added mortars were used in Figure 4.26 since their strengths were higher than that of gypsum added mortars. Reduction of ye'elimite amount by increasing red mud content in clinker raw meal led to lower strength gain at the first day, especially for W20RM. However, W20RM gained its >70 % compressive strength between 1 and 28 days which was approximately 10 % higher than others. This may be attributed to the participation of brownmillerite in hydration reactions compensating the strength-giving reactions of ye'elimite.

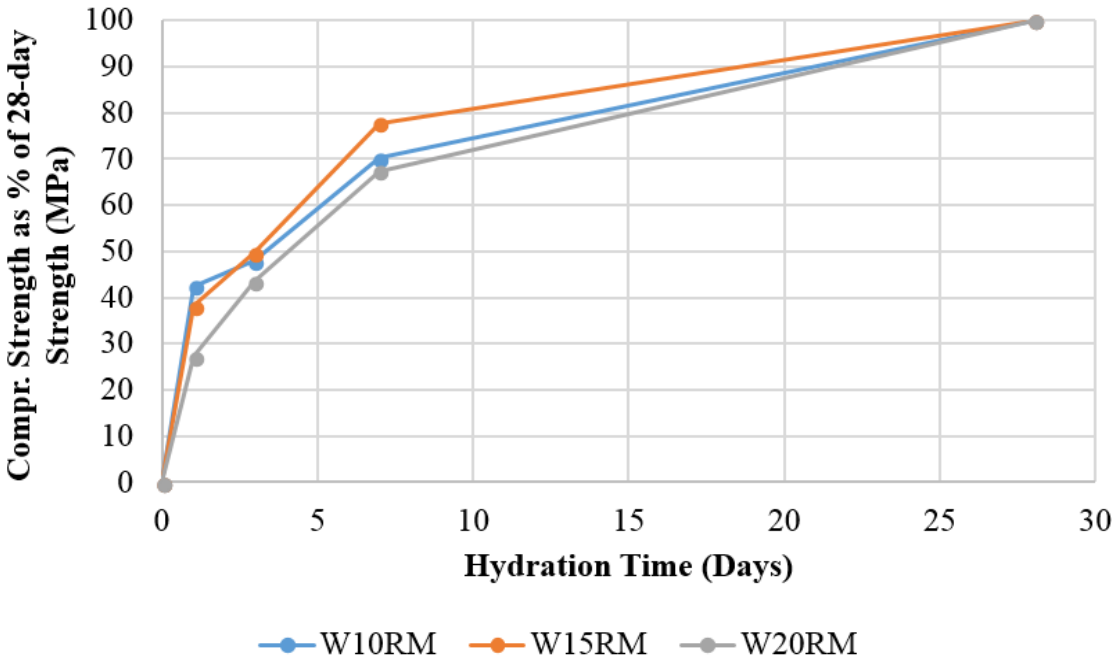

Figure 4.26 Compressive strength development of CS̄A cement mortars consisting of clinkers incorporated with red mud and desulfogypsum, as a percentage of 28-day strength

Compressive and flexural strengths of CS̄A cements consisting of clinkers W15RM5FA and W10RM13.5FA and added gypsum or desulfogypsum are shown in Table 4.26 and Table 4.27, respectively.

Table 4.26 proves the importance of the optimum amount of citric acid added and decreasing w/c ratio in terms of strength gain for W10RM13.5FA. Range between the compressive strengths of mortars prepared with W10RM13.5FA at different w/c ratios was great. This clinker nearly tripled its compressive strength at 1-day and 28-day with decreasing w/c ratio originated from the citric acid addition. Strengths of mortars with W10RM13.5FA were higher than that of W15RM5FA at every test age which is

important since W10RM13.5FA contained more waste materials (3.5 %) in its raw mixture than W15RM5FA.

Table 4.26 Strength development of C$\bar{S}$A cement mortars consisting of clinkers produced using red mud and fly ash as waste materials and gypsum with clinker-to-gypsum ratio of 81:19

Clinker ID	Flexural Strength (MPa)				Compressive Strength (MPa)			
	1 day	3 days	7 days	28 days	1 day	3 days	7 days	28 days
W15RM5FA	2.5	3.6	4.4	3.9	7.9	14.1	17.3	26.1
W10RM13.5FA	3.8	4.4	4.8	5.1	14.8	17.1	19.7	37.9
W10RM13.5FA*	1.6	1.8	2.3	3.0	5.7	8.0	10.2	13.5

*This cement paste did not contain citric acid and w/c ratio of 0.7 was used. Flow of this mortar was 80 %.

Table 4.27 Strength development of C$\bar{S}$A cement mortars consisting of clinkers produced using red mud and fly ash as waste materials and desulfogypsum with clinker-to-desulfogypsum ratio of 81:19

Clinker ID	Flexural Strength (MPa)				Compressive Strength (MPa)			
	1 day	3 days	7 days	28 days	1 day	3 days	7 days	28 days
W15RM5FA	2.4	2.3	3.5	3.0	9.0	12.1	24.1	31
W10RM13.5FA	4.0	4.2	4.8	5.0	15.8	17.7	22.9	40.3

Figure 4.27 gives the strength development of C$\bar{S}$A cements containing red mud and fly ash at different combinations, as a percentage of 28-day strength. Results of desulfogypsum added mortars were used in Figure 4.27 since their strengths were higher than those of gypsum added mortars.

The 1-day strength of W10RM13.5FA was nearly double that of W15RM5FA which can be explained by the ~2 % higher ye'elimite content in W10RM13.5FA than in W15RM5FA. On the other hand, W15RM5FA gained most of its compressive strength up to 7 days (~80 %) whereas W10RM13.5FA gained only ~55 % of its 28-day compressive strength until the same age. This can be explained by the higher belite content in W10RM13.5FA than in W15RM5FA (> 3 %) and the participation of belite in further hydration reactions. Also, a direct comparison can be made between W10RM13.5FA and W15RM from the strength gain point of view. Even though W15RM had almost 3 % more ye'elimite and 10 % more brownmillerite than

W10RM13.5FA, 28-day compressive strength of W10RM13.5FA was 6.1 MPa higher than that of W15RM (desulfogypsum containing mortars). This difference also highlights the importance of belite for later strength gain as W10RM13.5FA had ~10 % more belite than W15RM.

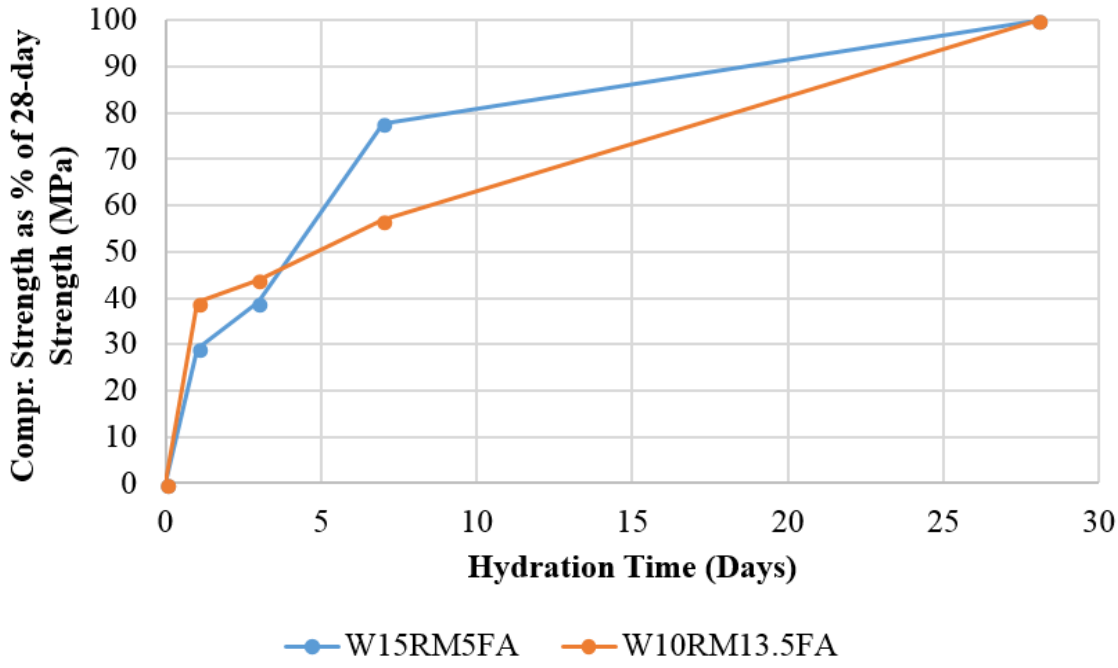

Figure 4.27 Compressive strength development of CS̄A cement mortars consisting of clinkers incorporated with red mud and fly ash, as a percentage of 28-day strength

Compressive and flexural strengths of CS̄A cements consisting of clinkers W5FA, W45FA and W48FA and added gypsum or desulfogypsum are given in Table 4.28, Table 4.29 (added desulfogypsum amount of 19 %) and Table 4.30 (added desulfogypsum amount of 24 %), respectively.

Some early strength results (1 and 3 days) could not be obtained from W45FA and W48FA, since the prism samples had splitted during demolding. This was related with the lower strength gain of such cements at early ages. Strength development of W5FA is not surprising as it contains only minor amounts of waste materials (5 % fly ash) in the clinker raw meal. W48FA showed similar strength gain with W45FA when w/c was 0.7 (Table 4.28). However, its strength development was not satisfying compared to W45FA when w/c was decreased to 0.6 (Table 4.29 and Table 4.30). Lower ye'elimite and belite content in W48FA may be the reasons for lower compressive strengths, but it was also observed that citric acid addition negatively affected the

system, in terms of strength gain. W48FA could not even reach 14,5 MPA, compressive strength achieved with w/c of 0.7 at 28 days, when w/c of 0.6 was used with citric acid addition. On the other hand, 28-day compressive strength of W45FA (23.4 MPa) is promising since the fly ash used almost constituted the half of its raw mixture, by mass.

Table 4.28 Strength development of C$\bar{S}$A cement mortars consisting of clinkers produced using only fly ash as a waste material and gypsum with clinker-to-gypsum ratio of 81:19

Clinker ID	**Flexural Strength (MPa)**				**Compressive Strength (MPa)**			
	1 day	**3 days**	**7 days**	**28 days**	**1 day**	**3 days**	**7 days**	**28 days**
W5FA	4.4	6.5	6.7	6.9	16.8	29.9	34.1	37.3
W45FA*	1.4	1.8	2.1	2.0	6.0	5.4	10.9	17.4
W48FA*	1.1	2.3	2.0	2.3	4.4	5.5	8.5	14.5

*These cement pastes did not contain citric acid and w/c ratio of 0.7 was used. Flow of the mortars were 100 %.

Table 4.29 Strength development of C$\bar{S}$A cement mortars consisting of clinkers produced using only fly ash as a waste material and desulfogypsum with clinker-to-desulfogypsum ratio of 81:19

Clinker ID	**Flexural Strength (MPa)**				**Compressive Strength (MPa)**			
	1 day	**3 days**	**7 days**	**28 days**	**1 day**	**3 days**	**7 days**	**28 days**
W5FA	5.5	6.4	6.3	6.2	25.7	30.4	38.7	39.1
W45FA	-	-	2.6	2.7	2.0	11.0	13.4	23.4
W48FA	-	-	-	2.6	-	2.2	8.5	10.1

Table 4.30 Strength development of C$\bar{S}$A cement mortars consisting of clinkers produced using only fly ash as a waste material and desulfogypsum with clinker-to-desulfogypsum ratio of 76:24

Clinker ID	**Flexural Strength (MPa)**				**Compressive Strength (MPa)**			
	1 day	**3 days**	**7 days**	**28 days**	**1 day**	**3 days**	**7 days**	**28 days**
W5FA	4.8	5.4	5.5	5.8	21.9	28.7	35.5	43.0
W45FA	-	1.9	2.8	2.9	1.8	7.4	13.6	20.4
W48FA	-	-	-	2.8	-	3.9	9.5	13.2

Figure 4.28 shows the strength development of C$\bar{S}$A cements containing fly ash at different proportions, as a percentage of 28-day strength. Results used in Figure 4.28 were determined according to the highest 28-day strengths achieved for each clinker.

W5FA achieved most of its compressive strength up to 3 days (~70 %) as expected from its high ye'elimite content. Different ranges of strength development between 7 and 28 days can be attributed to the belite content in these clinkers. Amount of belite in clinkers can be sorted as W45FA>W48FA>W5FA, which is similar to the order of the strength gained by these mortars between these curing ages.

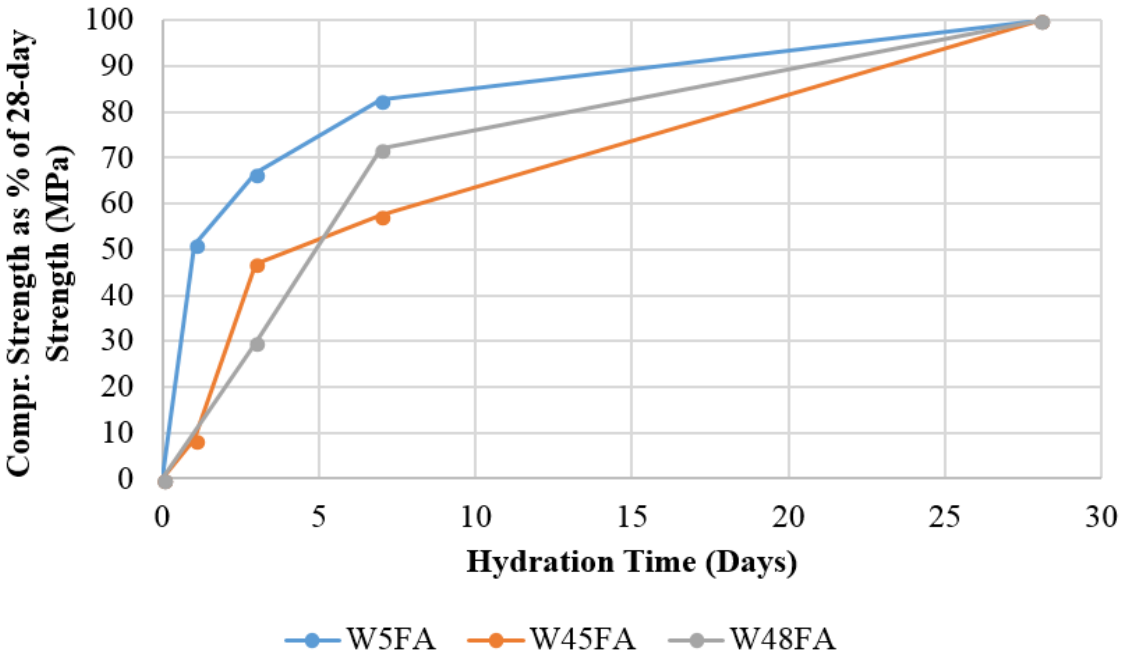

Figure 4.28 Compressive strength development of C$\bar{S}$A cement mortars consisting of clinkers incorporated with fly ash, as a percentage of 28-day strength

In light of the higher compressive strengths of mortars containing industrial wastes incorporated C$\bar{S}$A clinkers, when w/c ratio of 0.6 was used, different mortars consisting of clinkers named N2 and N4, were prepared using w/c of 0.6 and 0.5 % (wt.% of cement) citric acid to observe the effect of reduced w/c ratio (from 0.7 to 0.6) and citric acid to strength gain of C$\bar{S}$A clinkers produced using only natural materials. In order to maximize strength gain, clinker-to-gypsum (or desulfogypsum) ratio of 76:24 was used. Gypsum was added into N2 and desulfogypsum was added into N4 to compare calcium sulfates used. Results were given in below table (4.31) including strengths achieved when w/c of 0.7 and clinker-to-gypsum ratio of 76:24 were used

for N2 (Table 4.17), for direct comparison. For N4, clinker-to-calcium sulfate ratio of 76:24 has never been used when w/c ratio was 0.7. However, similar strength gain to N2 can be assumed for N4 based on their similar strength gain when clinker-to-gypsum ratio was fixed to 81:19 for each (Table 4.16).

As expected, N2 and N4 gained the highest strengths with w/c of 0.6 among all cements produced due to their highest ye'elimite content. Still, most of the compressive strength (~80 %) achieved within the first 3 days of hydration.

Table 4.31 Strength development of C$\bar{S}$A cement mortars consisting of clinkers produced using only natural materials and calcium sulfate with clinker-to-calcium sulfate ratio of 76:24

Clinker ID	**Flexural Strength (MPa)**				**Compressive Strength (MPa)**			
	1 day	**3 days**	**7 days**	**28 days**	**1 day**	**3 days**	**7 days**	**28 days**
N2*	3.7	4.8	4.8	5.2	19.0	26.9	27.6	30.9
N2	6.0	6.5	7.2	7.9	28.1	40.6	37.5	49.7
N4	5.8	6.9	7.5	7.4	33.3	38.7	44.7	50.6

*This cement paste did not contain citric acid and w/c ratio of 0.7 was used.

Table 4.32 summarizes all C$\bar{S}$A cements consisting of waste materials, with respect to the highest compressive strength achieved in 28 days at w/c ratio of 0.6. It can be concluded that C$\bar{S}$A clinkers were achieving higher compressive strengths when desulfogypsum was added instead of gypsum. This phenomenon may be related with the higher fineness of desulfogypsum (~10000 cm^2/g) than that of gypsum (~8300 cm^2/g) which leads to the desulfogypsum to be more reactive calcium sulfate source. The higher sulfur content in desulfogypsum might be another reason.

Table 4.32 Mixture proportioning of CS̄A cements consisting of waste materials, with respect to the highest compressive strength achieved in 28 days at w/c ratio of 0.6

Clinker ID	Citric Acid (wt.% of cement)	Used Calcium Sulfate Source	Clinker-to-Calcium Sulfate Ratio
W5FA	0.5	Desulfogypsum	76:24
W10RM	0.5	Desulfogypsum	81:19
W15RM	0.5	Desulfogypsum	81:19
W15RM5FA	0.5	Desulfogypsum	81:19
W10RM13.5FA	0.5	Desulfogypsum	81:19
W20RM	0.5	Desulfogypsum	81:19
W45FA	0.5	Desulfogypsum	81:19
W48FA	0.5	Desulfogypsum	76:24

Figure 4.29 compares the compressive strength development of all CS̄A cements introduced in this section. Each CS̄A clinker incorporated with waste materials, had two or three mixtures for the investigation of strength development therefore, Figure 4.29 would be so crowded if the results of all mixtures were used. Therefore, strength gain of cements provided in Table 4.32 were demonstrated in Figure 4.29. Results of N2 and N4 (Table 4.31) were also used in Figure 4.29 for comparison.

It can be inferred from Figure 4.29 that increasing waste content in clinker raw mixture caused reduction in compressive strengths. However, there is an exception with clinker named W10RM13.5FA that achieved higher 28-day compressive strength than some other CS̄A clinkers consisting of less waste materials in the clinker raw mixture such as W15RM, W15RM5FA and W20RM.

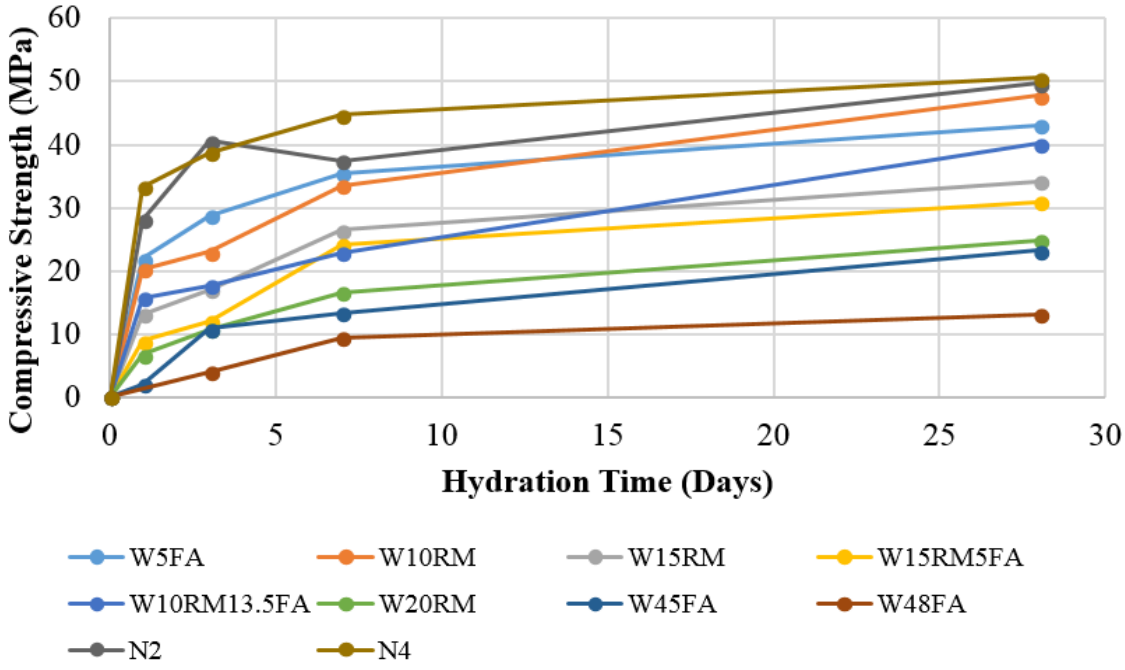

Figure 4.29 Compressive strength development of CS̄A cement mortars made of clinkers incorporated with waste materials and clinkers produced using only natural materials (N2 and N4)

4.6.2 X-ray diffraction

XRD patterns of all hydrated CS̄A cement pastes, given in Table 4.32, were obtained up to 28 days of hydration. However, XRD patterns of one representative paste from each group (groups; cements containing only red mud as a waste, cements containing red mud and fly ash as wastes, cements containing only fly ash as a waste) were demonstrated in this section, separately. Because, hydration product development of clinkers belonging to same group was not differing much. XRD patterns of others which were not demonstrated in this section, are provided in Appendix A.

Hydration product development of CS̄A cement pastes consisting of clinkers named W15RM, W10RM13.5FA and W45FA, and desulfogypsum with clinker-to-desulfogypsum ratio of 81:19 are shown in Figure 4.30, Figure 4.31 and Figure 4.32, respectively.

Minerals formed from the hydration of CS̄A clinkers incorporated waste materials were similar with CS̄A clinkers produced using only natural materials. These minerals were ettringite, gypsum and calcite at different quantities. However, unlike the hydration product development of CS̄A clinkers produced using only natural

materials, ye'elimite in W15RM and W10RM13.5FA was almost fully consumed (Figure 4.30 and Figure 4.31, respectively). Even though calcite could not be clearly identified in the XRD patterns of CS̄A clinkers consisting of only natural materials, it could be identified in the XRD patterns of W15RM, W10RM13.5FA and W45FA with its gradually increasing peak intensities up to 28 days of hydration which corresponds to the carbonation of pastes, especially for W15RM and W45FA (Figure 4.30 and Figure 4.32, respectively). Furthermore, ettringite formed in W45FA was observed to be fully carbonated as its peaks disappeared after 3 days of hydration while the peak intensities of gypsum and calcite were increasing. Belite in W45FA observed to be reacted as the intensity of its main peak (~32.05 °2θ) decreases ~30 % up to 28 days which could favor the later strength gain of W45FA. Any comments about the changing peak intensities of belite and brownmillerite present in W15RM and W10RM13.5FA cannot be made since they might be overlapped with the one of ettringite at 28 days of hydration. It was also observed that the amount of ettringite in W10RM13.5FA was gradually increasing with ongoing hydration unlike in others, which maintained the higher strength gain of W10RM13.5FA.

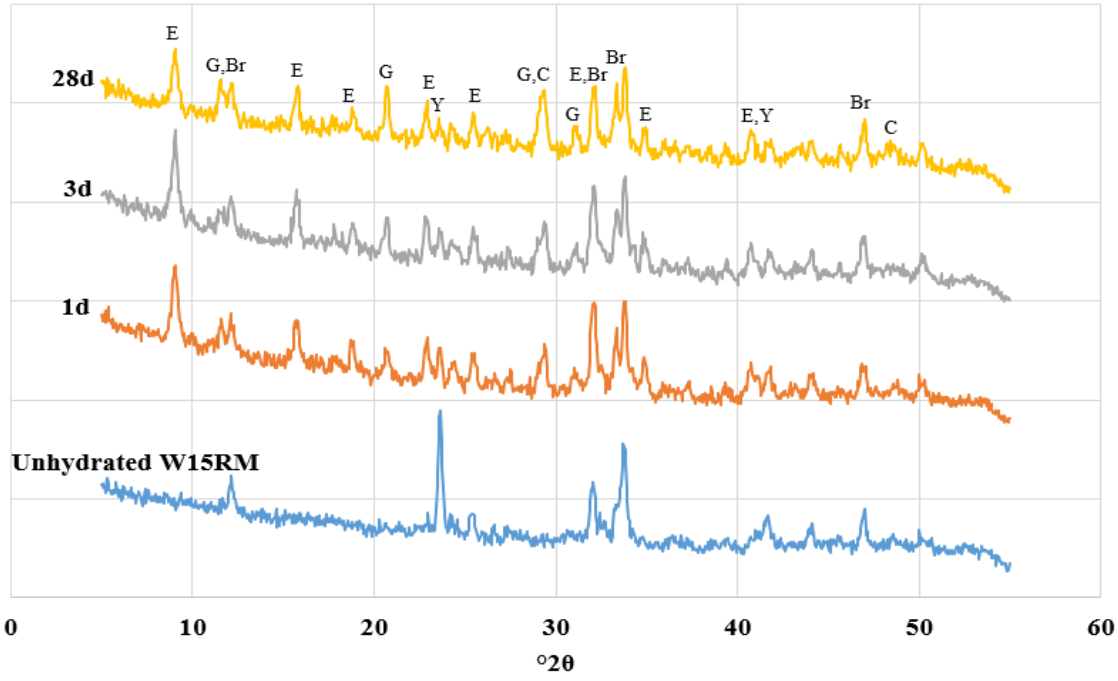

Figure 4.30 XRD patterns of cement paste consisting of W15RM and desulfogypsum with clinker-to-desulfogypsum ratio of 81:19, at 1, 3 and 28 days of hydration (Legend: Br – Brownmillerite; C – Calcite; E – Ettringite; G – Gypsum; Y – Ye'elimite)

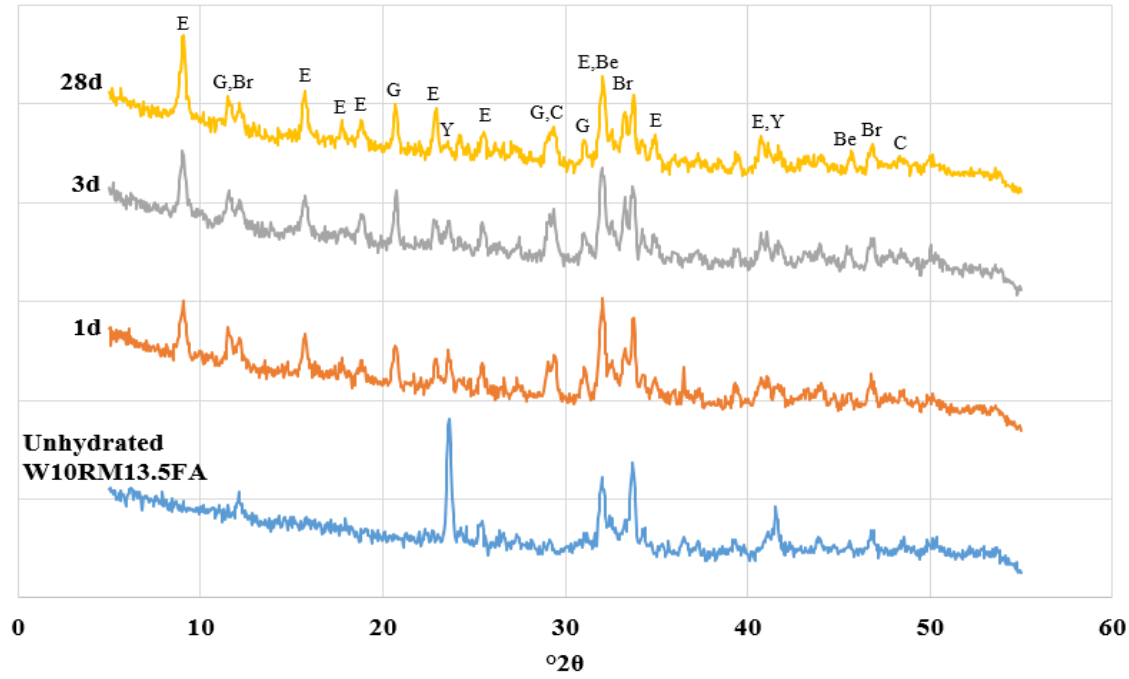

Figure 4.31 XRD patterns of cement paste consisting of W10RM13.5FA and desulfogypsum with clinker-to-desulfogypsum ratio of 81:19, at 1, 3 and 28 days of hydration (Legend: Be – Belite; Br – Brownmillerite; C – Calcite; E – Ettringite; G – Gypsum; Y – Ye'elimite)

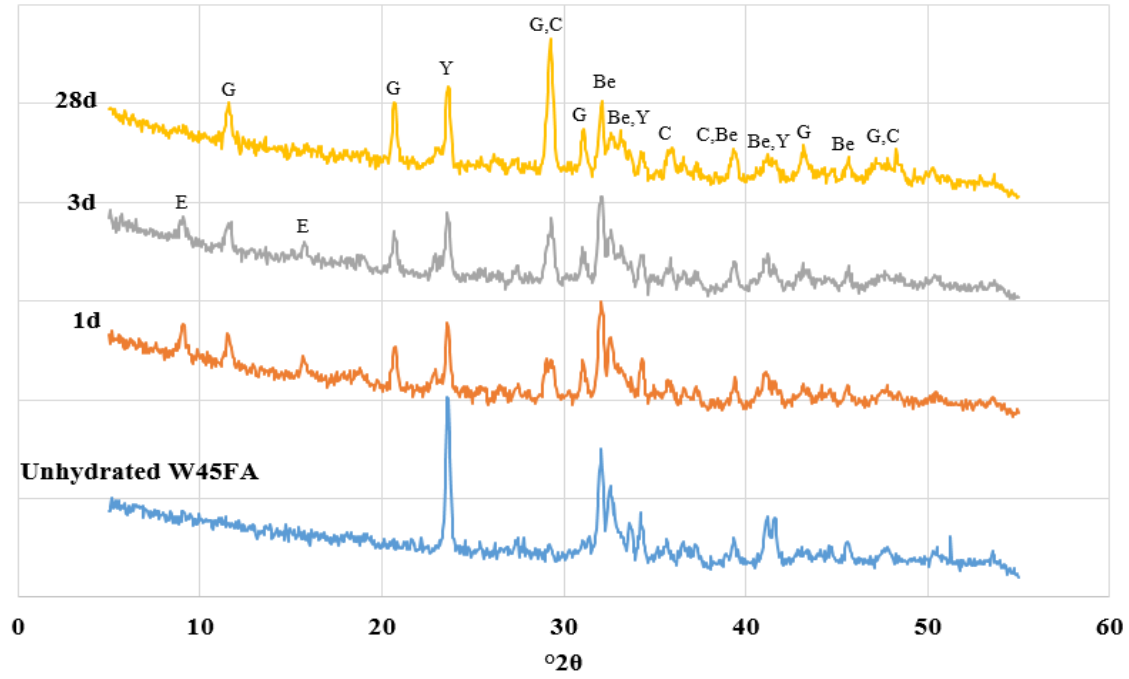

Figure 4.32 XRD patterns of cement paste consisting of W45FA and desulfogypsum with clinker-to-desulfogypsum ratio of 81:19, at 1, 3 and 28 days of hydration (Legend: Be – Belite; C – Calcite; E – Ettringite; G – Gypsum; Y – Ye'elimite)

4.6.3 Isothermal Calorimetry

Mixtures provided in Table 4.32, were subjected to calorimetery. Figure 4.33 and Figure 4.34 show the rate of heat evolution and cumulative heat evolution, respectively, for C$\bar{S}$A cement pastes containing only red mud as a waste material in the clinker raw mixture.

Figure 4.33 demonstrates decreasing induction period-lengths with increasing red mud content in clinker raw mixture. Such difference in induction periods, is interesting since the ye'elimite amount was also decreasing with increasing red mud content. This phenomenon may indicate some unidentified calcium aluminate phases such as $C_{12}A_7$ or CA present in such clinkers that are able to yield ettringite through the reaction with calcium sulfate (Eqn. (14) and (15)) or more possibly, accelerated ye'elimite reaction with increasing alkali content, mainly Na_2O, from the red mud incorporation (Winnefeld and Barlag, 2010; Chen and Juenger, 2012). The presence of unidentified calcium aluminate phases or increasing alkali contents in C$\bar{S}$A clinkers produced might be the reasons for rapid hardening and violent heat liberation within the first minutes of mixing therefore the necessity of a retarder use. Even though such pastes were prepared with citric acid (0.5 %, by weight of cement), their induction periods were ~1h shorter than that of gypsum added pastes whose clinkers contained only natural materials, without the existence of any retarder (Figure 4.9). Use of desulfogypsum instead of gypsum might be another reason for this phenomenon, beside of alkali effect and calcium aluminate phases. Bassanite which constitutes the major part of desulfogypsum used, is accepted to dissolve readily than other calcium sulfate sources (Burris and Kurtis, 2018). Monosulfate formation was not expected in such since the molar ratio of calcium sulfate-to-ye'elimite for each cement paste was more than 2 and increases with increasing red mud content because of the reducing ye'elimite content. Therefore, both peaks after the induction period (including small shoulder after the main peak of W10RM) can be attributed to the ettringite and AH_3 formation. Also, it has been reported that (Chen and Juenger, 2012), ettringite-giving reactions of ye'elimite and brownmillerite could be realized with two distinct peaks which can be seen from Figure 4.33. Cumulative heat evolved for red mud containing cement pastes (Figure 4.34) is compatible with their strength gain. It was observed that increasing red mud content from 10 % to 15 % did not affect much to total heat

production while additional 5 % red mud addition in clinker raw mixture (W20RM) lowered the cumulative heat evolved approximately 50 J/g.

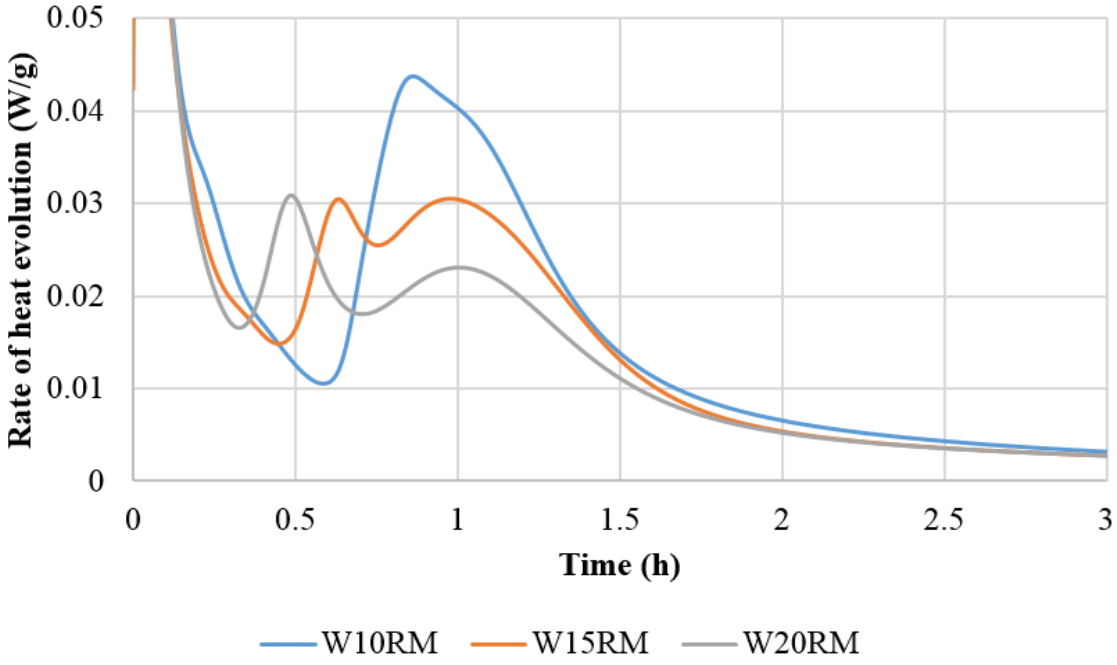

Figure 4.33 Rate of heat evolution for cement pastes containing W10RM, W15RM and W20RM, and desulfogypsum with clinker-to-desulfogypsum ratio of 81:19

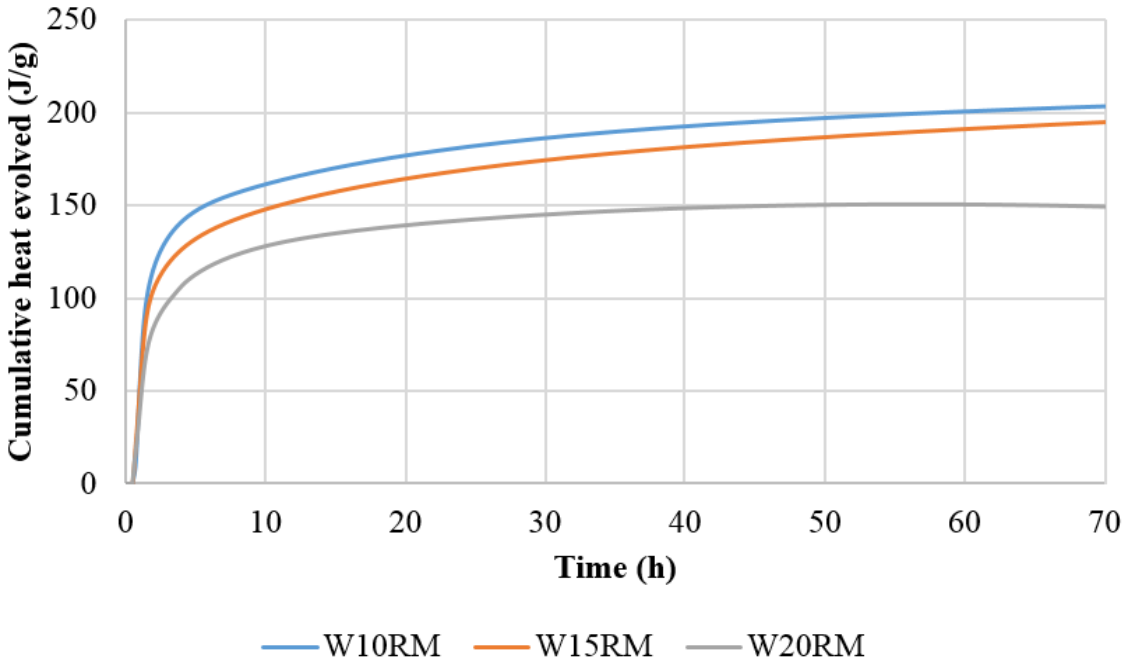

Figure 4.34 Cumulative heat evolved for cement pastes containing W10RM, W15RM and W20RM, and desulfogypsum with clinker-to-desulfogypsum ratio of 81:19

Figure 4.35 and Figure 4.36 show the rate of heat evolution and cumulative heat evolution, respectively, for $C\bar{S}A$ cement pastes containing red mud and fly ash as waste materials in the clinker raw mixture.

Figure 4.35 shows two distinct peaks after the induction period for W15RM5FA and W10RM13.5FA similar with the patterns of W15RM and W20RM (Figure 4.33). These peaks can also be attributed to the ettringite and AH_3 formation. W15RM5FA had slightly shorter induction period than W10RM13.5FA which may be explained by their difference in alkali contents from the red mud use. However, W10RM13.5FA demonstrates broader peaks than W15RM5FA as a result from its longer hydration reaction period and it evolved more total heat (Figure 4.36) which could support its later strength development.

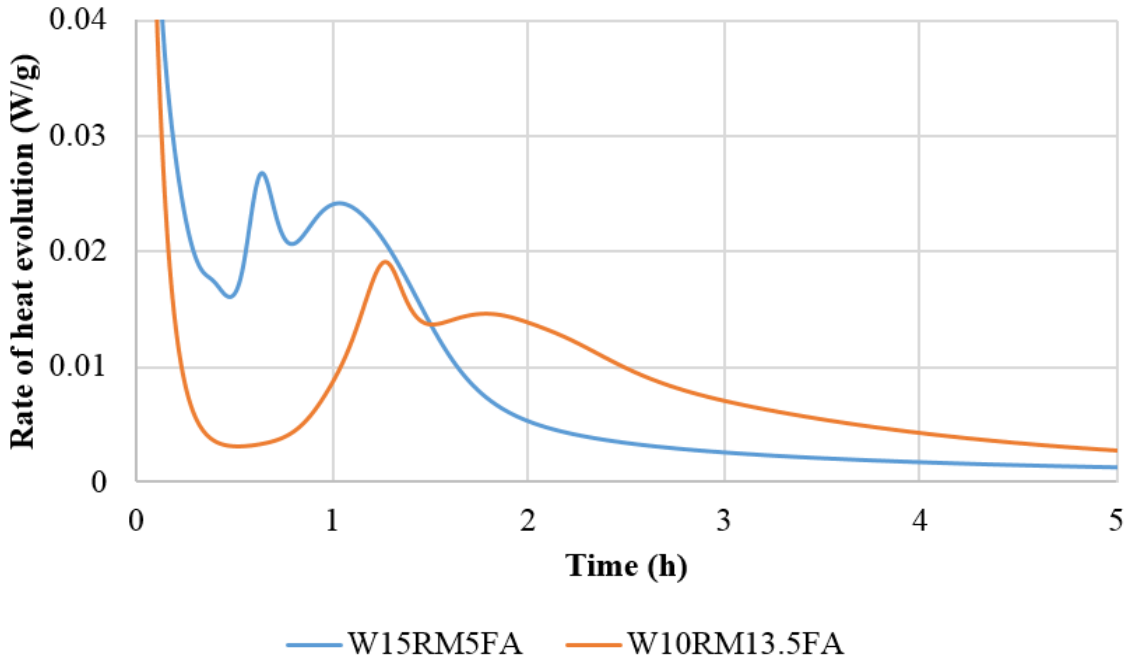

Figure 4.35 Rate of heat evolution for cement pastes containing W15RM5FA and W10RM13.5FA, and desulfogypsum with clinker-to-desulfogypsum ratio of 81:19

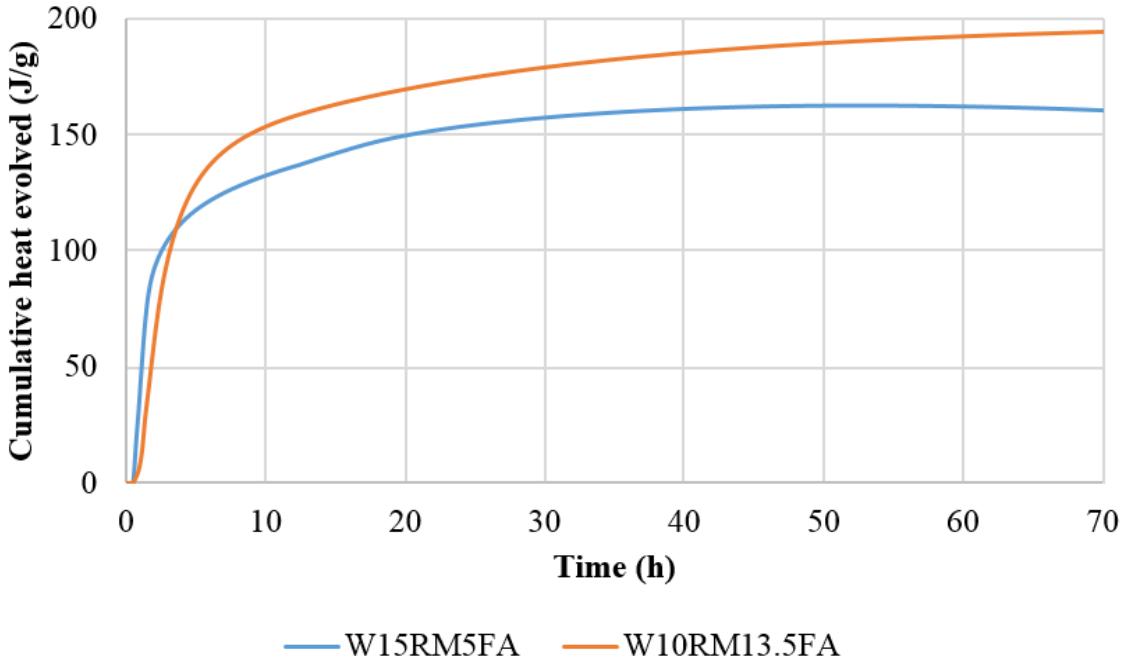

Figure 4.36 Cumulative heat evolved for pastes containing W15RM5FA, W10RM13.5FA, and desulfogypsum with clinker-to-desulfogypsum ratio of 81:19

Figure 4.37 and Figure 4.38 show the rate of heat evolution and cumulative heat evolution, respectively, for CS̄A cement pastes containing only fly ash as a waste material in the clinker raw mixture.

It can be seen in Figure 4.37 that W45FA and W48FA had ~2h shorter induction periods than W5FA which may also be explained by the increasing alkali content of such. W45FA and W48FA demonstrated similar heat evolution peaks while W5FA had a small peak between 2.5-3h prior to its main peak. This small peak probably shows the transformation of bassanite to gypsum (Burris and Kurtis, 2018). As expected from the phase compositions of such clinkers and their strength gain, W5FA evolved significantly more total heat (>50 J/g) than W45FA and W48FA (Figure 4.38).

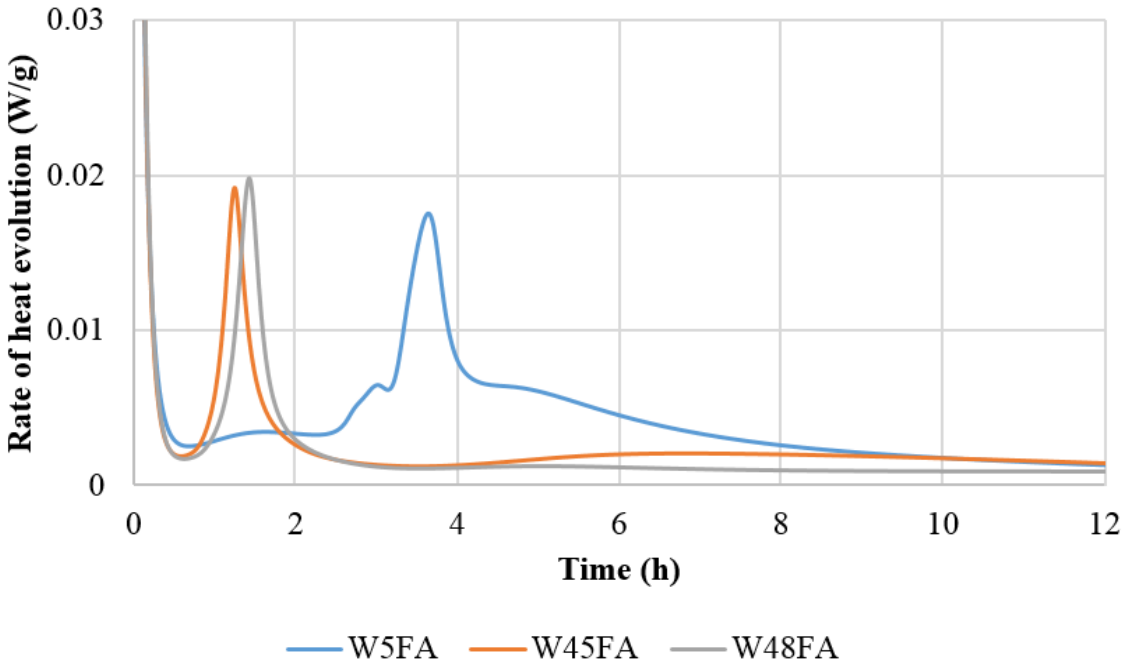

Figure 4.37 Rate of heat evolution for pastes containing W5FA, W45FA and W48FA, and desulfogypsum with clinker-to-desulfogypsum ratio of 76:24 for W5FA and W48FA, and 81:19 for W45FA

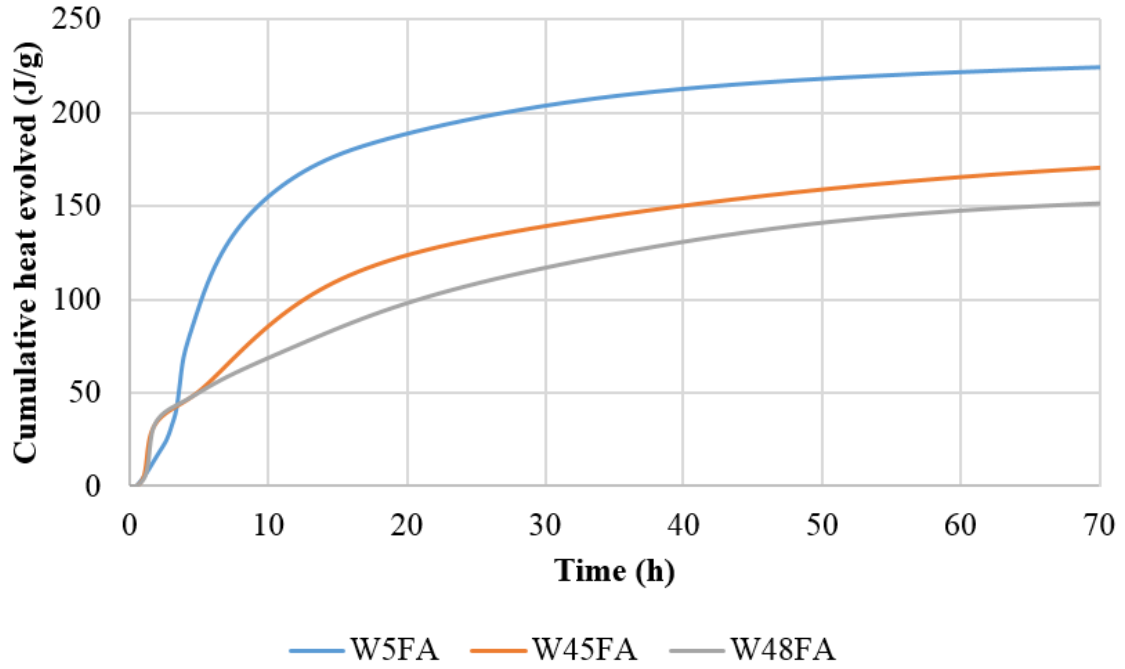

Figure 4.38 Cumulative heat evolved for pastes containing W5FA, W45FA and W48FA, and desulfogypsum with clinker-to-desulfogypsum ratio of 76:24 for W5FA and W48FA, and 81:19 for W45FA

4.6.4 Thermal Analysis

Mixtures provided in Table 4.32, were also subjected to thermal analysis. Figure 4.39 and Figure 4.40 comparatively show the heat flow and mass loss of pastes containing W10RM, W15RM and W20RM at various hydration times, respectively. Table 4.33 shows the relative proportions of loss of water and loss of CO_2 in total mass loss of such C$\bar{S}$A cement pastes.

Figure 4.39 shows the formation of ettringite (weight loss between 80-150 °C), gypsum (weight loss between 100-160 °C), AH_3 (weight loss between 250-280 °C) and calcite (weight loss at around 700-800 °C) for such pastes which is also in conjunction with their XRD analyses. Strong overlapping within the peaks of ettringite and gypsum can be observed for W10RM and W15RM at Figure 4.39b. Furthermore, Figure 4.39a shows small additional peaks around 270-340 °C and 900 °C for W15RM and W20RM. These small peaks could be related with the presence of monocarboaluminate or hemicarboaluminate phases beside of the dehydration of AH_3 (Duvallet, 2014). Figure 4.40 shows similar rates of total weight loss for these pastes, but it can be seen especially from Figure 4.40b that relative contributions to weight loss from hydrated (<600 °C) or carbonated phases (600-1100 °C) varied greatly for each clinker paste. Table 4.33 also confirms such phenomenon by demonstrating relatively sharp carbonation of W20RM than others with ongoing hydration.

Table 4.33 Calculated loss of water and CO_2 for cement pastes containing W10RM, W15RM and W20RM, and desulfogypsum with clinker-to-desulfogypsum ratio of 81:19, at 3 and 28 days of hydration, as % of their total mass loss

Clinker ID	**Loss of H_2O (%)**		**Loss of CO_2 (%)**	
	3 days	**28 days**	**3 days**	**28 days**
W10RM	91.8	80.3	8.2	19.7
W15RM	85.3	76.2	14.7	23.8
W20RM	85.9	64.6	14.1	35.4

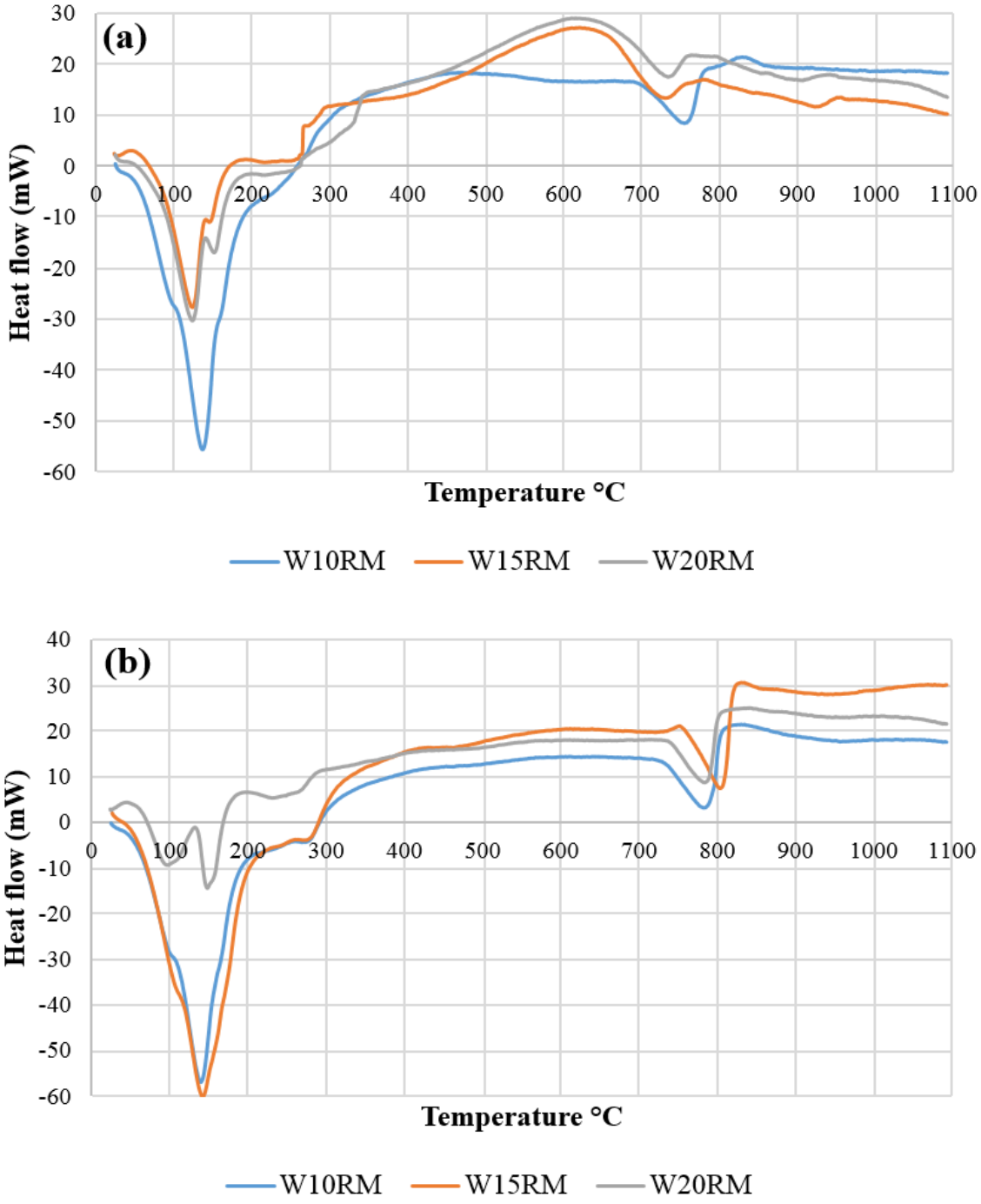

Figure 4.39 Heat flow of cement pastes containing W10RM, W15RM and W20RM, and desulfogypsum with clinker-to-desulfogypsum ratio of 81:19, a) 3 days of hydration; b) 28 days of hydration

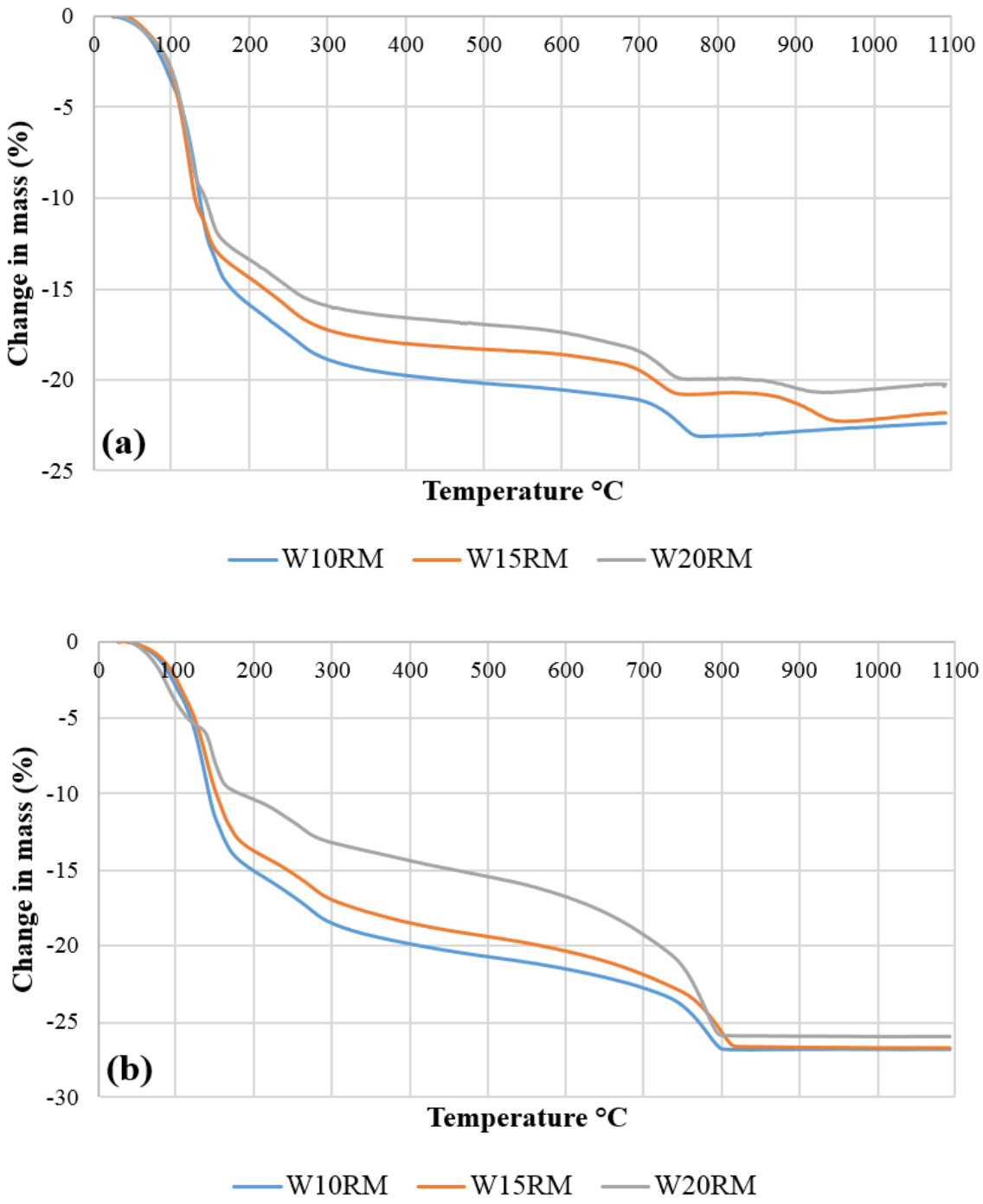

Figure 4.40 Mass loss of cement pastes containing W10RM, W15RM and W20RM, and desulfogypsum with clinker-to-desulfogypsum ratio of 81:19, a) 3 days of hydration; b) 28 days of hydration

Figure 4.41 and Figure 4.42 comparatively show the heat flow and mass loss of pastes containing W15RM5FA and W10RM13.5FA at various hydration times, respectively. Table 4.34 shows the relative proportions of loss of water and loss of CO_2 in total mass loss of such C$\bar{S}$A cement pastes.

Compared to the minerals formed within only red mud incorporated clinkers as waste materials, combination of fly ash with red mud in CS̄A clinker raw mixture could not make any significant impact as shown in Figure 4.41. Formation of ettringite, gypsum, AH_3 and calcite can also be identified in Figure 4.41. Similar with W15RM (Figure 4.39a), W15RM5FA also had a small peak around 900 °C which can be attributed to the mono- or hemicarboaluminate phases. Figure 4.42 shows similar total mass loss for W15RM5FA and W10RM13.5FA. However, Table 4.34 indicates more carbonated phases formed in W15RM5FA at 3 and 28 days of hydration than in W10RM13.5FA which confirms their XRD patterns.

Table 4.34 Calculated loss of water and CO_2 for cement pastes containing W15RM5FA and W10RM13.5FA, and desulfogypsum with clinker-to-desulfogypsum ratio of 81:19, at 3 and 28 days of hydration, as % of their total mass loss

Clinker ID	Loss of SBW (%)		Loss of CO_2 (%)	
	3 days	28 days	3 days	28 days
W15RM5FA	81.9	78.1	18.1	21.9
W10RM13.5FA	93.0	84.9	7.0	15.1

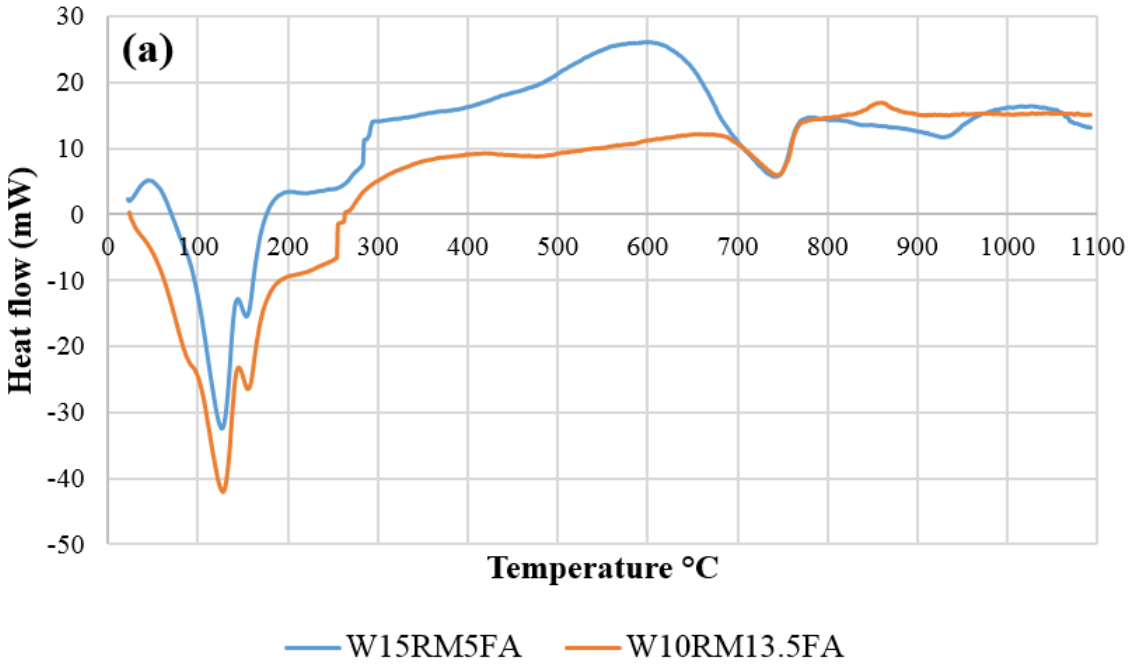

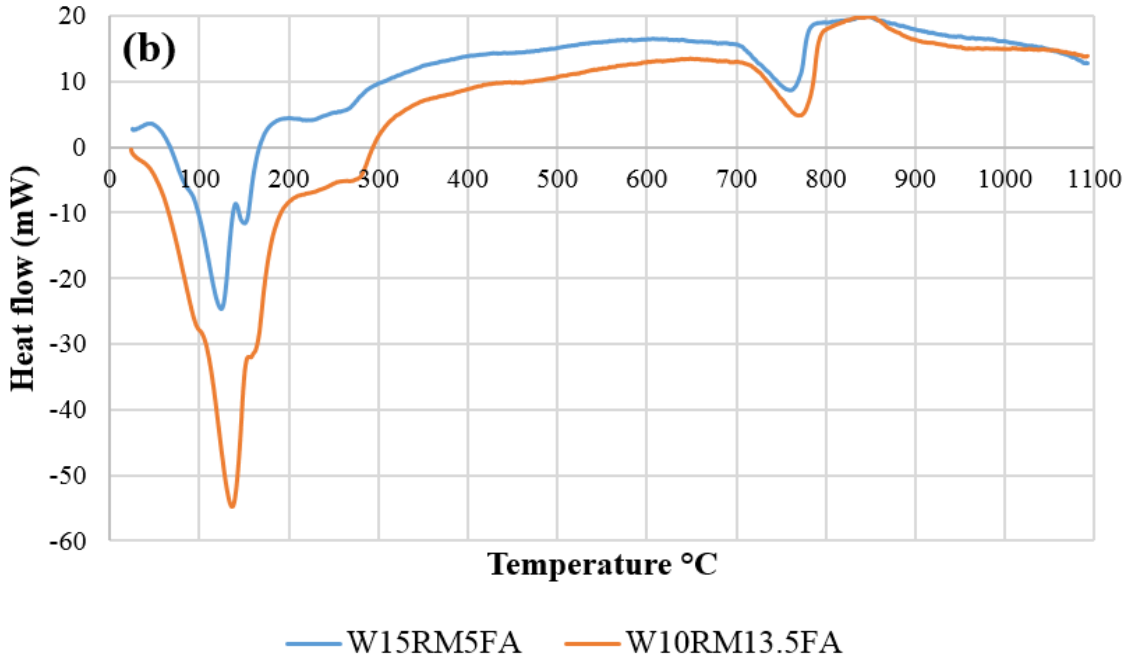

Figure 4.41 Heat flow of cement pastes containing W15RM5FA and W10RM13.5FA, and desulfogypsum with clinker-to-desulfogypsum ratio of 81:19, a) 3 days of hydration; b) 28 days of hydration

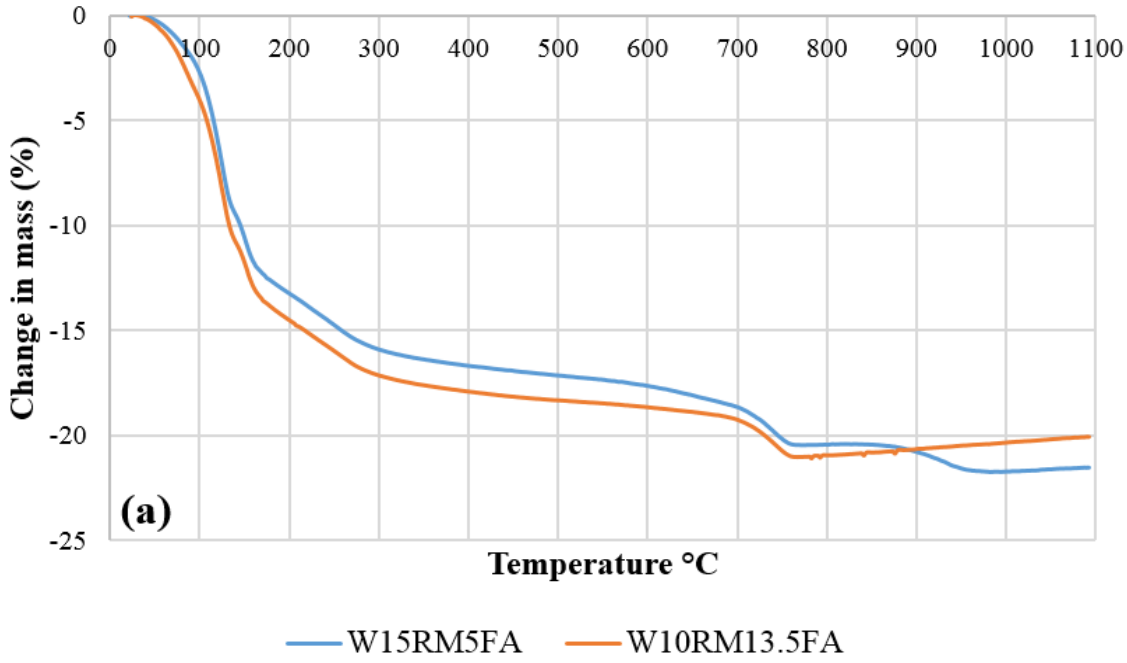

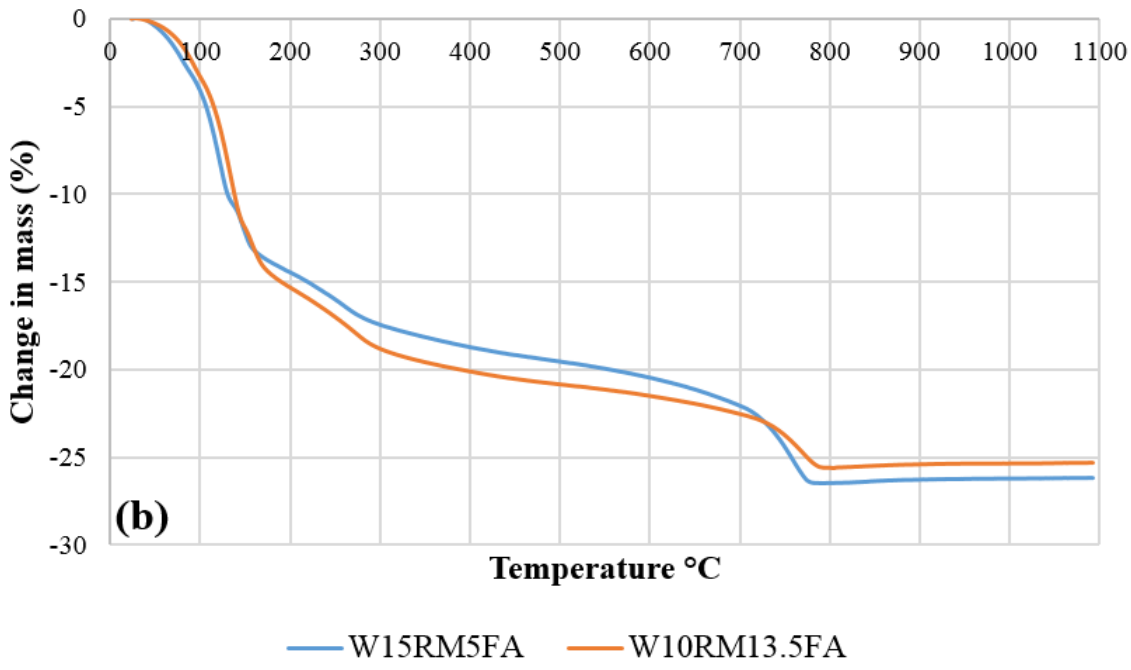

Figure 4.42 Mass loss of cement pastes containing W15RM5FA and W10RM13.5FA, and desulfogypsum with clinker-to-desulfogypsum ratio of 81:19, a) 3 days of hydration; b) 28 days of hydration

Figure 4.43 and Figure 4.44 comparatively show the heat flow and mass loss of pastes containing W5FA, W45FA and W48FA at various hydration times, respectively. Table 4.35 shows the relative proportions of loss of water and loss of CO_2 in total mass loss of such C$\bar{S}$A cement pastes.

Ettringite, gypsum, AH_3 and calcite were the identified minerals formed in such pastes. Mono- or hemicarboaluminate peaks between 900-1000 °C can be seen in Figure 4.43a for W5FA and W48FA. Figure 4.43b shows unidentified peaks around 900 °C for W45FA and W48FA which corresponded to small weight increase. These peaks may be associated with the oxidation of reduced sulfur ions (S^{-2}) which can lead to weight increase from its transformation to sulfate with oxidation (Scrivener et al., 2016b). Figure 4.44 shows that weight loss from ettringite decomposition (80-150 °C) in W5FA was significantly higher than that in W45FA and W48FA which is also compatible with the highest strength gain of W5FA among them. Even though all three pastes have lost similar weights up to 1100 °C (Figure 4.44b), relative weight loss from hydrated phases were significantly higher for W5FA than others (~15 %), as given in Table 4.35. Table 4.35 also proves that W48FA demonstrated relatively rapid carbonation, mostly until 3 days of hydration, while other pastes, especially W45FA,

were carbonated mostly between 3 and 28 days. The sharp increase in main calcite peak (29-30 °2θ) of W45FA, from 3-to-28 days, shown in Figure 4.32, also supports such phenomenon.

Table 4.35 Calculated loss of water and CO_2 for cement pastes containing W5FA, W45FA and W48FA, and desulfogypsum with clinker-to-desulfogypsum ratio of 76:24 for W5FA and W48FA and 81:19 for W45FA, at 3 and 28 days of hydration, as % of their total mass loss

Clinker ID	Loss of H_2O (%)		Loss of CO_2 (%)	
	3 days	28 days	3 days	28 days
W5FA	76.2	72.0	23.8	28.0
W45FA	89.8	57.2	10.2	42.8
W48FA	58.8	57.0	41.2	43.0

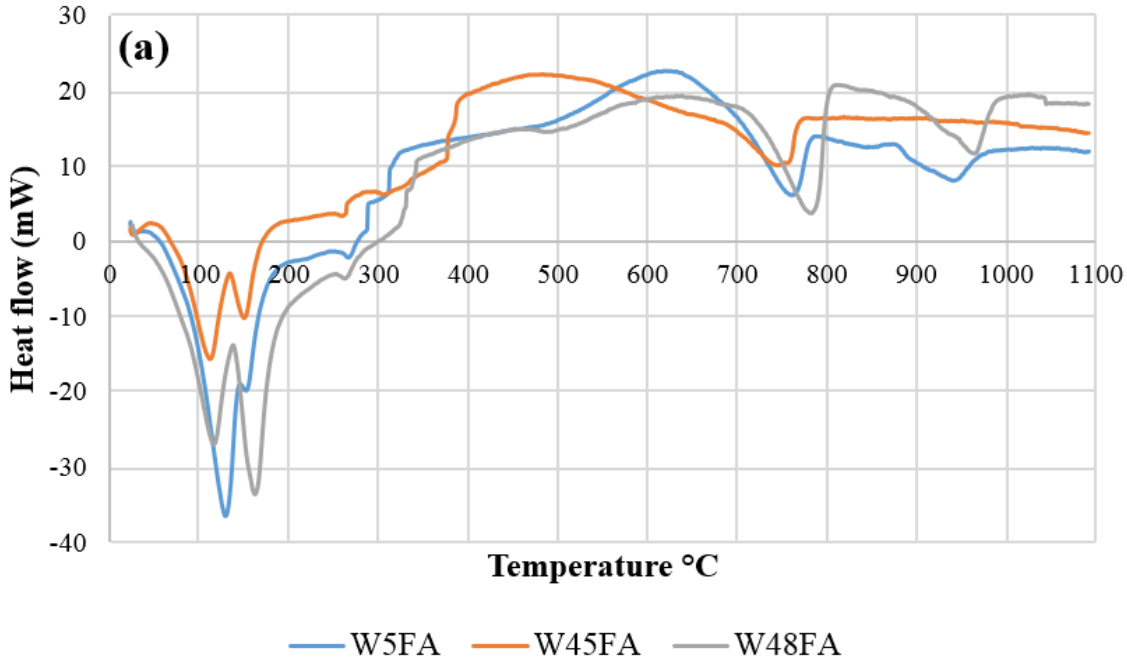

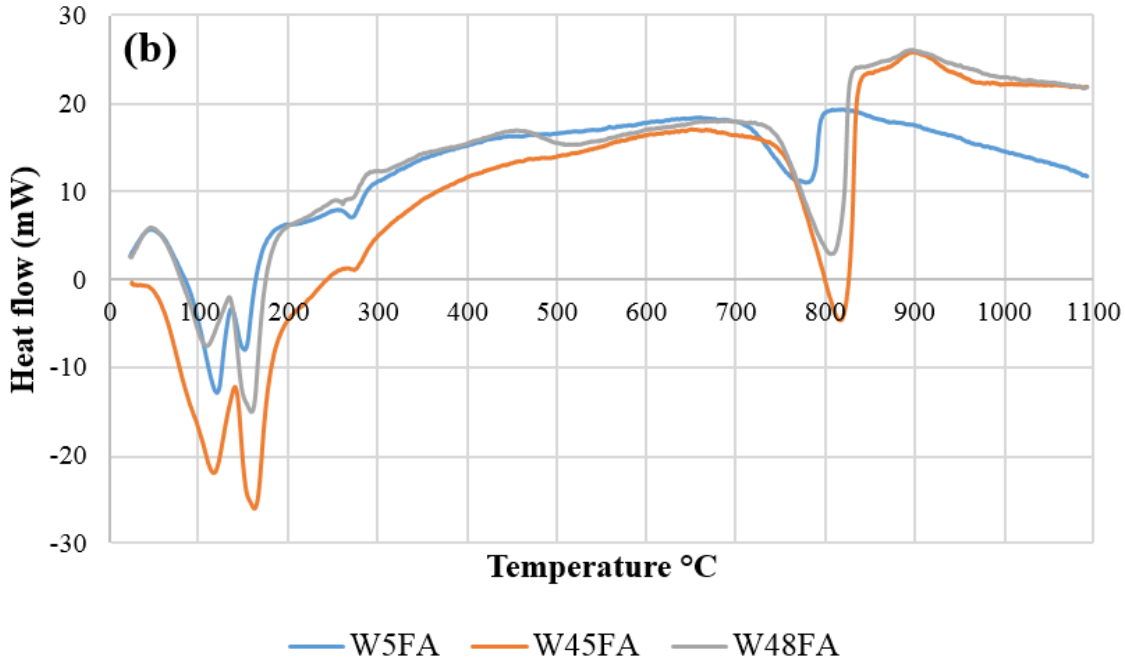

Figure 4.43 Heat flow of cement pastes containing W5FA, W45FA and W48FA, and desulfogypsum with clinker-to-desulfogypsum ratio of 76:24 for W5FA and W48FA and 81:19 for W45FA, a) 3 days of hydration; b) 28 days of hydration

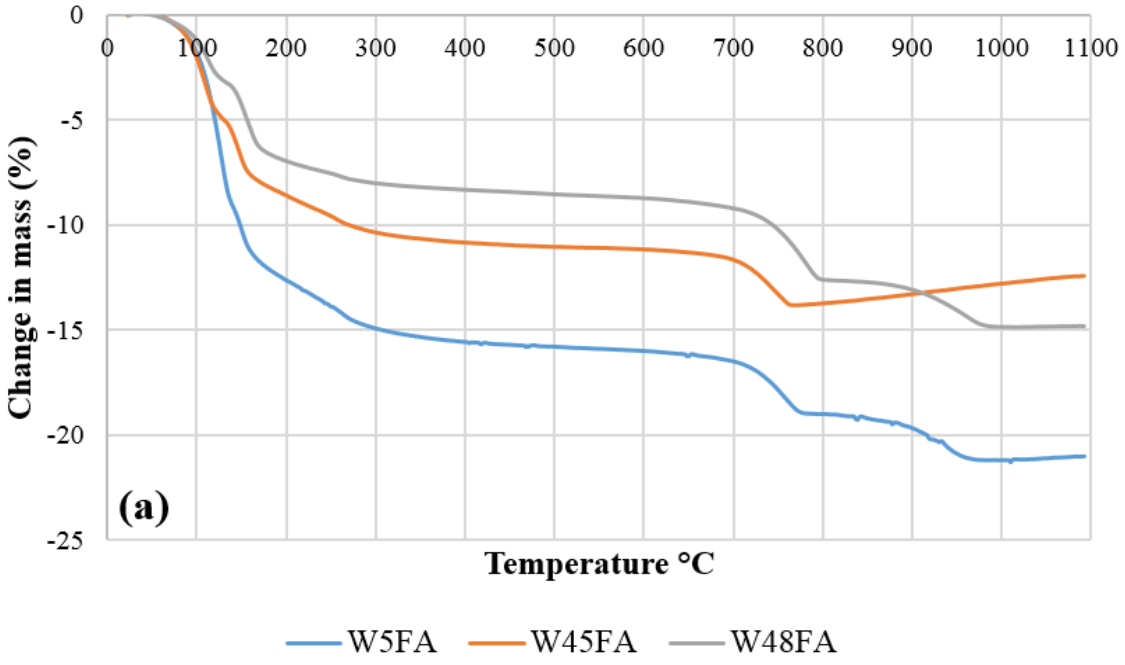

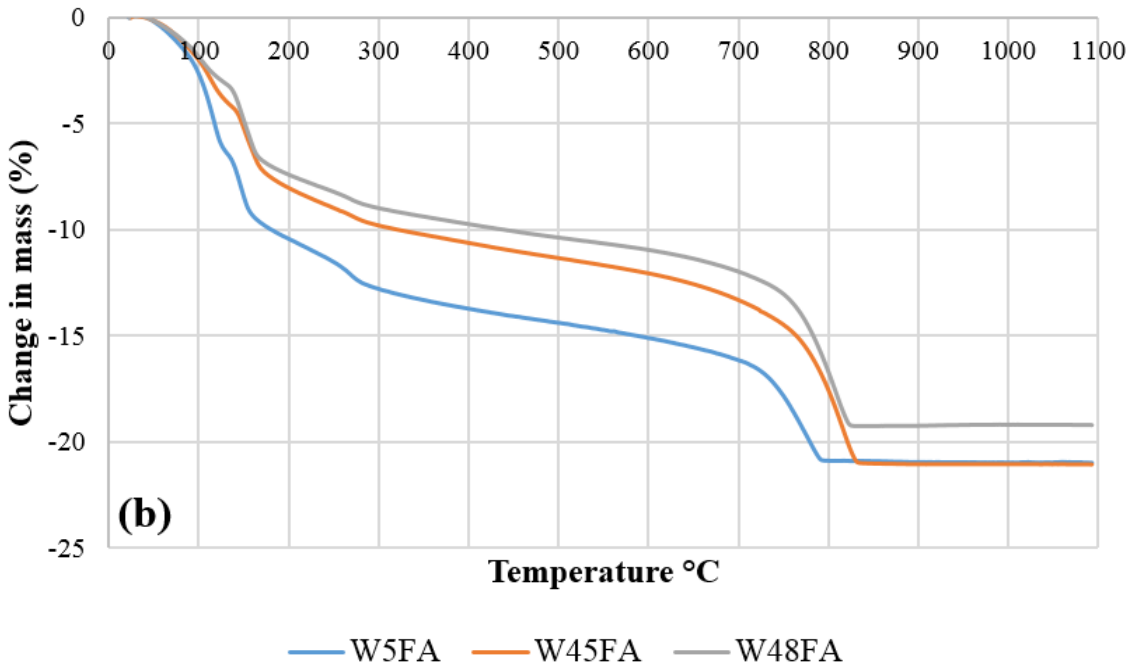

Figure 4.44 Mass loss of cement pastes containing W5FA, W45FA and W48FA, and desulfogypsum with clinker-to-desulfogypsum ratio of 76:24 for W5FA and W48FA and 81:19 for W45FA, a) 3 days of hydration; b) 28 days of hydration

4.7 Investigation of the Hydrated CS̄A Cements Using SEM

4.7.1 SEM Images of CS̄A Cements Produced Using Only Natural Materials

Figure 4.45 shows the SEM images of cement paste containing N2 at 3 days of hydration. A close-up of the region of interest (E1) marked in Figure 4.45a, is displayed in Figure 4.45b. Figure 4.46 demonstrates the microstructure of cement paste containing N6 at 3 days of hydration with two SEM images. A particle was marked in Figure 4.46b to be identified with EDX. Table 4.36 gives the elemental composition of E1 and E2 present in Figure 4.45a and Figure 4.46b, respectively, as atomic weight percentage. SEM images of cement pastes including N2 and N6 that were not demonstrated in this section, is provided in Appendix B.

Figure 4.45a shows ettringite crystals surrounded by some unhydrated particles and amorphous hydration products which could be AH_3. Also, the sponge-like fraction can be attributed to the ye'elimite with ettringite formed in its pores (El-Alfi and Gado, 2016). Table 4.36 reveals that E1 was the ye'elimite phase where partial substitution occurred between Al^{3+} and Fe^{3+} ions. Small needles in E1 which can be observed

clearly in Figure 4.45b, may be related with Fe^{3+} ions accumulated on the surface of ye'elimite. Figure 4.46 shows similar structure between the N2-cement paste and the N6-cement paste. The marked region of interest (E2) in Figure 4.46b indicates significant carbonation of an unhydrated phase which might be ye'elimite. Recently, this possibility has been reported in a study by Hargis et al. (2017) where 1 mole of ye'elimite has 3 moles of CO_2 binding capacity, mainly from CaO content, which corresponds to ~22 g CO_2 per 100 g of ye'elimite.

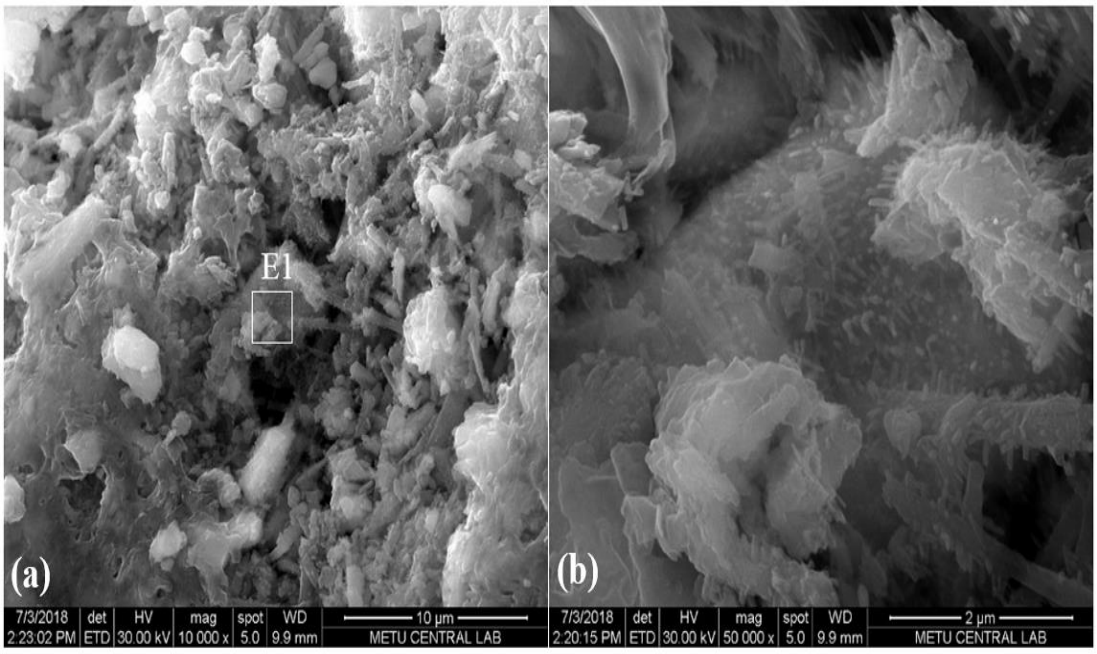

Figure 4.45 SEM images of hydrated cement paste containing N2 and gypsum with clinker-to-gypsum ratio of 76:24 at 3 days of hydration where the microstructure is displayed

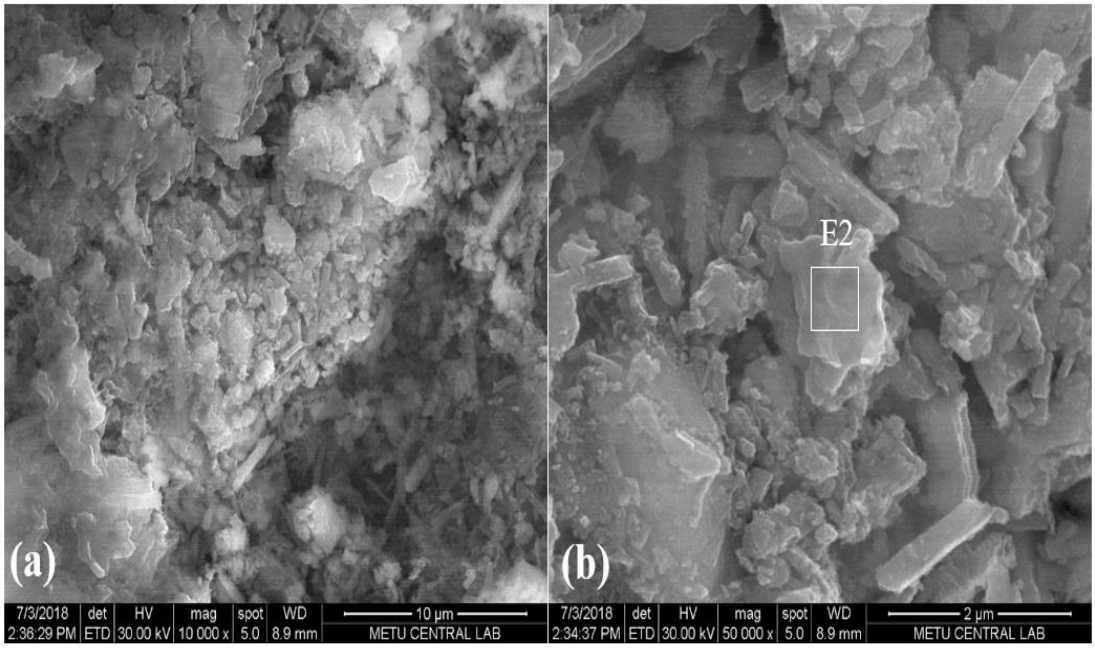

Figure 4.46 SEM images of hydrated cement paste containing N6 and gypsum with clinker-to-gypsum ratio of 76:24 at 3 days of hydration where the microstructure is displayed

Table 4.36 Atomic weight ratios of marked points (E1 and E2)

Element (%)	E1	E2
C	0	27.39
O	65.93	51.12
Al	10.72	7.24
Si	1.58	1.24
S	4.39	3.73
Ca	13.79	8.62
Cr	0.05	0
Mn	0.03	0
Fe	3.52	0.65

4.7.2 SEM Images of CS̄A Cements Containing Waste Materials

Figure 4.47 shows SEM images of cement paste containing W15RM at 3 days of hydration with a marked region of interest in Figure 4.47b corresponding to a particle surrounded by some hydration products. Figure 4.48 exhibits the microstructure of cement paste containing W10RM13.5FA at 3 days of hydration. A small particle was marked in Figure 4.48b to examine its elemental composition with EDX. Table 4.37 gives the elemental composition of E3 and E4 present in Figure 4.47b and Figure 4.48b, respectively, as atomic weight percentage. Figure 4.49 demonstrates the

microstructure of W45FA-cement paste. SEM images of cement pastes including W15RM, W10RM13.5FA and W45FA are not given in this section, but provided in Appendix B.

Figure 4.47 shows a denser accumulation for the W15RM-cement paste compared to others (Figure 4.48 and Figure 4.49). This could be associated with the enhanced reactivity of ye'elimite in the presence of alkalis as mentioned in Section 4.6.3 which corresponded to more hydration products up to 3 days. Also, EDX analysis of E3 in (Table 4.37) favors the alkali (Na and K) incorporation into ye'elimite with binded CO_2. Figure 4.48b shows a relatively higher amount of unhydrated clinker grains for W10RM13.5FA-cement paste which could be associated with its slower strength gain at early ages as ~40 % 28-day compressive strength achieved up to 3 days (Figure 4.27). EDX analysis of E4 shown in Table 4.37 indicates a CO_2 binded phase which could be ye'elimite with some caged silicon elements. Relatively higher silicon content may be related with the increased fly ash content in the raw mixture of W10RM13.5FA. Unlike the former cement pastes, EDX analysis was not performed on any specific particle present in W45FA-cement paste. However, it is observed from Figure 4.49 that ettringite crystals were the least visible in W45FA-cement paste among all clinkers investigated. This phenomenon can also be seen in the XRD pattern of W45FA-cement paste (Figure 4.32) which shows less intense ettringite peaks compared to others.

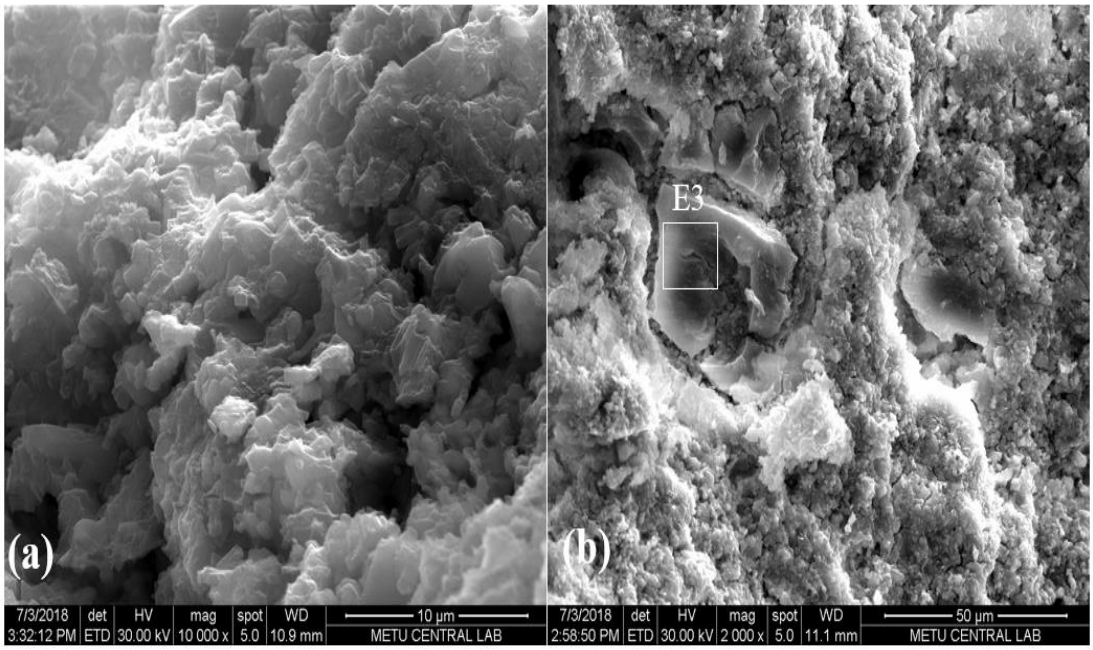

Figure 4.47 SEM images of hydrated cement paste containing W15RM and desulfogypsum with clinker-to-desulfogypsum ratio of 81:19 at 3 days of hydration where the microstructure is displayed

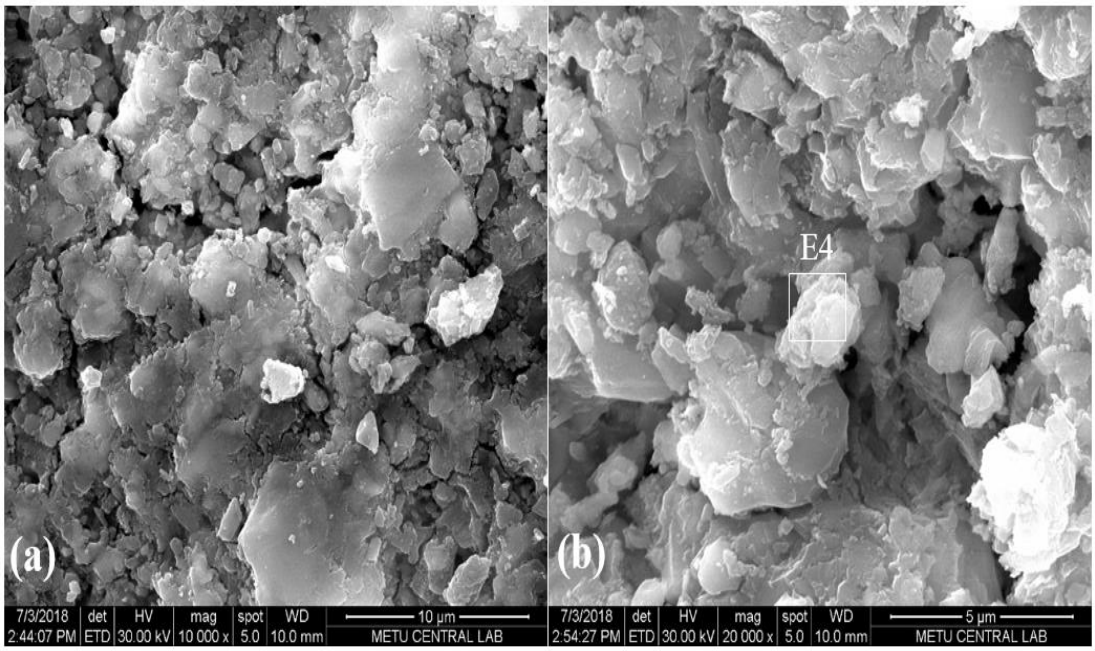

Figure 4.48 SEM images of hydrated cement paste containing W10RM13.5FA and desulfogypsum with clinker-to-desulfogypsum ratio of 81:19 at 3 days of hydration where the microstructure is displayed

Table 4.37 Atomic weight ratios of marked points (E3 and E4)

Element (%)	E3	E4
C	10.14	16.01
O	56.41	47.84
Na	2.89	0
Al	16.24	13.44
Si	0.68	2.67
S	5.56	3.75
K	0.33	0
Ca	7.21	15.22
Fe	0.54	1.00

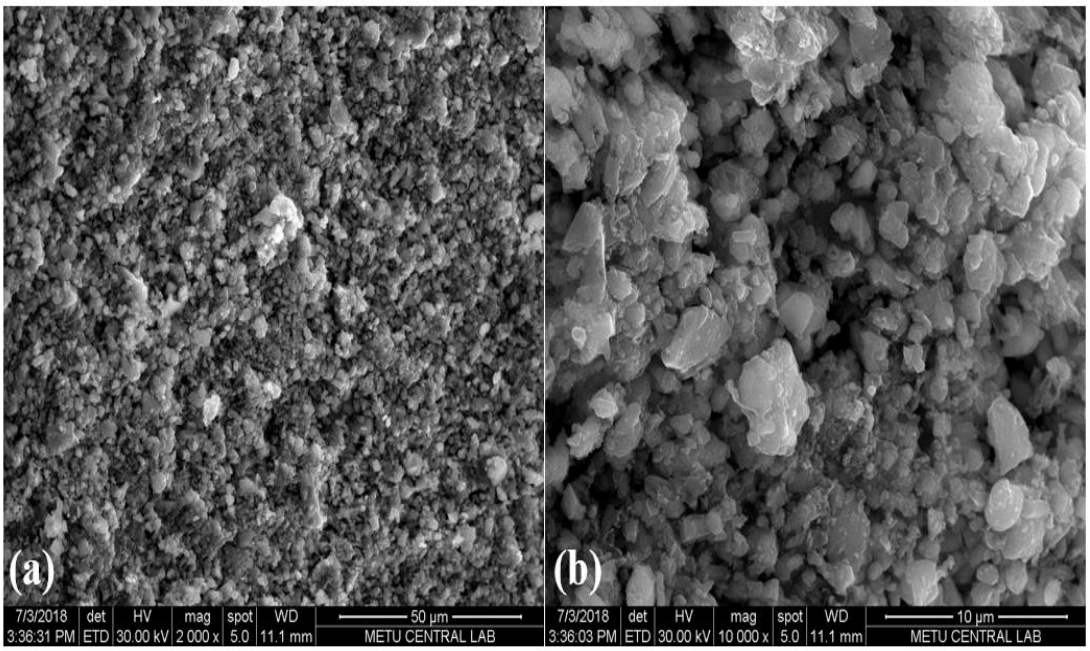

Figure 4.49 SEM images of hydrated cement paste containing W45FA and desulfogypsum with clinker-to-desulfogypsum ratio of 81:19 at 3 days of hydration where the microstructure is displayed

CHAPTER 5

CONCLUSIONS AND RECOMMENDATIONS

5.1 Conclusions

Even though laboratory production of CS̄A clinker has been realized many times, the method adopted in this study can be considered as a novel one. Mostly, CS̄A clinker production methods in the literature where presents both synthesis of reagent-grade chemicals and combination of natural and waste materials, are limited with small quantities. However, more than 60 kg of various CS̄A clinkers have been produced during this study where the method allowed 1 kg clinker production per trial. Furthermore, several parameters that affect the performance and characteristics of the CS̄A clinkers produced were investigated using different techniques. The following conclusions can be drawn:

- CS̄A clinker production is possible using both natural and industrial waste materials at appropriate levels. However, there are limitations to the raw mixture proportioning stemming from the oxide compositions of the raw materials which determines the phase composition of clinker produced.
- Ye'elimite, belite, ferrite and anhydrite were the main phases formed in the CS̄A clinkers produced. Especially, the amount of anhydrite and ye'elimite formed in CS̄A clinker, as determined by XRD quantitative analysis, can significantly deviate from those predicted by modified Bogue' s equations. However, both Bogue's equations and XRD quantitative analysis can predict the free lime formation which was suppressed in this study as a result of thorough clinkerization.
- Grindability of CS̄A clinkers is satisfactory due to their higher porosity compared to Portland cement. Even though increased red mud content in the

clinker raw mixture does not greatly affect their grindability, clinkers incorporating highly amounts of fly ash (W45FA, W48FA) exhibited relatively poor grindability.

- The main hydration products formed in C$\bar{S}$A cements were ettringite, gypsum and AH_3 up to 28 days of hydration. Most of the hydration takes place up to 3 days then slows down due to the coating of unhydrated particles with ettringite and AH_3.
- Strength development of C$\bar{S}$A clinker is not affected significantly by a change in fineness between 3000-6000 cm^2/g. However, producing clinker with higher fineness could increase the water demand of the clinker and increase the energy required during manufacturing.
- 1250 °C as the kiln temperature and 90 minutes as the kiln residence time were found to be favorable to produce C$\bar{S}$A clinker with good performance considering energetic and environmental impact. Temperatures higher than 1300 °C are not beneficial.
- Higher amounts of calcium sulfate to be added to C$\bar{S}$A clinker during cement production are preferable since it leads to dilution of clinker in the system which is better for environment. However, flow of hydraulic cement mortars can be significantly affected by the added gypsum amount because of the increased water demand if gypsum used was not 100 % dihydrate.
- Increased sulfate in the C$\bar{S}$A cement corresponds to a higher degree of reaction of phases, mainly ye'elimite, therefore, higher compressive strengths can be achieved at later ages. Desulfogypsum is more advantageous than gypsum to be added to the system in terms of strength gain, because of its higher sulfur content and reactivity.
- Use of a retarder (citric acid) is fruitful in terms of strength gain since it reduces the required water-to-cement ratio. Also, it is necessary to use a retarder for mixtures containing desulfogypsum because of its great water demand.
- Ye'elimite content in C$\bar{S}$A clinkers determines the early strength while other phases, especially belite, contribute to later strength gain. However, amount of ye'elimite to be formed is limited mainly by the alumina content of bauxite or other alternative materials used. Therefore, enhancing the reactivities of these phases should be focused on.

- It is possible to reach a 28-day compressive strength >50 MPa using natural materials only and >40 MPa with industrial waste materials in the clinker raw mixture where proportion of bauxite can be reduced up to 20 %, by mass.
- Presence of alkalies, especially in red mud, enhanced the reactivity of ye'elimite which corresponded to shorter induction periods of hydrated cement pastes. Sodium and potassium can be possibly accommodated in the ye'elimite structure. Also, total heat production of all produced C$\bar{S}$A clinkers generally varied between 150-200 J/g and was not affected much by the incorporation of waste materials.
- Carbonation of ettringite occurs in the hydrated C$\bar{S}$A cement pastes and it increases with increased hydration. The amounts of gypsum, AH_3 and calcite increase as ettringite decomposes. Strength gain of mortars up to 28 days was not affected by carbonation even though possible reinforcement corrosion due to the reduced alkalinity can be considered a possible drawback for such clinkers.

5.2 Recommendations

- Lower temperatures and shorter residence times (than 1250 °C and 90 minutes, respectively), should be used during the production of C$\bar{S}$A clinkers to investigate the possible clinker production at low levels of energy.
- Different methods to increase the reactivities of belite and ferrite phases such as quenching or using dopants should be tried to produce C$\bar{S}$A clinkers with better performance.
- Other industrial waste materials generated in high quantities in Turkey (such as blast furnace slag, soda waste sludge, pozzolans and fly ashes from other sources) should also be used in the clinker raw mixture.
- Concrete made of C$\bar{S}$A clinkers in this study should be produced and investigated to test the performance of C$\bar{S}$A clinkers in large-scale implementations.
- Effects of carbonation in C$\bar{S}$A cements should be further investigated until later ages (longer than 28 days).

- In addition to carbonation, other durability issues such as dimensional stability and alkali-aggregate reaction should be investigated for the C$\bar{S}$A clinkers produced.

REFERENCES

Alvarez-Pinazo, G., Santacruz, I., León-Reina, L., Aranda, M.A.G., De la Torre, A.G. (2013). Hydration Reactions and Mechanical Strength Developments of Iron-Rich Sulfobelite Eco-Cements. *Industrial & Engineering Chemistry Research*, 52, 16606–16614.

Andac, O., Glasser, F.P. (1994). Polymorphism of Calcium Sulphoaluminate ($Ca_4Al_6O_{16}SO_3$) and its Solid Solutions. *Advances in Cement Research*, 22, 57–60.

Andac, M., Glasser, F.P. (1999). Pore Solution Composition of Calcium Sulfoaluminate Cement. Advances in Cement Research, 11, 23–26.

ASTM C 109. (2016). Standard Test Method for Compressive Strength of Hydraulic Cement Mortars (Using 2-in. or [50-mm] Cube Specimens). ASTM International, West Conshohocken, PA

ASTM C 188. (2016). *Standard Test Method for Density of Hydraulic Cement*. ASTM International, West Conshohocken, PA.

ASTM C 204. (2016). *Standard Test Methods for Fineness of Hydraulic Cement by Air-Permeability Apparatus.* American Society of Testing and Materials, West Conshohocken, PA.

ASTM C 305. (2014). Standard Practice for Mechanical Mixing of Hydraulic Cement Pastes and Mortars of Plastic Consistency. American Society of Testing and Materials, West Conshohocken, PA.

ASTM C 1437. (2015). *Standard Test Method for Flow of Hydraulic Cement Mortar*. ASTM International, West Conshohocken, PA.

Beretka, J., Santoro, L., Sherman, N., Valenti, G.L. (1992). Synthesis and Properties of Low Energy Cements Based on $4CaO.3Al_2O_3.SO_3$. in *Proceedings of the*

9th International Congress on the Chemistry of Cement, New Delhi, India, 1, 292-318.

Beretka, J., Sherman, N., Maroccoli, M., Pompo, A., Valenti, G.L. (1997). Effect of Composition on the Hydration Properties of Rapid-Hardening Sulfoaluminate Cements. in *Proceedings of the 10th International Congress on the Chemistry of Cement*, Gothenburg, Sweden, Ed. H. Justnes, 2, 2ii029, 8pp.

Bernardo, G., Telesca, A., Valenti, G.L. (2006). A Porosimetric Study of Calcium Sulfoaluminate Cement Pastes Cured at Early Ages. *Cement and Concrete Research*, 36, 1042-1047.

Bernardo, G., Buzzi, L., Canonico, F., Paris, M., Telesca, A., Valenti, G.L. (2007). Microstructural Investigations on Hydrated High-Performance Cements Based on Calcium Sulfoaluminate. in *Proceedings of the 12th International Congress on the Chemistry of Cement*, Paper W3–11.4, Montreal, Canada.

Brunori, C., Cremisini, C., Massanisso, P., Pinto, V., Torricelli, L. (2005). Reuse of a Treated Red Mud Bauxite waste: Studies on Environmental Compatibility. *Journal of Hazardous Materials*, 117, 55-63.

Bullerjahn, F., Schmitt, D., Ben Haha, M. (2014). Effect of Raw Mix Design and of Clinkering Process on the Formation and Mineralogical Composition of (Ternesite) Belite Calcium Sulphoaluminate Ferrite Clinker. *Cement and Concrete Research*, 59, 87–95.

Burris, L. E., Kurtis, K. E. (2018). Influence of Set Retarding Admixtures on Calcium Sulfoaluminate Cement Hydration and Property Development. *Cement and Concrete Research*, 104, 105-113.

CEMBUREAU, Activity Report 2015, Brussels, 2016. http://www.cembureau.be/sites/ default/files/AR2015.pdf.

Chang, J., Zhang, Y., Shang, X., Zhao, J., Yu, X. (2017). Effects of Amorphous AH_3 Phase on Mechanical Properties and Hydration Process of $C_4A_3\bar{S}$-$C\bar{S}H_2$-CH-H_2O System, *Construction and Building Materials*, 133, 314–322.

Chen, I. (2009). Synthesis of Portland Cement and Calcium Sulfoaluminate-Belite Cement for Sustainable Development and Performance. Ph. D. thesis, University of Texas at Austin.

Chen, I.A., Juenger, M.C.G. (2012). Incorporation of Coal Combustion Residuals into Calcium Sulfoaluminate-Belite Cement Clinkers. *Cement & Concrete Composites*, 34, 893-902.

Damidot, D., Glasser, F.P. (1995). Investigation of the $CaO–Al_2O_3–SiO_2–H_2O$ System at 25 °C by Thermodynamic Calculations. *Cement and Concrete Research*, 25, 22–28.

Duvallet, T., Robl, T.L. (2013). Production of Alite-Calcium Sulfoaluminate-Ferrite Cements from Coal and other Industrial By-Products. *World of Coal Ash (WOCA) Conference*, Lexington, KY, USA, April 22-25.

Duvallet, T. (2014). Influence of Ferrite Phase in Alite-Calcium Sulfoaluminate Cements. Ph. D thesis, University of Kentucky, USA.

El-Alfi, E.A., Gado, R.A. (2016). Preparation of Calcium Sulfoaluminate-Belite Cement from Marble Sludge Waste. *Construction and Building Materials*, 113, 764–772.

EN 196-1. (2005). *Methods of Testing Cement – Part 1: Determination of Strength*. European Norm 196-1. Brussels: European Committee for Standardization.

FAO. (2013). Food Wastage Footprint Impacts on Natural Resources: Summary Report, Food and Agriculture Organisation of the United Nations, Rome.

Fukuda, N. (1961). On the Constitution of Sulfo-Aluminous Clinker. *Bulletin of the Chemical Society of Japan*, 34, 138-139

García-Maté, M., Angeles, G., León-Reina, L., Losilla, E.R., Aranda, M.A., Santacruz, I. (2015). Effect of Calcium Sulfate Source on the Hydration of Calcium Sulfoaluminate Eco-Cement. *Cement & Concrete Composites*, 55, 53–61.

Gartner, E. (2004). Industrially Interesting Approaches to “Low-CO2” Cements. *Cement and Concrete Research*, 34, 1489–1498.

Gartner, E. (2017). CSA and Belite-Rich Clinkers and Cements. in Conference of the Future of Cement, 200 years after Louis Vicat, UNESCO, Paris.

Glasser, F.P., Zhang, L. (2001). High-Performance Cement Matrices Based on Calcium Sulfoaluminate-Belite Compositions. *Cement and Concrete Research*, 31, 1881-1886.

Gosh, S.N., Rao, P.B., Paul, A.K., Raina, K. (1979). The Chemistry of Dicalcium Silicate Mineral. *Journal of Materials Science*, 14, 1554-1566.

Grooves, G.W. (1983). Phase Transformations in Dicalcium Silicate. *Journal of Materials Science*, 18, 1615–1624.

Hargis, C. W., Telesca, A., Monteiro, P. J. (2014). Calcium Sulfoaluminate (Ye'elimite) Hydration in the Presence of Gypsum, Calcite and Vaterite. *Cement and Concrete Research*, 65, 15-20.

Hargis, C.W., Moon, J., Lothenbach, B., Winnefeld, F., Wenk, H.R., Monterio, P.J. (2014). Calcium Sulfoaluminate Sodalite (Ca4Al6O12SO4) Crystal Structure Evaluation and Bulk Modulus Determination. *Journal of the American Ceramic Society*, 97, 892–898.

Hargis, C.W., Lothenbach, B., Müller, J.C., Winnefeld, F. (2017). Carbonation of Calcium Sulfoaluminate Mortars. *Cement and Concrete Composites*, 80, 123-134.

Huang, Y., Qian, J., Li, C., Liu, N., Shen, Y., Ma, Y., Sun, H., Fan, Y. (2017). Influence of Phosphorus Impurities on the Performances of Calcium Sulfoaluminate Cement. *Construction and Building Materials*, 149, 37–44.

Jansen, E., Schäfer, W., Will, G. (1994). R Values in Analysis of Powder Diffraction Data Using Rietveld Refinement. *Journal of Applied Crystallography*, 27, 492-496.

Juenger, M.C.G., Winnefeld, F., Provis, J.L., Ideker, J.H. (2011). Advances in Alternative Cementitious Binders. *Cement and Concrete Research*, 41, 1232–1243.

Kasselouri, V. Tsakiridis, P., Malami, C., Georgali, B., Alexandridou, C. (1995). A Study on the Hydration Products of a Non-Expansive Sulfoaluminate Cement. *Cement and Concrete Research,* 25**,** 1726–1736.

Kriskova, L., Pontikes, Y., Zhang, F., Cizer, Ö., Jones, P.T., van Balen, K., Blanpain, B. (2014). Influence of Mechanical and Chemical Activation on the Hydraulic Properties of Gamma Dicalcium Silicate. *Cement and Concrete Research*, 55, 59.

Krivoborodov, Y.R., Samchenko, S.V. (1992). *9th International Congress on Chemistry of Cements*, Proceedings, 3, 209.

Li, G.S., Walenta, G., Gartner, E.M. (2007). Formation and Hydration of Low CO_2 Cements Based on Belite, Calcium Sulfoaluminate and Calcium Aluminoferrite. in *12th International Congress on the Chemistry of Cement, Montreal*, Canada, paper TH3-15.3, July 8–13, 12 pp.

Li, J., Ma, H., Zhao, H. (2007). Preparation of Sulphoaluminate-Alite Composite Mineralogical Phase Cement Clinker from High Alumina Fly Ash. *Key Engineering Materials*, Vols. 334–335, pp 421–424.

Liu, X., Li, Y. (2005). Effect of MgO on the Composition and Properties of Alite-Sulphoaluminate Cement. *Cement and Concrete Research*, 35, 1685–1687.

Lutterotti, L., Matthies, S., Wenk, H. (1999). MAUD (Material Analysis Using Diffraction): A User-Friendly Java program for Rietveld Texture Analysis and More. in *Proceeding of the Twelfth International Conference on Textures of Materials (ICOTOM-12)*, Vol. 1, 1599.

Luz, C.A., Rocha, J.C., Cheriaf, M., Pera, J. (2009). Valorization of Galvanic Sludge in Sulfoaluminate Cement. *Construction and Building Materials*, 23, 595–601.

Mahyar, M., Erdoğan, S. T., (2015). Phosphate-Activated High-Calcium Fly Ash Acid-Base Cements. *Cement and Concrete Composites*, 63, 96–103

Majling, J., Sahu, S., Vlna, M., Roy, D.M. (1993). Relationship between Raw Mixture and Mineralogical Composition of Sulfoaluminate Belite Clinkers in the System CaO-SiO_2-Al_2O_3-Fe_2O_3-SO_3. *Cement and Concrete Research*, 23, 1351- 1356.

Malami, C., Philippou, T., Kasselouri, V., Tsakiridis, P. (1996). A study on the Behavior of Non-Expansive Sulfoaluminate Cement in Aggressive Media. *World Cement*, 27, 129-133.

Martín-Sedeño, M.C., Cuberos, A.J.M., Torre, A.G.D.L, Alvarez-Pinazo, G., Ordonez, L.M, Gateshki, M., Aranda, M.A.G. (2010). Aluminum-Rich Belite Sulfoaluminate Cements: Clinkering and Early Age Hydration. *Cement and Concrete Research*, 40, 359-369.

Mehta, P.K. (1980). Investigations on Energy Saving Cements. *World Cement Technology*, 11, 166–177.

Mehta, P. K, Monteiro, P.J.M. (2006). *Concrete: Microstructure, Properties and Materials*. 3rd. Edition, McGraw-Hill, New York.

Mindess, S., Young, J.F., Darwin, D. (2003). *Concrete*. 2nd. Edition, Pearson Education, Inc., Upper Saddle River, NJ.

Nedeljkovic, M., Arbi Ghanmi, K., Zuo, Y., Ye, G. (2016). Microstructural and Mineralogical Analysis of Alkali Activated Fly Ash-Slag Pastes. In C. Miao, W. Sun, J. Liu, H. Chen, G. Ye, & K. van Breugel (Eds.), in *3rd International RILEM Conference on Microstructure Related Durability of Cementitious Composites*, Nanjing, China., 117, pp. 1-10, RILEM publications S.A.R.L.

Odler, I. (2000). *Special Inorganic Cements*. E&FN Spon, New York, NY.

Ono, Y. (1980). Microscopical Estimation of Burning Condition and Quality of Clinker. in *7th International Congress on the Chemistry of Cement*, Paris, II, I-206 - I-211.

Osokin, A.P., Krivoborodov Y.R., Dukova, N.F. (1992). Sulfoferrite Cements. in *9th International Congress on Chemistry of Cements*, Proceedings, 3, 256.

Pelletier, L., Winnefeld, F., Lothenbach, B. (2010). The Ternary System Portland Cement– Calcium Sulphoaluminate Clinker–Anhydrite: Hydration Mechanism and Mortar Properties. *Cement & Concrete Composites*, 32, 497–507.

Péra, J., Ambroise, J. (2004). New Applications of Calcium Sulfoaluminate Cements. *Cement and Concrete Research*, 34, 671–676.

Puertas, F., Varela, M.T.B., and Molina, S.G. (1995). Kinetics of Thermal Decomposition of $C_4A_3\bar{S}$ in Air. *Cement and Concrete Research*, 25, 572–580.

Quillin, K. (2001). Performance of Belite-Sulfoaluminate Cements. *Cement and Concrete Research*, 31, 1341–1349.

Ragozina, T.A. (1957). Reaction of Calcium Sulphate with Aluminate at 1200 °C. *Zhurnal Pikladnoi Khimii*, 30, 1682–1684.

Ramachandran, V.S., Paroli, R.M., Beaudoin, J.J., Delgado, A.H. (2002). *Handbook of Thermal Analysis of Construction Materials*, Noyes Publications, Norwich, U.S.A.

Rietveld, H. M. (1969). A Profile Refinement Method for Nuclear and Magnetic Structures. *Journal of Applied Crystallography*, 2, 65–71.

Sahu, S., Havlica, J., Tomkova, V., Majling, J. (1991). Hydration Behavior of Sulphoaluminate Belite Cement in the Presence of Various Calcium Sulphates. *Thermochimica Acta*, 175, 45-52.

Sahu, S., Majling, J. (1994). Preparation of Sulfoaluminate Belite Cement from Fly Ash. *Cement and Concrete Research*, 24**,** 1065–1072.

Scrivener, K., Vanderley, M.J., Gartner, E.M. (2016a). Eco-Efficient Cements: Potential, Economically Viable Solutions for a Low-CO_2, Cement-Based Materials Industry. H. A, United Nations Environment Programme.

Scrivener, K., Snellings, R., Lothenbach, B. (2016b). *A Practical Guide to Microstructural Analysis of Cementitious Materials*. Taylor & Francis Group, LLC, Boca Raton.

Sharp, J.H., Lawrence, C.D., Yang, R. (1999). Calcium Sulfoaluminate Cements—Low-Energy Cements, Special Cements or What?, *Advances in Cement Research*, 11, 3-13.

Sherman, N., Beretka, J., Santoro, L., Valenti, G.L. (1995). Long Term Behavior of Hydraulic Binders Based on Calcium Sulfoaluminate and Calcium Sulfosilicate. *Cement and Concrete Research*, 25, 113-126.

Shi, C., Fernández Jiménez, A., Palomo, A. (2011). New cements for the 21st century: The pursuit of an Alternative to Portland Cement. *Cement and Concrete Research*, 41, 750-763.

Singh, M., Upadhayay, S.N., and Prasad, P.M. (1996). Preparation of Special Cements from Red Mud. *Waste Management*, 16, 665-670.

Singh, M., Upadhayay, S.N., Prasad, P.M. (1997). Preparation of Iron Rich Cements Using Red Mud. *Cement and Concrete Research*, 27, 1037–1046.

Singh, M., Kapur, P.C., Pradip. (2008). Preparation of Calcium Sulphoaluminate Cement Using Fertiliser Plant Wastes. *Journal of Hazardous Materials*, 157, 106–113.

Song, F., Yu, Z., Yang, F., Lu, Y., Liu, Y. (2015). Microstructure of Amorphous Aluminum Hydroxide in Belite-Calcium Sulfoaluminate Cement. *Cement and Concrete Research*, 71, 1–6.

Strigac, J., Palou, M.T., Kristin, J., Majling, J. (2000). Morphology and Chemical Composition of Minerals inside the Phase Assemblage C-C_2S-$C_4A_3\bar{S}$-C_4AF-$C\bar{S}$ Relevant to Sulphoaluminate Belite Cements. *Ceramics-Silikaty*, 44, 26-34.

Su, M., Wang, Y., Zhang, L., Li, D. (1997). Preliminary Study on the Durability of Sulfo/Ferro-Aluminate Cements, in *Proceedings of the 10th International Congress on Chemistry of Cements*, Göteborg, vol. 4, paper 4iv029, 12pp.

Sudoh, G., Ohta, T., Harada, H. (1980). High Strength Cement in the CaO-Al_2O_3-SiO_2-SO_3 System and its Application. in *Proceedings of the 7th International Congress on Chemistry of Cements*, Paris, Vol. 3, pp. V 152-157.

Taylor, H.F.W. (1997). *Cement Chemistry*. 2nd ed., Thomas Telford, London.

Telesca, A., Marroccoli, M., Pace, M.L., Tomasulo, M., Valenti, G.L., Monteiro, P.J.M. (2014). A Hydration Study of Various Calcium Sulfoaluminate Cements. *Cement & Concrete Composites*, 53, 224–232.

Thomas, G. H., Stephenson, I.M. (1978). The Beta to Gamma Dicalcium Silicate Phase Transformation and its Significance on Air-Coiled Slag Stability. *Silicates Industriels*., 195-200.

Tokyay, M. (2016). *Cement and Concrete Mineral Admixtures*. CRC Press. Boca Raton.

Velazco, G., Almanza, J.M., Cortés, D.A., Escobedo, J.C., Escalante-Garcia, J.I. (2014). Effect of Citric Acid and the Hemihydrate Amount on the Properties of a Calcium Sulphoaluminate Cement. *Materials de Construccion*, Vol. 64, No. 316.

Wang, Y., Su, M., Yang, R., Liu, B. (1992). A Quantitative Study of Paste Microstructure and Hydration Characteristics of Sulfoaluminate Cement. in *Proceedings of the 9th International Congress on Chemistry of Cements*, New Delhi, Vol. 4, pp. 454–460.

Wang, Y., Su,, M. (1997). The Third Cement Series in China, *World Cem*., 25, 6-10.

Winnefeld, F., Barlag, S. (2010). Calorimetric and Thermogravimetric Study on the Influence of Calcium Sulfate on the Hydration of Ye'elimite. *Journal of Thermal Analysis and Calorimetry*, 101, 949-957.

Winnefeld, F., Lothenbach, B. (2010). Hydration of Calcium Sulfoaluminate Cements-Experimental Findings and Thermodynamic Modelling. *Cement and Concrete Research*, 40, 1239-1247.

Winnefeld, F., Martin, L.H.J., Müller, C.J., Lothenbach, B. (2017). Using Gypsum to Control Hydration Kinetics of CS̄A cements. *Construction and Building Materials*, 155, 154-163.

Wu, K., Shi, H., Guo, X. (2011). Utilization of Municipal Solid Waste Incineration Fly ash for Sulfoaluminate Cement Clinker Production. *Waste Management*, 31, 2001–2008.

Xi, Y. (1992). 9th International Congress on Chemistry of Cements, Proceedings, 4, 377.

Zdorov, A., Bemshtein, V. (1987). 1st NCB International Seminar on Cement, Concrete and Building Materials, Proceedings, 6, 82.

Zhang, P., Chen, Y., Shi, L., Zhang, G., Huang, W., Wu, J. (1992). The Crystal Structure of $C_4A_3\bar{S}$. in *Proceedings of the 9th International Congress on Chemistry of Cements*, New Delhi, Vol.3, pp. 201–208.

Zhang, L., Su, M., Wang, Y. (1999). Development of the Use of Sulfo- and Ferroaluminate Cements in China. *Advances in Cement Research,* 11, 15–21.

Zhang, L. (2000). Microstructure and Performance of Calcium Sulfoaluminate Cements. Ph.D. thesis, University of Aberdeen.

Zhang, L., Glasser, F.P. (2002). Hydration of Calcium Sulfoaluminate Cement at less than 24 h. *Advances in Cement Research*, 14, 141–155.

Zhang, G., Li, G., Li, Y. (2016). Effects of Superplasticizers and Retarders on the Fluidity and Strength of Sulphoaluminate Cement. *Construction and Building Materials*, 126, 44– 54.

Zivica, V. (2000). Properties of Blended Sulfoaluminate Belite Cement. *Construction and Building Materials*, 14, 433–437.

APPENDICES

APPENDIX A: XRD PATTERNS OF HYDRATED CALCIUM SULFOALUMINATE CEMENTS

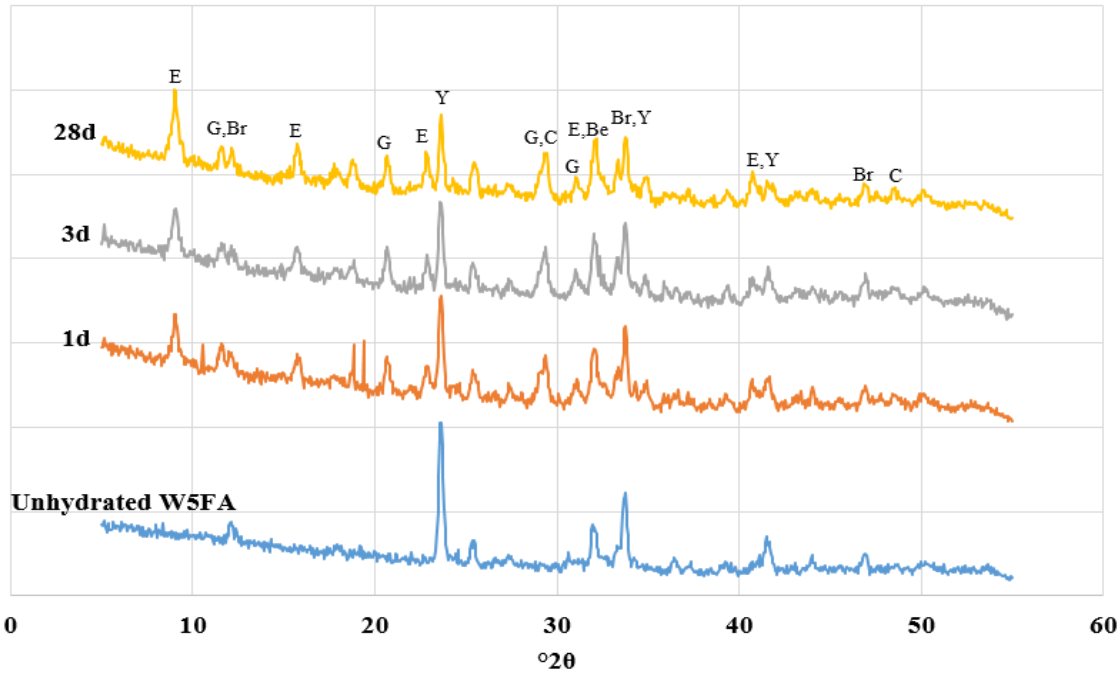

Figure A.1 XRD patterns of cement paste consisting of W5FA and desulfogypsum with clinker-to-desulfogypsum ratio of 76:24, at 1, 3 and 28 days of hydration (Legend: Be – Belite; Br – Brownmillerite; C – Calcite; E – Ettringite; G – Gypsum; Y – Ye'elimite)

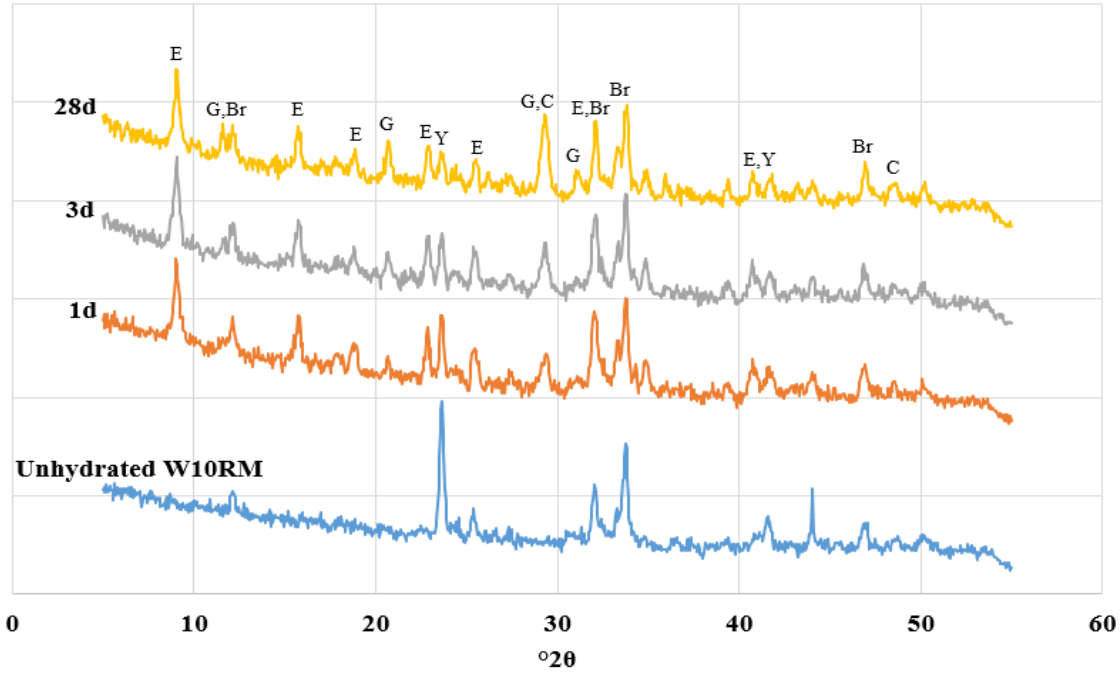

Figure A.2 XRD patterns of cement paste consisting of W10RM and desulfogypsum with clinker-to-desulfogypsum ratio of 81:19, at 1, 3 and 28 days of hydration (Legend: Br – Brownmillerite; C – Calcite; E – Ettringite; G – Gypsum; Y – Ye'elimite)

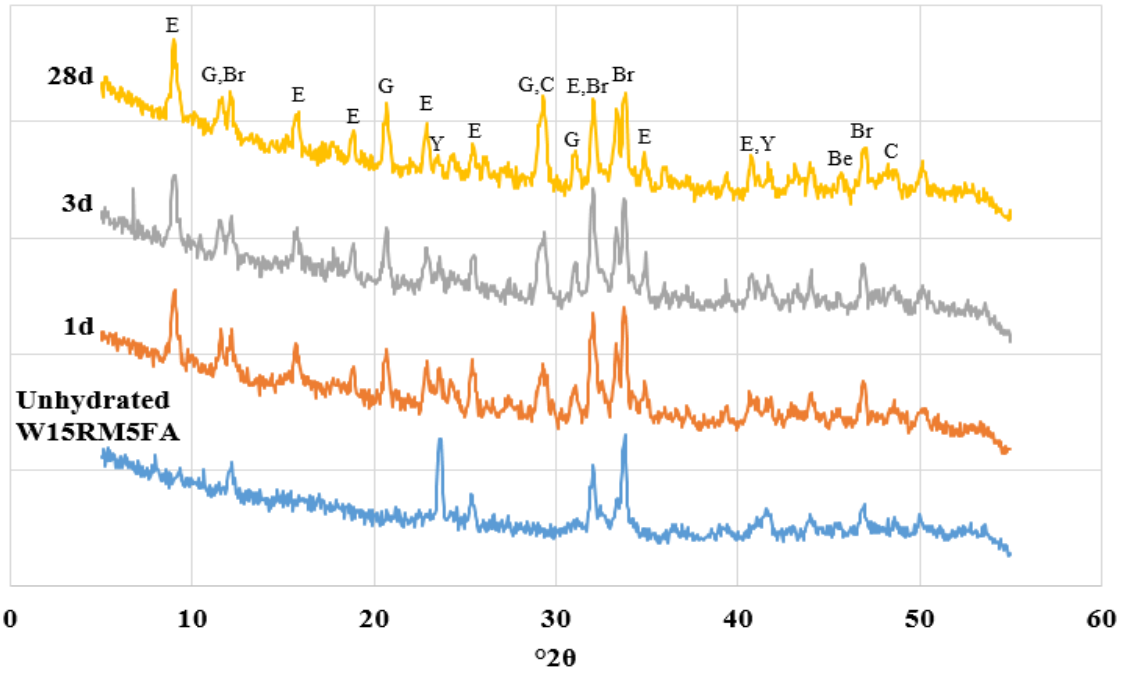

Figure A.3 XRD patterns of cement paste consisting of W15RM5FA and desulfogypsum with clinker-to-desulfogypsum ratio of 81:19, at 1, 3 and 28 days of hydration (Legend: Be – Belite; Br – Brownmillerite; C – Calcite; E – Ettringite; G – Gypsum; Y – Ye'elimite)

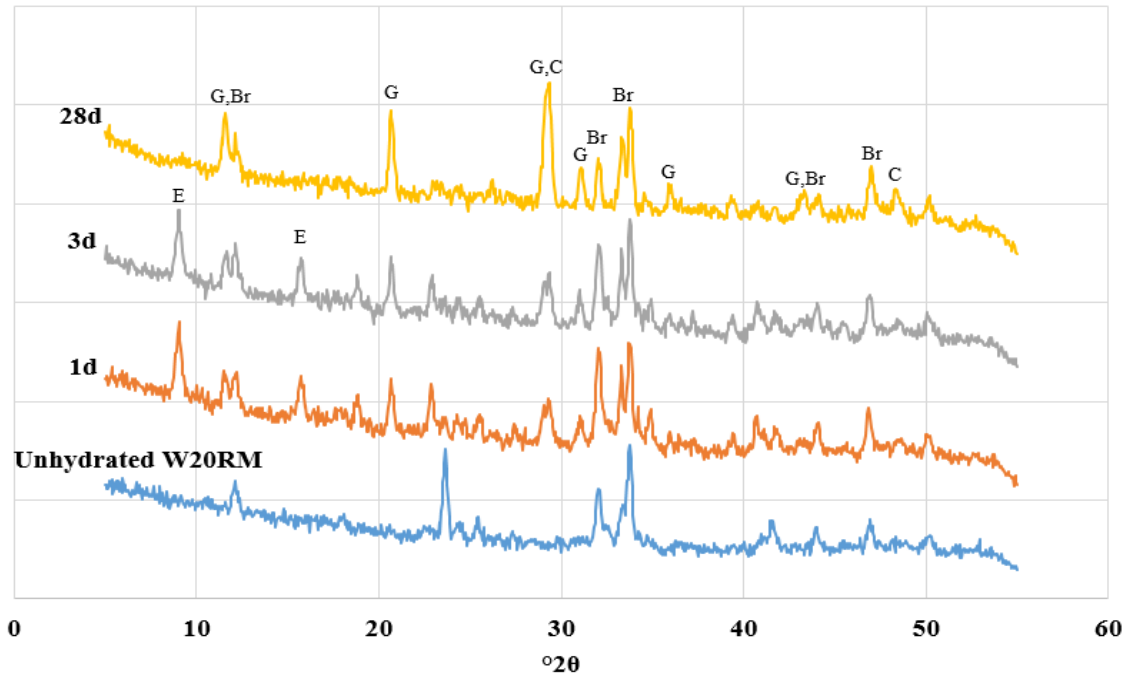

Figure A.4 XRD patterns of cement paste consisting of W20RM and desulfogypsum with clinker-to-desulfogypsum ratio of 81:19, at 1, 3 and 28 days of hydration (Legend: Br – Brownmillerite; C – Calcite; E – Ettringite; G – Gypsum; Y – Ye'elimite)

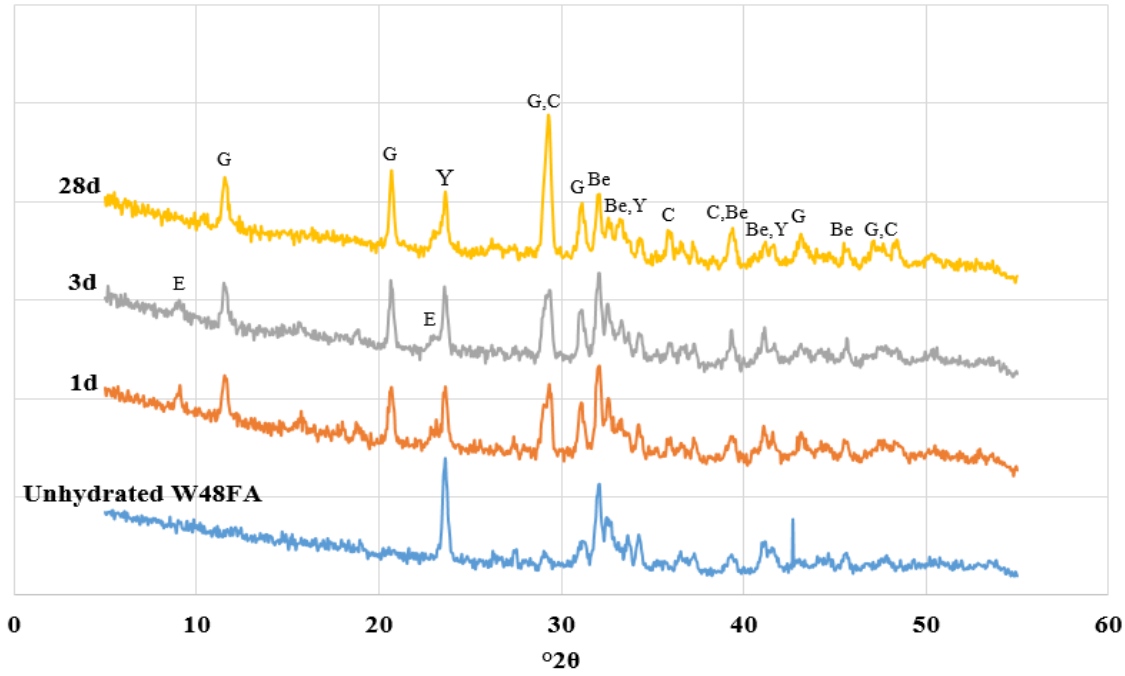

Figure A.5 XRD patterns of cement paste consisting of W48FA and desulfogypsum with clinker-to-desulfogypsum ratio of 76:24, at 1, 3 and 28 days of hydration (Legend: Be – Belite; C – Calcite; E – Ettringite; G – Gypsum; Y – Ye'elimite)

APPENDIX B: SEM IMAGES OF HYDRATED CALCIUM SULFOALUMINATE CEMENTS

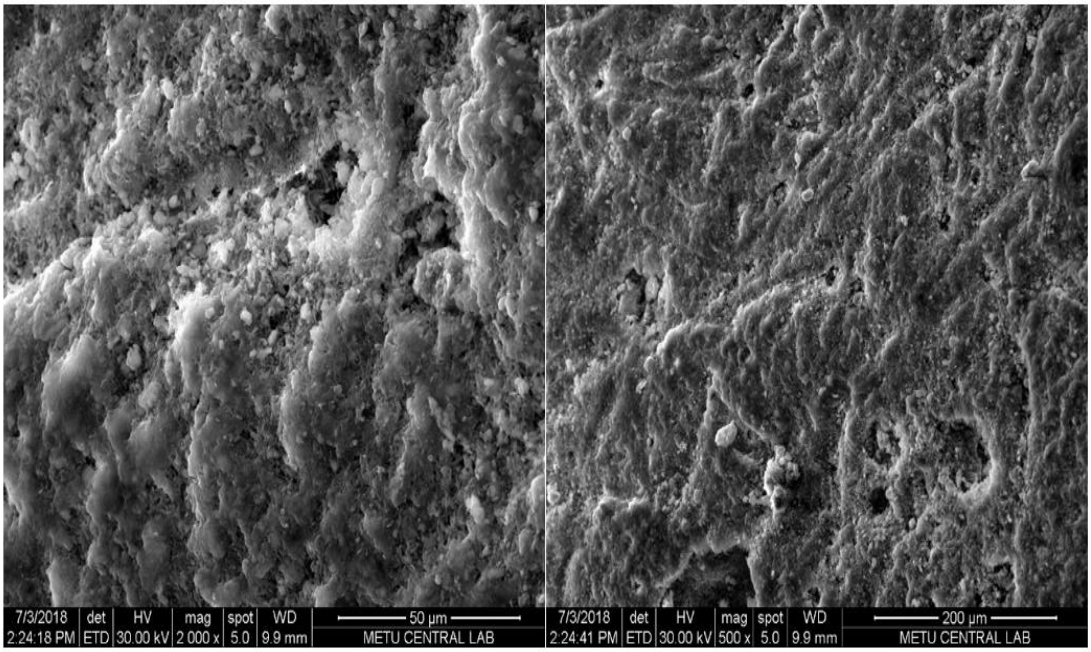

Figure B.1 SEM images of hydrated cement paste containing N2 and gypsum with clinker-to-gypsum ratio of 76:24 at 3 days of hydration

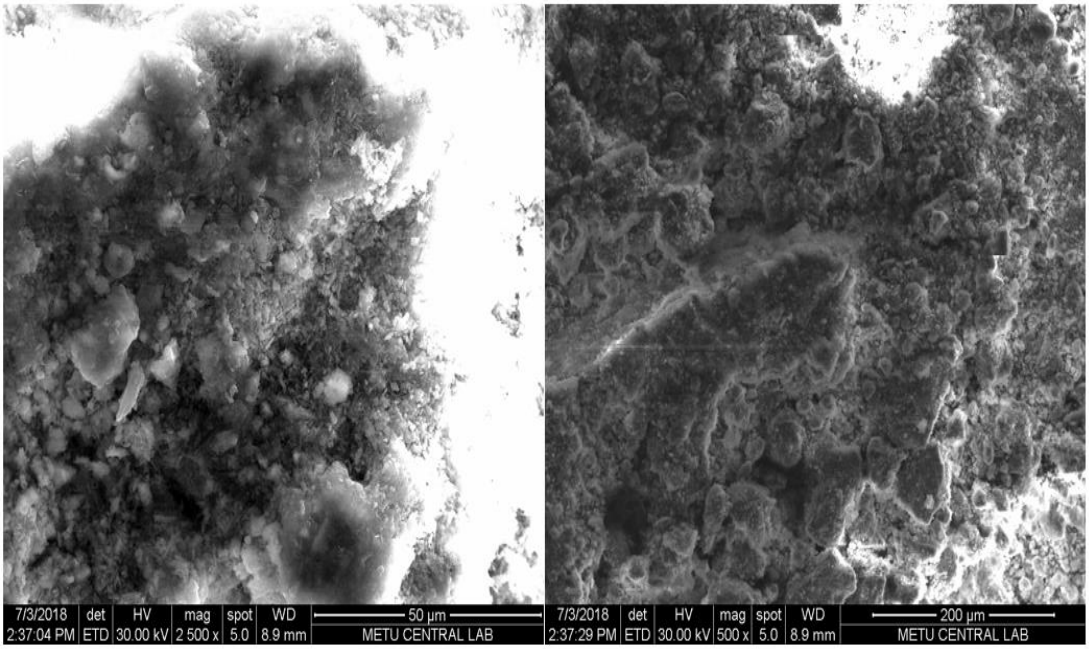

Figure B.2 SEM images of hydrated cement paste containing N6 and gypsum with clinker-to-gypsum ratio of 76:24 at 3 days of hydration

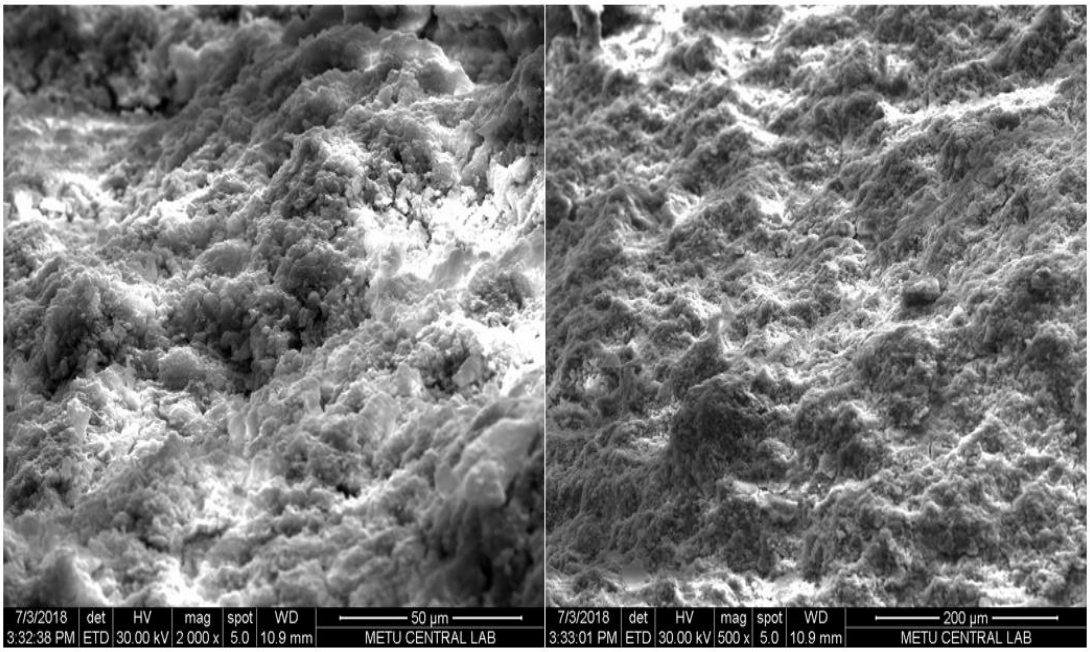

Figure B.3 SEM images of hydrated cement paste containing W15RM and gypsum with clinker-to-desulfogypsum ratio of 76:24 at 3 days of hydration

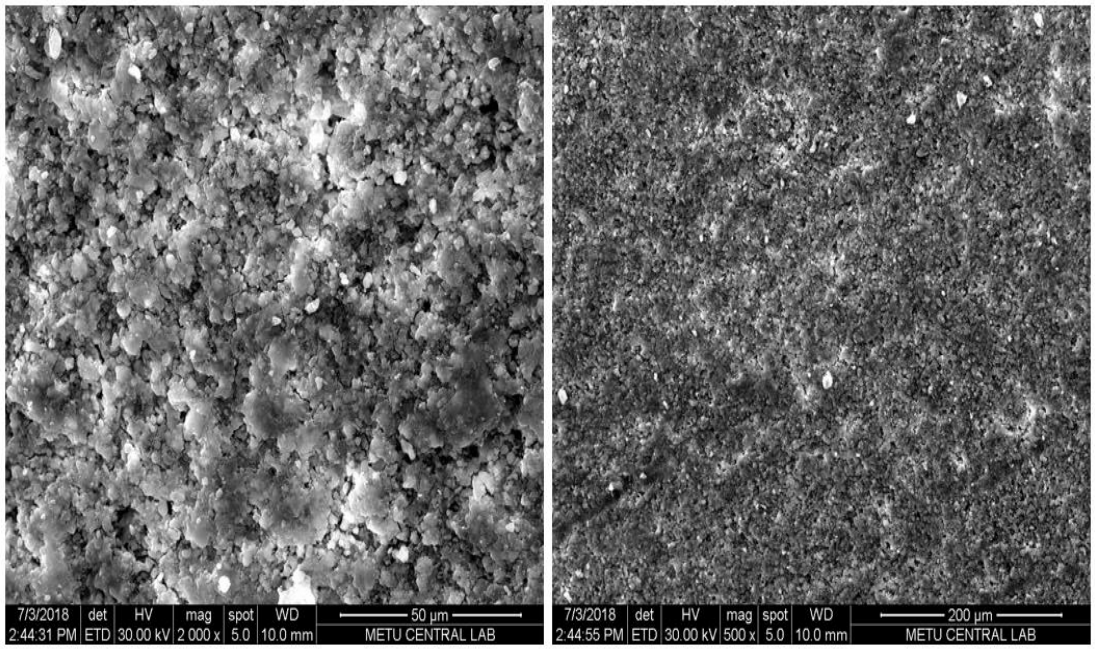

Figure B.4 SEM images of hydrated cement paste containing W10RM13.5FA and desulfogypsum with clinker-to-desulfogypsum ratio of 81:19 at 3 days of hydration

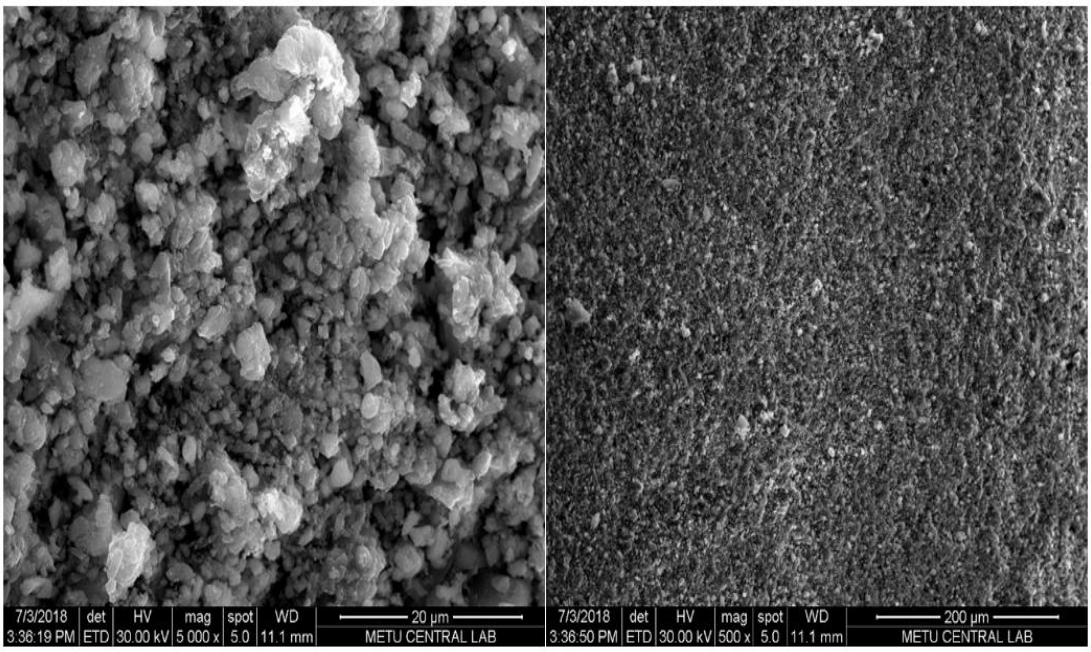

Figure B.5 SEM images of hydrated cement paste containing W45FA and desulfogypsum with clinker-to-desulfogypsum ratio of 81:19 at 3 days of hydration